

# The mechanism of estrogen`s effect in the hypothalamic regulation of energy homeostasis and circadian rhythm

Ph.D. Dissertation

**Gábor C. Mezei M.D.**

Semmelweis University  
School of Ph.D. Studies  
Clinical Medicine



Supervisor: Prof. János Rigó Jr., M.D., Ph.D.

Official reviewers: Beatrix Sármán M.D., Ph.D.  
Csaba Fekete M.D., Ph.D.

Chairman of the committee: Prof. Ferenc Túry M.D., Ph.D.  
Members of the committee: Prof. Janina Kulka M.D., Ph.D.  
Bence Rác Ph.D.

Budapest  
2010

## TABLE OF CONTENT

<b>ABBREVIATION .....</b>	<b>3</b>
<b>1. INTRODUCTION .....</b>	<b>6</b>
<b>1.1. Estrogen as metabolic hormone .....</b>	<b>6</b>
1.1.1. Obesity epidemic; focus on estrogen's antiobesity effect .....	6
1.1.2. Hypothalamic regulators of energy homeostasis; the role of leptin .....	8
1.1.3. The mechanism of estrogen's anorexigenic effect .....	11
1.1.4. Cross-talk between estrogen and leptin .....	13
1.1.5. Synaptic plasticity in the hypothalamus .....	14
<b>1.2. Estrogen and the biological clock .....</b>	<b>16</b>
1.2.1. Suprachiasmatic nucleus, the hypothalamic rhythm generator .....	16
1.2.2. The sexually dimorphic biological clock; estrogen's developmental effect ...	17
1.2.3. Estrogen's effect on the biological clock during adulthood .....	19
<b>2. AIM OF THE STUDY AND HYPOTHESIS .....</b>	<b>21</b>
<b>3. MATERIALS AND METHODS .....</b>	<b>23</b>
<b>3.1. Experiment 1; estrogen's effect on the energy homeostasis .....</b>	<b>23</b>
3.1.1. Animals .....	23
3.1.2. Surgical and hormonal manipulations .....	23
3.1.3. Determination of estrus cycle .....	25
3.1.4. Energy expenditure, respiratory quotient, lean body mass, body composition and nasal-anal length .....	25
3.1.5. Fixation and tissue preparation .....	25
3.1.6. Immunocytochemistry .....	26
3.1.7. Image analysis for light and fluorescence microscopy .....	28
3.1.8. Electron microscopy and postembedding immunostaining .....	29
3.1.9. Quantitative synaptology .....	30
3.1.10. Immunoblotting .....	31
3.1.11. Electrophysiology .....	31
<b>3.2. Experiment 2; estrogen's effect on the biological clock during early         development .....</b>	<b>33</b>
3.2.1. Animals .....	33
3.2.2. Hormon treatment, mitotic marker injection and tissue preparation .....	33
3.2.4. Immunocytochemistry and immunofluorescence .....	34
<b>3.3. Experiment 3; estrogen's effect on the biological clock during adulthood ....</b>	<b>37</b>
3.3.1. Animals .....	37
3.3.2. Surgical and hormonal manipulations .....	37
3.3.3. Light shifting procedures .....	37
3.3.4. Fixation and tissue preparation .....	38

3.3.5. Immunocytochemistry .....	38
3.3.6. Image analysis .....	39
<b>3.4. Statistical analyses .....</b>	<b>42</b>
<b>4. RESULTS .....</b>	<b>43</b>
<b>4.1. Experiment 1; estrogen's effect on the energy homeostasis .....</b>	<b>43</b>
4.1.1. Estrogen increases the number of excitatory synapses on POMC perikarya in wild-type animals .....	43
4.1.2. Estrogen enhances POMC tone; the dynamics of feeding behavior and synaptic rewiring .....	45
4.1.3. Estrogen exerts an antiobesity effect independent on leptin .....	48
4.1.4. Estrogen mimics leptin's effect on the rewiring of POMC cells .....	50
<b>4.2. Experiment 2; estrogen's effect on the biological clock during early         development .....</b>	<b>54</b>
4.2.1. Distribution of BrdU-labeled cells in the SCN .....	54
4.2.2. Sex differences in BrdU labeling in the SCN .....	55
4.2.3. Phenotypical characterization of BrdU-labeled cells .....	57
<b>4.3. Experiment 3; estrogen's effect on the biological clock during adulthood ....</b>	<b>60</b>
4.3.1. Estrogen enhances light-induced Fos expression in the SCN .....	60
4.3.2. Estrogen's effect on p-CREB expression in the SCN .....	61
4.3.3. Estrogen has no effect on the calbindin-D (28K), egr-1 and CBP expression in the SCN .....	62
4.3.4. Estrogen has no effect on the light-induced p-CREB and calbindin-D (28K) immunoreactivity in the IGL .....	63
4.3.5. Light induced Fos expression in the DRN, but not in MRN .....	64
4.3.6. Estrogen increases the proportion of serotonin cells expressing Fos after a phase shift in the DRN .....	66
<b>5. DISCUSSION .....</b>	<b>69</b>
<b>5.1. Estrogen and the hypothalamic regulation of energy homeostasis .....</b>	<b>69</b>
<b>5.2. Estrogen and the hypothalamic regulation of circadian rhythm .....</b>	<b>75</b>
<b>6. CONCLUSIONS .....</b>	<b>86</b>
<b>7. SUMMARY .....</b>	<b>89</b>
<b>8. REFERENCES .....</b>	<b>91</b>
<b>9. THE AUTHOR'S PUBLICATIONS ASSOCIATED WITH THESIS .....</b>	<b>109</b>
<b>10. THE AUTHOR'S PUBLICATIONS NOT ASSOCIATED WITH THESIS ...</b>	<b>111</b>
<b>11. ACKNOWLEDGEMENTS .....</b>	<b>116</b>

## ABBREVIATIONS

BMI	Body mass index
CNS	Central nervous system
E2	17- $\beta$ -estradiol
P450aro	Cytochrome P450 aromatase
ARC	Arcuate nucleus
VMH	Ventomedial hypothalamus
DMH	Dorsomedial hupothalamus
PVN	Paraventricular nucleus of the hypothalamus
LH	Lateral hypothalamus
AVPV	Anteroventral periventricular nucleus
GnRH	Gonadotropin releasing hormon
POMC	Proopiomelanocortin
LH	Luteinizing hormone
FSH	Follice-stimulating hormon
$\alpha$ -MSH	$\alpha$ -Melanocyte-stimulating hormone
ACTH	Adenocorticotrophic hormon
MC4R	Melanocortin 4 receptor
AMPA	Amino-3-hydroxy-5-methylisoxazole-4-propionic acid
GluR1 and 2	AMPA glutamate receptor subunit 1 and 2
GABA	$\gamma$ -Aminobutyric acid
ER $\alpha$ and $\beta$	Estrogen receptor $\alpha$ and $\beta$
ERE	Estrogen response element
LRb	Leptin receptor b (long) form
NPY	Neuropeptid Y
AgRP	Agouti-related peptide
PV	Parvalbumin
<i>ob/ob</i>	Leptin-deficient transgenic mice

<i>db/db</i>	Leptin receptor-deficient transgenic mice
STAT3	Signal transducer and activator of transcription 3
SDN-POA	Sexual dimorphic nucleus of the preoptic area
SCN	Suprachiasmatic nucleus
LGN	Lateral geniculate nucleus
IGL	Intrageniculate leaflet of the thalamic lateral geniculate nucleus
VIP	Vasoactive intestinal peptides
AVP	Vasopressin
Fos	a member of immediate early gene transcription factors
CREB	cAMP response element
p-CREB	Phosphorylated cAMP response element
<i>egr-1</i>	Early growth response protein-1
CBP	CREB binding protein
DRN	Dorsal raphe nucleus
MRN	Median raphe nucleus
GFP	Green fluorescent protein
POMC-GFP	POMC promoter-derived green fluorescent protein
OVX	Ovariectomized
h	hour(s)
min	minute(s)
ZT	Zeitgeber time
CT	Circadian time
5-HT	Serotonin
RT	room temperature
PB	Phosphate buffer
TBS	Tris-buffered saline
VO <sub>2</sub>	Oxygen consumption
i.c.v.	Intracerebroventricular
VCO <sub>2</sub>	Carbon dioxide production

RQ	Respiratory quotient (calculated as $V_{CO2}/V_{O2}$ )
EE	Energy expenditure
DDW	Double distilled water
aCSF	Artificial cerebrospinal fluid
HRP	Horseradish peroxidase
SDS-PAGE	Sodium dodecyl sulfate polyacrylamide gel electrophoresis
EPSCs	Excitatory postsynaptic currents
IPSCs	Inhibitory postsynaptic currents
mEPSCs	Miniature excitatory postsynaptic currents
mIPSCs	Miniature inhibitory postsynaptic currents
BrdU	5-bromo-2'-deoxyuridine
TP	Testosterone propionate
ANOVA	Analysis of variance
CBP/P300	CREB binding protein/P300
GFAP	Glial fibrillary acidic protein
TGF- $\alpha$	Tumor growth factor- $\alpha$
DNA	Desoxy ribonucleotid acid
NcoA/SRC1a	Nuclear co-activator SRC1a
MAPK	Mitogen-activated protein kinase
Src-kinase	Short for sarcoma-kinase
JAK	The Janus kinase
PI3K	Phosphoinositide-3 kinase
PSD-95	Postsynaptic density-95
BDNF	Brain-derived neurotropic factor
PKA	cAMP-dependent protein kinase
AKAP79/150	A-kinase-anchoring protein 79/150

## **1. INTRODUCTION**

The gonadal steroid estrogen is thought to be primarily a reproductive hormone regulating the female reproductive functions. In the second half of the last century the exploration of the mechanism of the hypothalamus-pituitary-ovarian axis has revolutionized reproductive endocrinology. The discovery of estrogen-induced gonadotropin surge, also known as “positive feedback”, in the brain has led us to understand the physiological mechanisms responsible for menses, ovulation, pregnancy, lactation and menopause. Furthermore it opened revenues for newly born fields such as assisted reproduction, hormonal contraception and menopause medicine.

There is emerging substantial evidence that steroid hormones, in particular estrogen, modulate a variety of centrally regulated physiological functions in addition to their well-described role in the regulation of reproductive function. Within the central nervous system (CNS), estrogen plays a role in the mechanisms modulating processes such as learning and memory, motivation, mood, sleep, circadian rhythms and energy homeostasis (McEwen and Alves, 1999; McEwen, 2001). Cessation of ovarian function (natural or iatrogenic menopause) correlates with deregulation of these processes leading to learning and/or memory impairments, mood disturbances, unpredictable mood swings, anxiety, depression, temporal and erratic disturbances in thermoregulation (hot flushes, night sweats), altered sleep patterns and circadian rhythms and imbalanced energy homeostasis favoring obesity (McEwen, 2001). In the regulation of these central nervous functions several brain regions are involved, which are directly (estrogen receptors) or indirectly (through neural pathways) sensitive to the circulating estrogen levels. This thesis is focusing on the effects of estrogen in the hypothalamic regulation of energy homeostasis and circadian rhythm.

## **1.1. Estrogen as a metabolic hormone**

### **1.1.1. Obesity epidemic; focus on estrogen's antiobesity effect**

In the last couple of decades obesity has become an enormous health problem in the developed world. In the United States 25 years ago only 15% of adults were considered obese (BMI>30), today this number is more than 34% and is rapidly increasing. Furthermore, more than half of the adults are now considered overweight (BMI>25). The population is getting more overweight and this process is starting at a younger age. Obesity is by definition a metabolic state characterized by enhanced food intake (hyperphagia) and reduced energy expenditure that results in the accumulation of body fat. Sustained obesity has profound consequences on one's life, spanning from superficial psychological symptoms to serious diseases and also accounts for one of the largest financial burdens on our health care system. It is well established, that obesity is a major risk factor of various diseases including metabolic disorders (diabetes, metabolic syndrome), cardiovascular diseases (atherosclerosis, hypertension, stroke, myocardial infarct), musculoskeletal diseases and as well as cancer. It markedly diminishes both the quality and length of one's life. Thus, it is not surprising, that the demand (of the patients and of the pharmaceutical industry) for an efficient and safe magical anti-obesity drug is high. An enormous amount of research is targeting all the factors which are thought to be involved in the central energy balance regulation and this is how estrogen moved into the center of the recent obesity research. It has been known for a while, that the estrogen, namely its most potent form the 17- $\beta$ -estradiol (E2), is a very potent antiobesity hormone (Duduc, 1985; Wade et al., 1985). E2 reduces food intake and body adiposity and increases energy expenditure in animals and humans of both sexes (Milewicz et al., 2000; Poehlman, 2002). In human females the food intake varies across the menstrual cycle, with daily food intake being lowest during the periovulatory period when estrogen levels are at a maximum (Asarian and Geary, 2006). Menopausal women tend to gain body fat, which is thought to be a consequence of the decline in endogenous estrogen levels (Carr, 2003; Augoulea et al., 2005). Rodents exhibit a 4 day estrus cycle in which

estrogen levels fluctuate, as does energy homeostasis, such that decreased food intake and body weight, and increased energy expenditure coincide with high levels of estrogen (Parker et al., 2001). In accordance with this finding, in animal models ovariectomy induces an increase in food intake and decreases ambulatory and wheel running activities, leading towards prolonged positive energy balance and ultimately obesity. All these effects can be reversed with estrogen replacement (Colvin and Sawyer, 1969; Asarian and Geary, 2002). Based on the above mentioned evidences, it is well supported, that hypo-estrogenic states are associated with decreased activity and an increase in body weight in females. This effect of estrogen is thought to be mediated through the actions of the CNS, predominantly through the hypothalamus. This is based on the observations that direct injections of estrogen into specific hypothalamic regions are the most effective in reducing food intake, body weight and increasing wheel running activities (Butera and Czaja, 1984; Dubuc, 1985; Palmer and Gray, 1986). This theory is further supported by the fact, that these hypothalamic nuclei are particularly rich in estrogen receptors (Mitra et al., 2003). However, the mechanism by which estrogen exerts its central anti-obesity effect is still poorly understood and is currently under extensive investigation.

### **1.1.2. Hypothalamic regulators of energy homeostasis; the role of leptin**

In the 1940s and 1950s various degeneration/lesion studies were conducted to identify the regions of the brain involved in the regulation of energy homeostasis. Of these various regions, the hypothalamus emerged as one of the critical sites for the regulation of energy homeostasis. Destruction of the hypothalamic ventromedial (VMH), paraventricular (PVN), or dorsomedial (DMH) nuclei induced hyperphagia and obesity, whereas lesions in the lateral hypothalamus (LH) decreased food intake and triggered weight loss (Hetherington and Ranson, 1940; Anand and Brobeck, 1951). These findings led to the proposal of the “dual center model” that identified the VMH as the “satiety center” and the LH as the “hunger center” (Stellar, 1954).

These nuclei also must be able to constantly monitor the amount of fuel available in the body and the amount of existing body energy stores (fat tissue and/or glycogen) in order to adequately modulate energy intake and expenditure. Parabiosis studies on hypothalamic lesioned rodents concluded the existence of humoral signal(s) in relation to an animal's lipostatics (Hervey, 1959). In these studies, two live animals, one with a lesion in the VMH, were joined by surgical means, which allowed humoral factors to pass from one animal to the other. As obesity developed in the lesioned rat, its partner became hypophagic and lost weight, suggesting that a signal, in proportion to the amount of fat mass, is highly potent in inhibiting food intake. Additional parabiosis studies on genetically obese mutant mice, *ob/ob* and *db/db* (Coleman and Hummel, 1969; Coleman, 1978), concluded that *ob/ob* mice lack this lipostatic signal, whereas *db/db* mice are insensitive to it.

A fundamental breakthrough in the field of metabolic research came in 1994 and 1995, when these hypotheses were confirmed by cloning the *ob* gene that encodes leptin (Zhang et al., 1994) and the *db* gene that encodes leptin receptor (Tartaglia et al., 1995). Leptin is a key player in regulating energy intake and expenditure, including appetite and metabolism, and it is thought to be the most potent hormone resulting in a markedly decreased food intake and in an increased energy expenditure. Leptin is a 16 kDa protein its gene, the so called *ob* gene, is located on chromosome 7 in humans. It is secreted to the blood stream by the adipocytes. The circulating leptin levels reflect the amount of adipose tissue present. It enters the CNS in proportion to its plasma concentration and acts on its receptors located in the hypothalamic nuclei (Mercer et al., 1996), some of which had been implicated in the regulation of metabolism by lesion studies. However, leptin bound and its receptors accumulated predominantly in a ventromedial hypothalamic structure, the arcuate nucleus (ARC), which was not specifically suggested by these lesion studies; and only in a lesser degree in the PVN, VMH and LH nuclei (Schwartz et al., 1996). Based on these results the ARC has become the focus of recent research. Further support for the role of this small hypothalamic nucleus in energy homeostasis came when the melanocortin system was found to be significantly involved

in obesity (Huszar et al., 1997). Melanocortin is also found in neurons of the ARC, and leptin affected energy homeostasis is mainly mediated by the ARC melanocortin system (Seeley et al., 1997). An attractive model emerged from further analysis of the components of the central melanocortin system (Ollmann et al., 1997), which today is considered to be the key component in the regulation of feeding and energy expenditure. In this model the role of the ARC turned out to be critical for two major reasons. First, the neurons within the ARC are located in an anatomically strategic place. They are close to fenestrated capillaries at the median eminence, a region with no blood-brain barrier between vessels and the parenchyma, giving them access to various humoral signals that are restricted from other portions of the brain. Second, these neurons are innervated by axons containing all major neurotransmitters and synthesize receptors for most metabolic hormones (Benoit et al. 2000). Two subsets of neurons that have opposite effects on feeding are found in the ARC; both contain the inhibitory neurotransmitter  $\gamma$ -Aminobutyric acid (GABA) (Horvath et al. 1997). One set of these neurons expresses proopiomelanocortin (POMC); when stimulated they produce anorectic effects. The POMC precursor is cleaved into melanocyte-stimulating hormones ( $\alpha$ -,  $\beta$ -, and  $\gamma$ -MSH),  $\beta$ -endorphin, and adrenocorticotrophic hormone (ACTH). Of these,  $\alpha$ - and  $\beta$ -MSH reduce food intake and body weight and increase energy expenditure in animals and humans. Both  $\alpha$ - and  $\beta$ -MSH act on melanocortin receptor subtypes 3 and 4 (MC3/4R), which are abundant particularly in the ARC, PVN, LH, and DMH. The second group of cells in which increased activity leads to orexigenic responses contains neuropeptide Y (NPY) and aguti-related peptide (AgRP). NPY/AgRP potently stimulates feeding and reduces energy expenditure, by two distinguished methods. First, NPY/AgRP neurons are directly inhibiting the POMC neurons through the release of GABA. Second, NPY/AgRP neurons are releasing AgRP from their neuronal axon terminals, which are directly antagonizing the effect of  $\alpha$ - and  $\beta$ -MSH on the MC3/4Rs in the VMH and PVN (Horvath, 2005).

Under normal physiological conditions, when the leptin mechanism is intact, leptin functions as a fat reporter, an index of the body energy storage. When the energy

storages are full, the case of positive energy balance, the circulating leptin levels are high, leptin activates POMC neurons, triggers the release of  $\alpha$ - and  $\beta$ -MSH from POMC axon terminals, which in turn activates MC3/4Rs, leading to suppressed food intake and increased energy expenditure. Simultaneously, leptin suppresses the activity of NPY/AgRP neurons of ARC, blocks their inhibitory effects, and thus further suppresses food intake and increasing energy expenditure. In case of intact leptin signaling, the administration of leptin in animals and humans reduces food intake and increases energy expenditure, resulting in decreased fat storage.

On the other hand, mutations that disrupt the functions of leptin signaling result in obesity and diabetes (Coleman, 1978; Zhang et al., 1994). However, most obese people are not leptin or leptin receptor deficient, but rather, leptin resistant with elevated plasma leptin levels and poor responsiveness to leptin signal (Maffei et al., 1995). In the case of impaired leptin signaling, the energy homeostasis machineries recognize a state of extreme negative energy balance and initiate various behavioral and physiological responses regardless of actual body energy stores. Animals and human with impaired leptin signaling are not only hyperphagic but also have extreme difficulty utilizing stored energy resulting in morbid obesity. Taken together, obesity simulates a state of prolonged negative energy balance.

The manner by which this leptin effect is translated to appropriate neural responses in hypothalamic feeding circuits is unclear. Mechanisms for developing leptin resistance are largely unknown. Complex metabolic signal interactions, therefore, are an important aspect of energy homeostasis and are in the center of the current research.

### **1.1.3. The mechanism of estrogen's anorexigenic effect**

Although leptin thought to carry out the most potent anorexigenic effect, numerous other metabolic signals are also known with significant anorexigenic or orexigenic effect on the central regulation of energy homeostasis, such as insulin, ghrelin, estrogen, prolactin, the glucocorticoids, resistin, interleukins, as well as nutrients such as glucose and free fatty acids. All of these, to a certain extent, modify energy balance and body weight, and

also target the hypothalamic melanocortin system presumably in coordination with leptin function. Ghrelin, for example, is considered the counterpart of leptin, is a protein substance released from the stomach and pancreas and is thought to be the most potent orexigenic hormone promoting hunger.

Estrogen, as discussed previously, is a very potent antiobesity hormone and its effect thought to take place in the hypothalamic nuclei involved in the regulation of energy balance. Thus, it is not a surprise that estrogen became the focus of the recent metabolic research. Despite all efforts, the mechanism, by which estrogen exerts its anorexigenic effect in the hypothalamus and its interaction with leptin, is mainly unclear. Estrogen can be produced locally from the aromatization of testosterone and/or androstenedione by cytochrome P450 aromatase (P450aro). The levels of P450aro in male brains are higher than in females (Lephart, 1996). Aromatase-deficiency results in the accumulation of excess adipose tissue in both sexes and this is associated with hypogonadotropic hypogonadism, a phenotype shared by leptin deficiency, in both sexes in humans (Jones et al., 2000). This suggests that local estrogen levels are important for the regulation of energy homeostasis and reproduction. Indeed, P450aro is highly and selectively expressed in the regions associated with metabolism and reproduction, i.e., VMH (Naftolin et al., 2001).

The effect of estrogen is mediated by estrogen receptors (ERs), members of the nuclear hormone receptor family. Upon estrogen binding, the ERs undergo conformational changes and nuclear translocation, acting as transcription factors to regulate gene expression (genomic effect) by binding to estrogen response element (ERE) sequences in target genes and recruiting co-regulatory proteins. Two ERs,  $\alpha$  and  $\beta$  have been identified. Estrogen receptor  $\alpha$  (ER $\alpha$ ) has been suggested as the main nuclear estrogen receptor that mediates estrogen's antiobesity effect in both sexes (Heine et al., 2000; Roesch, 2006, Geary et al., 2001). ER $\alpha$ -null animals develop obesity with a more than 100% increase of their fat tissue when compared to controls, whereas estrogen receptor  $\beta$  (ER $\beta$ ) mice are lean. In the arcuate nucleus, ER $\alpha$  is the dominant estrogen receptor and levels of ER $\beta$  are negligible (Osterlund et al., 1998). Notably, levels of circulating

estrogen in obese ER $\alpha$ -null animals are 10 times higher than those in their wild-type littermates (Couse et al., 1995), revealing estrogen resistance of these mice, which results in adiposity. Additional administration of estrogen does not reduce either food intake or body weight (Geary et al., 2001). Despite differential expression of ERs in various neuroendocrine nuclei in the brain in males and females, ERs are equally expressed in the ARC in both sexes (Brown et al., 1992) suggesting that estrogen's effect on the melanocortin system is not sexually dimorphic. Although the evidence implicating ER $\alpha$  in metabolism is strong, other mechanisms that involve novel membrane-associated ER and intracellular signaling, by which estrogen affects energy homeostasis cannot be ruled out (Qiu et al., 2006). The molecular nature of membrane-associated ER is less understood.

#### **1.1.4. Cross-talk between estrogen and leptin**

Estrogen and leptin both act in overlapping neurons in the hypothalamus to regulate long-term energy balance and fertility. Both hormones exert a potent antiobesity effect. It has been suggested, that chronic estrogen withdrawal, as in ovariectomy in rodents and postmenopause in women, and subsequent hormone replacement revealed that estrogen may be a potent regulator of leptin signaling (Ainslie et al., 2001; Clegg, 2006); when estrogen levels are low, leptin resistance is developed resulting obesity. In contrast, however, the effect of estrogen appears independent of the key antiobesity signal, leptin, since estrogen reduces appetite and adiposity effectively in both leptin (*ob/ob*) and leptin receptor (*db/db*) mutant obese animals (Dubuc, 1986; Grasa et al., 2000). The mechanism underlying estrogen's antiobesity effect is not clearly understood. The similarity between leptin's and estrogen's effect on homeostasis and molecular cellular adaptations in the hypothalamus raises the possibility that estrogen and leptin signaling target common mechanisms. Further supports this notion, that the primary sites of ER $\alpha$  within the hypothalamus include the same areas where the leptin receptors are located. In fact, all the neurons that express the estrogen receptor in hypothalamic regions related to energy regulation also express the long form (b) of the leptin receptor (LRb) (Diano et

al., 1998). The signal transducer and activator of transcription 3 molecule (STAT3) is thought to have a central role in the intracellular signal transduction of leptin's anti-obesity effect. The brain-specific STAT3 knockout mice were obese and diabetic, highly resembling leptin mutant phenotypes (Gao et al.; 2004), suggesting that STAT3 plays a dominant role in mediating leptin signaling. A study showed that estrogen increases leptin-induced STAT3 activities in ARC neurons (Clegg, 2006). The brain STAT3 knockout animal model, thus, provides a unique experimental system for dissecting the interactive mechanism between leptin-STAT3 and estrogen signaling. Taken together, we hypothesize that estrogen exerts its antiobesity effect by activating the key leptin downstream effector, STAT3, in the hypothalamic feeding nuclei.

#### **1.1.5. Synaptic plasticity in the hypothalamus**

By now it is well known that estrogen has a potent anorexigenic effect, but the manner by which this estrogen effect is translated to appropriate neural responses in the hypothalamic feeding circuits are unclear. A large body of data has emerged regarding the intracellular signaling of various hormones, i.e. estrogen in the hypothalamus. Transcriptional events have been described to support overall cellular alterations. However, Cajal's neuronal doctrine predicts that functional outcomes of circuit alteration should stem from altered firing and/or connection (synaptology) of neuronal networks. Mounting evidence suggests that peripheral hormones accomplish just this in the hypothalamus as well. Supporting this idea, the hypothalamus retains plasticity throughout life, and immature synapses can frequently be found in the adult hypothalamus. For example, the magnocellular system shows plasticity during changes in water homeostasis (Theodosios et al., 1991; Miyata et al., 1994), in the ARC the synaptic organization of unidentified neurons exhibited changes in response to a varying gonadal steroid milieu (Garcia-Segura et al., 1994; Parducz et al., 2003), the synaptology of the perikarya of luteinizing hormone-releasing hormone neurons varies during changes in the gonadal steroid milieu (Zsarnovszky et al., 2001; Naftolin et al., 2007) or in photoperiod lengths (Xiong et al., 1997). Nevertheless, synaptic plasticity was not

considered an important aspect in daily energy regulation. Recent observations, however, suggest that it may be a regulatory component in the hypothalamic control of energy balance. First, leptin replacement in *ob/ob* mice indicated that synaptic rearrangement of feeding circuits is part of an ongoing general phenomenon. Furthermore, robust effects of peripheral ghrelin injections on the input organization of POMC neurons of mice led to wiring different from that induced by leptin (Pinto et al., 2004). In addition, leptin robustly regulated the synaptic organization of lateral hypothalamic hypocretin/orexin neurons (Horvath and Gao, 2005), and ghrelin produced a rapid effect on synaptic formation in the ARC (Pinto et al., 2004), in the hippocampus (Diano et al., 2006) and in the ventral tegmentum (Abizaid et al., 2006). Based on the aforementioned evidences it is likely, that estrogen trigger similar neuronal adaptations in the hypothalamic melanocortin feeding circuits further supporting the notion that the plasticity is an inherent element of the hypothalamic regulation of energy control.

## **1.2. Estrogen and the biological clock**

### **1.2.1. Suprachiasmatic nucleus, the hypothalamic rhythm generator**

The capacity of the CNS to carry out higher brain functions, including learning, memory processing, and cognition, in general, is highly dependent on adequately organized autonomic and endocrine mechanisms. In the CNS of mammals, including humans, the synchronization of the activity of different brain mechanisms with each other and with the environment is largely organized by the biological clock (Rusak and Zucker, 1975; Moore, 1983). The main biological clock resides in the suprachiasmatic nucleus (SCN) of the hypothalamus and is primarily entrained by the light/dark cycle via direct retinal projections to its core region. The SCN is the master clock that generates and maintains circadian and seasonal rhythms by integrating changes in photic conditions to the brain. The mechanism, by which this entrainment occurs within the SCN is heavily investigated but is still not clearly understood. Transduction of photic signals within the SCN involves a multi-signaling process that ultimately generates rhythms. The SCN via paracrine action (Silver et al., 1996) and neural projections (Watts and Swanson, 1987) affects a wide variety of regions and related functions of the brain by providing synchronized rhythms for these CNS mechanisms (Rusak and Zucker, 1975; Moore, 1983). The SCN also receives processed visual input via a subdivision of the thalamic lateral geniculate nucleus (LGN), i.e., the intergeniculate leaflet (IGL) of the LGN (Swanson et al., 1974). It has been suggested that the geniculohypothalamic tract exerts feedback action on the SCN, modulating the entrainment of circadian rhythms to the light/dark cycle after phase-shifting (Moore, 1983).

Growing evidences support, that gonadal steroids, estrogen in particular, have significant effects on the biological clock during both development (Horvath and Wicker, 1999; Horvath et al., 1998; Gorski et al., 1978) and adulthood (Albers, 1981; Morin and Cummings, 1982; Morin et al., 1977) maintaining the synchrony of endocrine and autonomic mechanisms. Estrogen excites its effect directly or indirectly on the neurons in the biological clock, by which it has significant implications for a wide array of

physiological functions including the regulation of gonadotropins, sleep/wake cycles, cognitive functions and psychiatric disorders, such as depression and attention deficit disorder (McEwen and Alves, 1999; McEwen, 2001). For example, the gonadotropin releasing hormone (GnRH), the releasing hormone for the pituitary luteinizing hormone (LH) and follicle-stimulating hormone (FSH), is secreted in a circadian and sexually dimorphic manner into the portal vasculature at the level of the median eminence (Albers et al., 1984; Turek et al., 1984). It is well established that females possess a neurogenic mechanism that allows the activation of the GnRH neuronal system by estrogen (positive gonadotropin feedback) and thereby induces the ovulatory surge of LH and FSH. Destruction of the SCN blocks the preovulatory LH surge and induces persistent estrus in intact female rats (Brown-Grant and Raisman, 1977). GnRH neurons are receiving multiple inputs from the SCN and IGL. SCN and IGL efferents target and synapse on GnRH-containing neurons in the preoptic area and in the anteroventral periventricular nucleus (AVPV) (Van der Beek et al., 1997). In males, GnRH neurons are under tonic inhibition by circulating gonadal steroids and the positive feedback action of estrogen to induce circadian LH secretion is absent. Taking together, it is strongly suggested, that this sexually dimorphic, clock-dependent positive feedback of gonadotropins is due, in part, to gonadal hormone-dependent development and/or adult activity of the SCN and IGL. However, the mechanism by which estrogen exerts its effect in the neuronal circuits of the biological clock is still ill-defined.

### **1.2.2. The sexually dimorphic biological clock; estrogen's developmental effect**

Several areas of the brain exhibit gender differences, which thought to be due, in part, to gonadal steroid hormone-dependent development. Most sexually dimorphic nuclei within the hypothalamus are larger in males than in females. Of these, the most extensively studied is the sexual dimorphic nucleus of the medial preoptic area (SDN-POA), which is significantly bigger in males (Gorski et al., 1978; Jacobson et al., 1985). They demonstrated that this difference is due to the prenatal and neonatal levels of locally formed estrogen from testosterone that is significantly higher in males than in

females. While they succeeded in reversing the size of this nucleus in females by perinatal administration of testosterone (masculinization), administration of dihydrotestosterone to females did not induce masculinization, but estrogen had a masculinizing effect. These findings demonstrated that during early development of the CNS, testosterone converted to estrogen by the enzyme, aromatase, regulates the maturation and sexual differentiation of certain brain areas.

The key enzyme for brain sexual differentiation, aromatase, is present in distinct nuclei of the CNS. Biochemical approaches revealed the highest aromatase activity to be present in limbic structures, including the amygdala, hippocampus, bed nucleus of the stria terminalis, lateral septum, and medial preoptic area of the hypothalamus (Roselli and Resko, 1993). Corresponding to the notion that aromatase is related to sexual phenotype, all of these limbic and hypothalamic areas participate in the regulation of reproductive functions. However, later its presence was demonstrated in extra-limbic structures as well, strikingly, the vast majority of these regions belong to different sensory systems including the circadian visual system, such as optic tract, SCN, ventral lateral geniculate body (most abundantly in the IGL), and superior colliculus (Horvath and Wikler, 1998; Horvath et al., 1994). A feature of aromatase immunoreactivity in the SCN and IGL is that it is transiently expressed, it is found to be present during late prenatal and early postnatal ages, but in lower in adult (Horvath et al., 1998). However, the visual cortex seemed to lack aromatase immunoreactivity.

Among other hypothalamic nuclei, the SCN has been demonstrated to be sexually dimorphic. Three-dimensional images of the SCN of males and females showed that the volume of the SCN is larger in males and contains more nuclei (Le Blond et al., 1982; Gorski et al., 1978). Furthermore, morphological studies demonstrated that SCN efferents, which contain vasopressin (AVP) or vasoactive intestinal peptide (VIP), develop in a gender specific manner (Horvath et al., 1998).

The synaptology and efferent projections of the IGL and SCN start to develop from embryonic day 16 and 19, respectively (Bunt et al, 1983). This coincides with the appearance of aromatase immunoreactivity in axons and axon terminals in the SCN and

IGL with a peak at embryonic day 18. Plasma testosterone levels of males start to elevate at embryonic day 17 and peak between embryonic day 18 and 19. After a transient decrease, blood testosterone concentrations increase after birth. During this perinatal period (between embryonic day 18 and postnatal day 21), the afferent and efferent connections of the SCN and IGL are established (Lenn et al., 1977). It was also shown, that the developing SCN and IGL contain ERs, predominantly ER $\beta$  (Shughrue et al., 1997; Nilsen et al., 2000).

The demonstration of the presence of aromatase in the developing biological clock along with the results showing the existence of ERs in these same areas and the differential availability of substrate androgen in males and females indicate that parts of the biological clock develop in a gender specific/hormone-dependent manner. However, the mechanism, by which of this developmental effect taking place is not well-understood.

### **1.2.3. Estrogen's effect on the biological clock during adulthood**

The effects of ovarian hormones on the biological clock during adulthood have been extensively studied. In female hamsters, estrogens modulate circadian locomotor rhythms by shortening the free-running period and advancing the phase angle of entrainment (Morin et al., 1977). Ovariectomy also reduces the amount of daily activity in rats, hamsters, and mice (Morin et al., 1977; Ogawa et al., 2003). Treatment with estrogen restores the activity levels to normal. Estrogen also modulates overall locomotor activity levels in males as well (Ogawa et al., 2003). Treatment with estrogen reduces the number of rhythm desynchronizes in ovariectomized female hamsters housed in constant light, but no effect of either testosterone or estrogen is seen in males (Morin and Cummings, 1982). Furthermore, the effects of activity on circadian rhythmicity are well known, and it is likely that a component of the estrogenic effect on circadian timing is a result of indirect activity effects that can then modulate rhythmicity. Despite the extensive investigations, the effects of estrogen on mechanisms underlying the entrainment of SCN activity to changes in light/dark cycles remain undetermined. Advances in the onset of light increase SCN expression of transcription factors like c-

fos, early growth response protein-1 (egr-1), and phosphorylated cAMP response element (pCREB) (Aronin et al., 1990; Gau et al., 2002). Also, light modulates the expression of the CREB binding protein (CBP) and calbindin-D (28K) (Gau et al., 2002). These transcription factors thought to be the key players in the entrainment of biological rhythms within the SCN. Light-induced changes in SCN expression of these intracellular and nuclear proteins correlate with light-induced changes in behavioral and physiological rhythms. Furthermore, estrogen modulates SCN expression of cell surface proteins, which are also important in the generation of the biological rhythms (Shinohara et al., 2002).

Estrogen may excite its effect directly and/or indirectly on the neurons in the biological clock. The estrogen's effect on the induction of transcription factors in the SCN may occur by a direct action of estrogen on ER $\beta$  receptors located in the SCN and/or IGL (Shughrue et al., 1997; Su et al., 2001). However, SCN appears to be minor target for estrogen (Shughrue et al., 1997). Alternatively, estrogen could act at other ER-rich brain sites that project to the SCN to modulate the expression of light-induced gene transcription in the SCN such as preoptic area, corticomедial amygdala, bed nucleus of the stria terminalis, and arcuate nucleus and the raphe nuclei. The serotonin (5-HT) neural system in the midbrain raphe may be a good candidate in modulating the effects of estrogen on the biological clock for many reasons. First, the dorsal raphe nucleus (DRN) receives direct projections from the retina (Shen and Semba, 1994). Second, the DRN and median raphe nucleus (MRN) contain both ER $\alpha$  and  $\beta$  (Leranth et al., 1999; Shughrue et al., 1997; Mitra et al., 2003). Finally, the raphe releases 5-HT into the SCN to regulate circadian rhythms (Pickard et al., 1996; Pickard and Rea, 1997; Meyer-Bernstein and Morin, 1999; Morin, 1999). Alternatively, estrogenic effects on circadian rhythms could be a result of indirect actions of estrogens on SCN afferents as well as through the effects of general activity on the circadian clock. Based on these evidences, it is plausible that estrogen enhances light-induced transcription in the SCN indirectly by modulating 5-HT release from the raphe into the SCN.

## 2. HYPOTHESIS

It is well known, that the estrogen has a significant role in the neural control of energy homeostasis and circadian rhythms. However, the mechanisms underlying these effects are poorly understood. The aim of our research, therefore, was to explore the inter- and intra-cellular mechanisms by which the estrogen's effect is translated to appropriate neuronal responses in the hypothalamus.

*Hypothesis 1.* The estrogen's antiobesity effect is mediated through rapid synaptic changes of the hypothalamic feeding circuits independently from leptin. Thus, the synaptic plasticity is an inherent element in the hypothalamic regulation of energy homeostasis. We sought to test this hypothesis by determining the followings:

1. To test the effect of estrogen on synaptology of hypothalamic feeding circuits, whether the estrogen reorganizes the synapses of hypothalamic melanocortin cells.
2. To investigate the type of the excitatory synapses on POMC perikarya.
3. To study whether estrogen enhances the activity of POMC neurons.
4. To demonstrate the effect of estrogen on the synaptology of POMC neurons under physiological conditions as well.
5. To elucidate the relationship between synaptic changes and energy homeostasis by studying the dynamics of feeding behavior and synaptic rewiring induced by estrogen.
6. To determine whether estrogen-induced synaptic changes on POMC neurons are reflected at the electrophysiological level.
7. To test whether the estrogen-triggered anorexigenic behavior is independent of leptin.
8. To study whether estrogen mimics leptin's effect on the rewiring of POMC cells and enhancing their tone.

9. To demonstrate whether estrogen is able to acutely activate the downstream target of leptin signaling, STAT3, independent of leptin in the hypothalamus.
10. To test the role of ER $\alpha$  in the estrogen's antiobesity effect.

*Hypothesis 2.* The locally formed estrogen's organizational/developmental effect on the biological clock is responsible for the sexually dimorphism of the adult SCN and IGL, and it is taking place mostly late prenatally at the peak of aromatase activity in the brain.

We sought to test this hypothesis by determining the followings:

1. To test, whether the number and the distribution of SCN and IGL neurons, which are newly originated during the late prenatal period, are gender specific.
2. To study, whether the testosterone treatment during the late prenatal period alters the number and distribution of the newly originated cells in the SCN and IGL of both genders through aromatisation.
3. To investigate the phenotypical characterization of these newly originated cells in the SCN and IGL.

*Hypothesis 3.* Estrogen modulates the light-induced activity of SCN and IGL neurons in adulthood either directly and/or indirectly through the raphe serotonin system and therefore, estrogen is important for optimal responses of the biological clock to changes of photic conditions. We sought to test this hypothesis by determining the followings:

1. To test, whether estrogen modulates the light-induced expression of various transcription factors in the SCN or in the IGL.
2. To demonstrate, whether light enhances the activity of the neurons in the raphe nuclei and whether this effect is modulates by estrogen.

### **3. MATERIALS AND METHODS**

#### **3.1. Experiment 1; estrogen's effect on the energy homeostasis**

##### **3.1.1. Animals**

All together, eight different types of rodents were used in this experiment.

*Rats.* Female Sprague Dawley rats were delivered by Charles River Farms (Kingston, NY, USA). Male Sprague Dawley rats with intracerebral ventricular cannula were from Taconic Farms (Germantown, NY, USA).

*Mice.* The male and female *ob/ob* and *db/db* transgenic mice on a C57BL/6 background as well as wild-type mice were purchased from Jackson Laboratory (Bar Harbor, ME, USA). The brain-specific STAT3-knockout mice were generated by crossing nestin-cre mice (B6.Cg(SJL)-TgN(Nes-cre)1Kln) to a conditional STAT3 allele 21. The ER $\alpha$ -knockout (-null) mice were from the colony of D.T.-A. at Columbia University (New York, NY, USA). POMC-green fluorescent protein (GFP) mice were from Dr. Jeffrey Friedman's laboratory, Rockefeller University (New York, NY, USA). This transgenic mouse line with a POMC promoter-derived green fluorescent protein (POMC-GFP) transgene is established with more than 95% of the POMC neurons expressing GFP (Pinto et al., 2004).

All animals were kept under standard laboratory conditions with tap water and lab chow available ad libitum with monitored food intake in a 12- hour (h) light/dark cycle (lights on from 6:30 to 18:30). All procedures were in accordance with USA National Institutes of Health animal care guidelines and were conducted with the approval of the Yale University Animal Care and Use Committee.

##### **3.1.2. Surgical and hormonal manipulations**

*Rats.* Ten-week-old wild type female rats were ovariectomized (OVX) under general anesthesia (ketamine, 100 mg/kg; xylazine, 5 mg/kg; intraperitoneally). Two weeks after OVX, rats were implanted with silastic capsules (Dow Corning, Midland, MI, USA)

filled with crystalline 17- $\beta$ -estradiol (E2; Sigma-Aldrich, St Louis, MO, USA; n = 6). Controls received empty implants (n = 6). Capsules were 0.5 cm in length with an internal diameter of 1.98 mm and were placed subcutaneously in the intrascapular space under ether anesthesia. This hormone treatment has been shown to elevate plasma levels of estradiol within physiological ranges and to produce daily LH surges in OVX female rats (Legan and Karsch, 1975). These animals were sacrificed three days after treatment and were used to investigate the synaptic changes in the ARC.

Another set of OVX female rats were received a single subcutaneous injection of either 50 mg E2 solved in 0.1 ml ethanol or only vehicle for control (n = 5 per group). These animals for killed four hours after the treatment and examined for c-Fos immunoreactivity. The Sprague-Dawley male rats with intracerebral ventricular cannula were used for the studies investigating the dynamics of synaptic rewiring induced by E2. Water-soluble E2 (cyclodextrin-encapsulated 17- $\beta$ -estradiol, 2  $\mu$ g in 4  $\mu$ l saline; Sigma-Aldrich, St Louis, MO, USA) was infused into the third ventricle through the intracerebral ventricular cannula of these rats (n = 7). Food intake was measured 4 h and 14 h after E2 infusion. Another set of these animals were used to study the parvalbumin expression 6 h after third ventricle E2 infusion.

*Mice.* The male and female *ob/ob* and *db/db* mice (n = 6 each group) were also implanted with silastic capsules in a similar fashion (0.5 cm in length with an internal diameter of 1.98 mm filled with E2 or empty for controls under ether anesthesia) and were kept for four weeks to investigate the estrogen's effect on food intake/energy expenditure.

For the immunoblotting studies wild-type and *ob/ob* mice were treated with a single intraperitoneal injection of water-soluble E2 (cyclodextrin-encapsulated 17- $\beta$ -estradiol, 2  $\mu$ g in 4  $\mu$ l saline; Sigma-Aldrich, St Louis, MO, USA; 200  $\mu$ g/kg) or saline for control. Animals were sacrificed 0, 15, 30, 60, 90, 120 or 150 min after treatment respectively, and their hypothalami were used to investigate the E2-induced STAT3 phosphorylation (n = 2-4 each group).

The brain-specific STAT3-knockout and the ER $\alpha$ -knockout male mice were treated with E2 capsules a similar fashion (n = 6 per group).

The POMC-GFP mice, these animals were used for fluorescence microscopy the electrophysiological studies, were also OVX and treated with E2 as described above (n = 6 per group).

### **3.1.3. Determination of estrus cycle**

Wild-type female rats that exhibited three consecutive normal estrus cycles were used. The days of the estrus cycle - that is, metestrus, diestrus, proestrus and estrus - were determined by microscopic examination of vaginal smears. Groups (n = 5 per group) of animals were killed at 18:00 o'clock on each day of the cycle and were processed for electron microscopic analyses of POMC perikaryal synapses.

### **3.1.4. Energy expenditure, respiratory quotient, lean body mass, body composition and nose-anal length**

Energy expenditure (EE) and respiratory quotient (RQ) were determined using a comprehensive mouse metabolic monitoring system (Oxymax calorimeter, Columbus Instruments). A 24-h, automated, noninvasive collection of metabolic and behavioral parameters was performed on male ob/ob mice (n = 4). The rates of oxygen consumption (VO<sub>2</sub>) and carbon dioxide production (VCO<sub>2</sub>) were determined. RQ was calculated as the ratio of VCO<sub>2</sub> to VO<sub>2</sub>. Energy expenditure was calculated as  $EE = VO_2 \times (3.815 + 1.232) \times RQ$ . Rectal body temperature was measured using a mouse Type T thermometer probe (Model BAT-12, Physitemp Instruments, Clifton, NJ, USA). Petroleum jelly was used to protect the animals. The lean body mass was assessed after anatomical preparation of the torsos of the animals. The body composition was measured by standard MRI technology and reported in grams. The body length (nose to anus, measured in cm) was determined with a linear ruler after the animals were killed.

### **3.1.5. Fixation and tissue preparation**

Animals for immunocytochemistry were perfused transcardially under deep anesthesia with ketamine (100 µg/kg body weight) and xylazine (10 µg/kg body weight) with 100

(rats), or 30 ml (mice) of isotonic heparinized saline, followed by 250 ml (rats) and 60 ml (mice) of fixative (4% paraformaldehyde, 15% picric acid and 0.1% glutaraldehyde in 0.1 M sodium phosphate buffer (PB, pH 7.3). The brains were dissected out and post-fixed for an additional 12 h in the same fixative at 4°C. Subsequently, the brains were rinsed in several changes of PB, and 50 µm coronal sections were cut on a vibrotome (Lancer, St Louis, MO, USA) at room temperature (RT). The brain sections containing the ARC were selected using the Paxinos and Watson rat and mice atlases (Paxinos and Watson, 1998) (**Figure 1**) were collected in vials, washed several times and stored in 0.02% sodium azide in PB at 4°C until immunocytochemistry was conducted.

The POMC-GFP animals - which were for electrophysiological studies - were deeply anesthetized with halothane and decapitated without fixation.

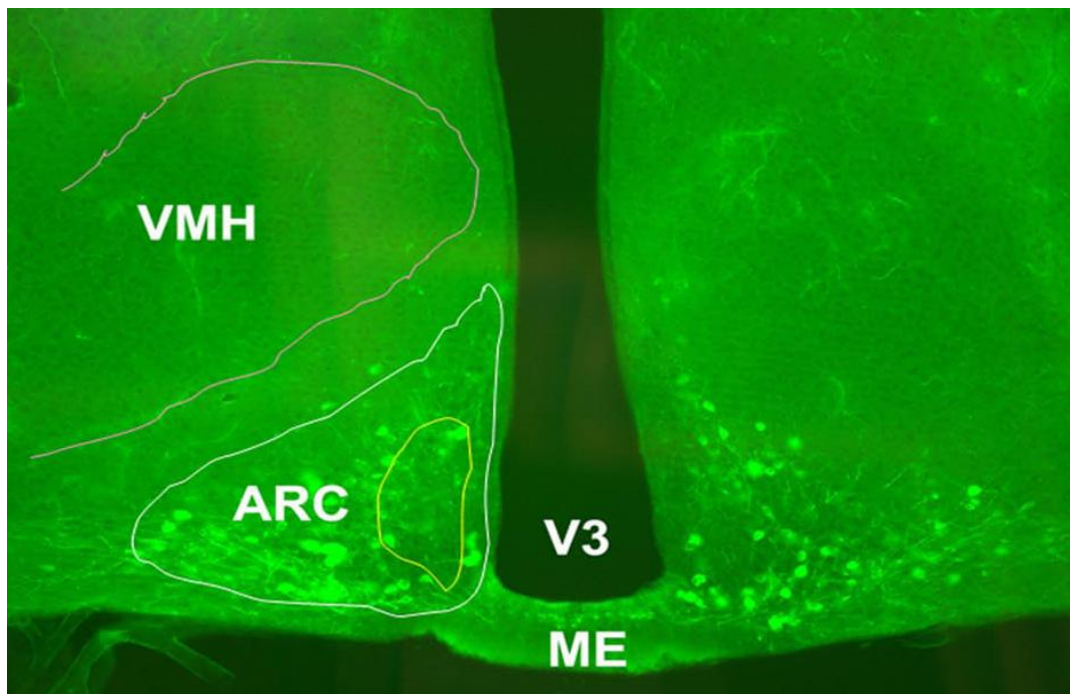


**Figure 1.** Proopiomelanocortin (POMC) neurons in the arcuate nucleus (ARC). GFP (green fluorescent protein)-labeled POMC neurons of the ARC are encircled by the white line delineating the ARC. The neuropeptide Y (NPY) neurons tend to localize within more medial portion of the ARC (circled in yellow, no staining), with a significant degree of overlap between the two populations. The ventromedial hypothalamus (VMH), the „satiety center” also plays an important role in the central regulation of energy homeostasis. ME=median eminence; V3=third ventricle; VMH=ventromedial hypothalamus.

### **3.1.6. Immunocytochemistry**

*Single labeling immunostaining for POMC.* Sections containing the ARC were rinsed in PB followed by 30 min incubation in a 1% hydrogen peroxide solution to remove endogenous peroxidase activity. After several rinses in PB, tissue sections were incubated at RT in blocking solution containing 3% normal goat serum (Vector Laboratories, Burlingame, CA, USA), 1% bovin serum albumin (Sigma-Aldrich, St. Louis, MO, USA) and 0.3% Triton X-100 for 1 h followed by incubation in primary antibody polyclonal rabbit anti-beta-endorphin at a dilution of 1:50,000 for 48 h at -4°C. After several washes sections were incubated in a solution containing 1:200 dilution of biotinylated goat anti-rabbit IgG secondary antibody (Vector Laboratories, Burlingame, CA, USA) for 2 hr at RT. Following several washes in PB, sections were incubated with avidin-biotin-horseradish peroxidase complex (ABC; Vectastain Elite ABC kit, Vector Laboratories, Burlingame, CA, USA), in 1:200 dilution in PB at RT for an additional 90 min. After adequate washing, the tissue-bound peroxidase were visualized by a nickel-diaminobenzidine reaction (NiDAB; 15 mg DAB, 6.5 mg ammonium chloride, 780 µl of nickel ammonium sulfate, 16 ml PB, and 425 µl of 0.03% hydrogen peroxidase) at room temperature for several minutes resulting in a black reaction product. The reaction was stopped by rinses in PB. The sections were mounted on gelatin-coated slides, dehydrated, cleared in xylene and coverslipped using DePex mounting medium (Electron Microscopy Sciences, Washington, PA, USA) either for electron microscopic or light microscopic analysis.

For fluorescence microscopy the POMC-GFP mice brain slices were incubated with Alexa Fluor secondary antibody conjugates (Molecular Probes, Carlsbad, CA, USA) for 2 h at RT. The tissue was then mounted on slides, coverslipped with anti-fade media and stored at 4°C until analysis was performed.

*Double labeling immunostaining for Fos, Parvalbumin, GluR1, and GluR2.* Selected sections were processed for double labeling immunocytochemistry. First washed and then incubated with 1% hydrogen peroxide solution for 10 min at RT to remove excess peroxidase activity. Sections were then incubated in a mixture of 3% normal goat serum

(Vector Laboratories, Burlingame, CA, USA), 1% bovine serum albumin (Sigma-Aldrich, St. Louis, MO, USA) and 0.3% Triton X-100 as blocking agent diluted in PB for 30 min also at RT. Subsequently, the sections were incubated in the primary antisera (c-Fos, rabbit antibody to human Fos, AB-5, diluted 1:50,000, Oncogene Research Products, San Diego, CA, USA; mouse anti-parvalbumin antibody, diluted 1:2,000, Sigma, St. Louis, MO, USA; GluR1 and GluR2 rabbit antisera diluted 1:500, Chemicon, Billerica, MA, USA) for 24 h at RT. After this, the tissue was incubated in a solution containing the adequate biotinylated secondary antibody IgG, Vector; 1:200 in PB, Vector Laboratories, Burlingame, CA, USA) followed by ABC (Vector Elite Kit; 1:200, Vector Laboratories, Burlingame, CA, USA), for 2 and 1.5 h, respectively, at RT. The double labeling immunostaining was visualized by a diaminobenzidine reaction (5 mg DAB, 9 mL PB and 250  $\mu$ L 1% hydrogen peroxide) resulting in a light brown reaction product. The colors of the two reaction products were readily distinguishable. The reaction was terminated after 2 min for all antisera by a thorough wash of the tissue sections. Between each incubation step, sections were properly washed (four times for 10 min each). All the sections were mounted on gelatin-coated slides, dehydrated, cleared in xylene and coverslipped using DePex mounting medium (Electron Microscopy Sciences, Washington, PA, USA).

In control double immunostaining experiments, in which one of the primary antisera was replaced with normal serum, only single immunostaining could be detected. Experiments to control the specificity of the antisera included preabsorption of the various antisera with their target peptide, or peptide sequence and elimination of the secondary or primary antisera from the incubating solution.

### **3.1.7. Image analysis for light and fluorescence microscopy**

For light microscopic evaluation pictures were captured using a Zeiss Axiophot microscope (Zeiss, Oberkochen, Germany), for fluorescence microscopy the sections were visualized under a Zeiss Axioplan 2 fluorescent microscope (Zeiss, Oberkochen, Germany). Subsequently these pictures were imported into the Scion Image analysis

system. The tissue sections were coded then the cell counts were performed without prior knowledge of the experimental treatments by two independent raters.

### **3.1.8. Electron microscopy and and postembedding immunostaining**

After the immunostaining sections were postosmicated (1% OsO<sub>4</sub> in PB) for 30 min, dehydrated through increasing ethanol concentrations (using 1% uranyl acetate in 70% ethanol for 30 min), flat embedded in Durcupan (ACM/Fluka; Sigma-Aldrich, St Louis, MO, USA), Electron Microscopy Sciences, Fort Washington, PA, USA) between liquid release-coated slides (Electron Microscopy Sciences), and placed in an oven at 60°C for 48 h. After capsule embedding, blocks were trimmed and cut on a Reichert-Jung ultramicrotome (Leica, Deerfield, IL, USA) collected on Formvar-coated single-slot grids and analyzed with a Tecnai 12 Biotwin (FEI Company, Hillsboro, OR, USA) electron microscope.

*Postembedding immunostaining for GluR1, GluR2, Glutamate and GABA.* Ribbons of ultrathin sections were collected on filtered solutions (Millipore, Bedford, MA, USA) in humid chambers and processed as follows: 1) 10 min in periodic acid; 2) rinse in double distilled water (DDW); 3) 10 min in 2% sodium metaperiodate in DDW; 4) rinse in DDW; 5) three 2-min rinses in Tris-buffered saline (TBS), pH 7.4; 6) 30 min in ovalbumin in TBS; 7) three 10-min periods in normal goat serum in TBS; 8) first incubation for 1-2 h in rabbit anti-GluR1 and GluR2 (Chemicon, Billerica, MA, USA) diluted 1:500, or in rabbit anti-GABA (Incstar, Stillwater, MN) diluted 1:200, or in rabbit anti-glutamate (Abcam, Cambridge, MA, USA) diluted 1:100; 9) two 10-min washes in TBS and a 10-min rinse in 0.05 M Tris buffer (pH 7.5) containing gold-conjugated goat antirabbit IgG (Amersham, Piscataway, NJ, USA) diluted 1:10 in the same buffer; 10) two 5-min washes in DDW; and 11) contrasting with saturated uranyl acetate (30 min) and lead citrate (20-30 seconds). Ultrathin sections were then examined using a Tecnai 12 Biotwin (FEI Company, Hillsboro, OR, USA) electron microscope. This approach has been widely used for postembedding labeling of GABA and glutamate.

### 3.1.9. Quantitative synaptology

The quantitative analysis of synapse numbers was performed in a double-blind fashion on electron micrographs from rats and mice of different experimental groups. To obtain a complementary measure of axo-somatic synaptic number, unbiased for possible changes in synaptic size, the disector technique was used. On consecutive 90-nm-thick sections, we determined the average projected height of the synapses and used about 30% of this value as the distance between the disectors. On the basis of this calculation, the number of axo-somatic synapses was counted from 7 perikaryal profiles in two consecutive serial sections roughly 270 nm apart (the "reference" and "look-up" sections) from each tissue block. In order to increase the sampling size, the procedure was repeated in such a way that the reference and look-up sections were reversed. The number of symmetrical, asymmetrical and the total contacts were collected independently from serial sections. Synapse characterization was performed at 20,000x magnifications, while all quantitative measurements were performed on electron micrographs at a magnification of 11,000. Symmetric and asymmetric synapses were counted on all selected neurons only if the pre- and/or postsynaptic membrane specializations were clearly seen and synaptic vesicles were present in the presynaptic bouton. Synapses with neither clearly symmetric nor asymmetric membrane specializations were excluded from the assessment. The plasma membranes of selected cells were outlined on photomicrographs and their length was measured with the help of a chartographic wheel. Plasma membrane length values measured in the individual animals were added and the total length was corrected to the magnification applied. Synaptic densities were evaluated according to the formula  $NV=Q/Vdis$  where  $Q$ - represents the number of synapses present in the "reference" section that disappeared in the "look-up" section.  $Vdis$  is the disector volume (volume of reference) which is the area of the perikaryal profile multiplied by the distance between the upper faces of the reference and look-up sections, i.e. the data are expressed as numbers of synaptic contacts per unit volume of perikaryon. Section thickness was determined by using the Small's minimal fold method. The synaptic counts were

expressed as numbers of synapses on a membrane length unit of 100  $\mu\text{m}$ . The morphometric analysis was carried out in a blinded fashion.

### **3.1.10. Immunoblotting**

E2-treated hypothalami of *ob/ob*, and wild-type mice were collected at desirable time points and homogenized in the immunoprecipitation lysis buffer by sonication. The lysates were centrifuged at 4°C for 10 min at 13,000g, and supernatants were assayed for protein content (Pierce Chemical, Rockford, IL, USA). The samples were separated using sodium dodecyl sulfate polyacrylamide gel electrophoresis (SDS-PAGE), transferred to polyvinylidene difluoride membranes and incubated with antibody to pSTAT3 (Y705), antibody to STAT3 (Cell Signaling Technology, Beverly, MA, USA) and horseradish peroxidase (HRP) -conjugated donkey antibody to rabbit IgG (Jackson ImmunoResearch Laboratories, West Grove, PA, USA). The blots were visualized using chemiluminescent substrate (SuperSignal; Pierce Chemical, Rockford, IL, USA).

### **3.1.11. Electrophysiology**

Adult POMC-GFP mice were deeply anesthetized with halothane prior to decapitation and removal of the entire brain. The brain was immediately submerged in ice cold, carbogen-saturated (95% O<sub>2</sub> and 5% CO<sub>2</sub>) artificial cerebrospinal fluid (aCSF), and a brain block containing the hypothalamus was made. The aCSF contained (in mM): 126 NaCl, 2.5 KCl, 2.4 CaCl<sub>2</sub>, 1.2 NaH<sub>2</sub>PO<sub>4</sub>, 1.2 MgCl<sub>2</sub>, 21.4 NaHCO<sub>3</sub>, and 11.1 glucose. Coronal sections (180  $\mu\text{m}$ ) were cut with a vibrotome (Lancer, St Louis, MO, USA), and the slices were incubated at 37°C for approximately 30 min followed by incubation at RT until used. Slices were transferred to the recording chamber and allowed to equilibrate for 10-20 min prior to use. The slices were bathed in oxygenated aCSF heated to approximately 29-30°C at a flow rate of 1.7-2 ml/min. GFP-positive POMC cells in the ARC were visualized using epifluorescence and IR-DIC imaging on an upright Zeiss Axioskop 2FS Plus microscope (Zeiss, Oberkochen, Germany) equipped with a fixed stage and a Sony XC-75 CCD camera. Filter sets were from Chroma Technology Corp

(Rockingham, VT, USA). The characteristics of the filter sets were as follows (values are exciter, emitter, beamsplitter): Topaz GFP (POMC) HQ500/20, HQ535/30, Q515lp. GFP neurons were identified via epifluorescence and then patched under IR-DIC optics. Recordings were made using a HEKA EPC9/2 amplifier under the control of Pulse software. Cells were voltage clamped at -60 mV, and sampled at a frequency of 20 kHz. Currents were recorded for 1 second every 3 seconds, and postsynaptic currents (PSCs) were detected using the MiniAnalysis Program. The frequency of PSCs was then calculated at either 15-second intervals or for 3-min periods before and after tetrodotoxin (TTX) addition. All membrane potentials reported were not corrected for liquid junction potentials. For measurement of excitatory postsynaptic currents (EPSCs), a cesium-methanesulfonate based internal solution (in mM: 125 CsMeSO<sub>3</sub>, 10 CsCl, 5 NaCl, 10 HEPES, 1 EGTA, 2 MgCl<sub>2</sub>, 5 MgATP, 0.3 NaGTP, pH~7.35 with NaOH) was used, and picrotoxin (100 μM) was added in the bath to block inhibitory postsynaptic currents (IPSCs). Electrodes had resistances of ~2.7-3.3 MΩ when filled with the Cs-Methanesulfonate internal solution and ~1.8-2 MΩ when filled with the CsCl internal solution. Series resistance was monitored over the course of the recordings, and values were generally <10 MΩ and were not compensated. Cells were excluded if the series resistance increased significantly during the experiment. TTX (1 μM) was added in the bath to isolate miniature PSCs. Data analysis was performed using PulseFit, IgorPro, Microsoft Excel, and S-Plus. All figures were created using PulseFit and IgorPro.

## **3.2. Experiment 2; estrogen's effect on the biological clock during early development**

### **3.2.1 Animals**

Timed-pregnant female Sprague-Dawley rats were purchased from Charles River Farms (Kingston, NY, USA) 10 days into their pregnancy (embryonic day 10) with embryonic day 1 being the day on which mating was verified by the supplier. Animals were kept under standard laboratory conditions, with tap water and regular rat chow available *ad libitum*, in a 12-h light/dark cycle (lights on from 6:30 to 18:30). The pregnant rats were housed individually in plastic cages during the pregnancy and remained with their pups for 21 days after giving birth. At that time, pups were weaned from their mothers. The day of birth of the pups was considered as day 0 of postnatal life. The pups in each litter were weighed and examined for presence of any abnormality and kept until they were 60 days old, when they were killed. All procedures used in this study were in accordance with USA National Institutes of Health animal care guidelines and were conducted with the approval of the Yale University Animal Care and Use Committee.

### **3.2.2. Hormon treatment, mitotic marker injection and tissue preparation**

Five pregnant rats received daily subcutaneous injections of testosterone propionate (TP; 10 mg/0.1 mL sesame oil; Sigma-Aldrich, St Louis, MO, USA) from the 15th day of gestation until giving birth. Five other pregnant rats received injections with vehicle alone on the same days. All pregnant rats received a single intraperitoneal injection of a mitotic marker 5-bromo-2'-deoxyuridine (BrdU, 50 mg/kg body weight; Sigma-Aldrich, St Louis, MO, USA) on the 18th day of gestation (embryonic day 18). This particular treatment has been used previously to label mitotic cells in developing fetuses given that BrdU crosses the placental barrier and incorporates into the mitotic cells (al-Shamma and De Vries, 1996). Sixty days following their birth, male and female pups treated with oil or testosterone during gestation were randomly selected to be killed. The fixation, the cutting and the tissue handling were performed as described above in Experiment 1.

### **3.2.3. Immunocytochemistry and immunofluorescence**

*Single labeling immunostaining for BrdU.* Immunostaining for BrdU was performed in all sections containing the SCN and IGL. Sections were selected using the Paxinos and Watson rat brain atlas (Paxinos and Watson, 1998). The immunostaining was performed as described above in Experiment 1 using an overnight incubation in BrdU antisera (mouse monoclonal; Becton Dickinson, San Jose, CA, USA; 1:500) at RT and the tissue-bound peroxidase was visualized by a nickel-diaminobenzidine reaction at RT for 4 min, resulting in a black reaction product.

*Double labeling immunostaining.* To investigate the phenotypical characterization of these newly originated BrdU-stained cells, selected sections were processed for double labeling immunocytochemistry using with primary antisera for AVP, GFAP, calbindin-D (28K) and VIP utilizing the previously described methods (rabbit polyclonal anti-AVP, ICN Biochemicals, Irvine CA, USA, 1:5000; mouse monoclonal anti-calbindin-D (28K), Sigma-Aldrich, St Louis, MO, USA, 1:5000; rabbit polyclonal anti-GFAP, Sigma-Aldrich, St Louis, MO, USA, 1:4000, or rabbit polyclonal anti-VIP, ImmunoStar, Hudson, WI, USA; 1:10000) for 24 h at RT. After this, the tissue was incubated in the appropriate secondary antibody (biotinylated goat anti-rabbit IgG, Vector; 1:200 in PB for the polyclonal IgGs; biotinylated horse anti-mouse IgG, Vector; 1:200) followed by ABC (Vector Elite Kit; 1:200), for 2 and 1.5 h, respectively, at RT. The double labeling immunostaining was visualized by a diaminobenzidine reaction resulting in a light brown reaction product as previously described.

*Immunofluorescence staining.* Additional sections from the same animals were processed for immunofluorescence detecting BrdU and GFAP or VIP. In these protocols, tissue sections were incubated in the primary antisera for BrdU and VIP, or BrdU and GFAP, except that the antibody solutions were five times more concentrated than in the protocols in which diaminobenzidine was used as a chromagen. Twenty-four hours later, tissue was incubated in a solution containing Texas-red-conjugated anti-rabbit plus fluorescein-conjugated anti-mouse IgG (Vector; 1:200) for 2 h at RT. The tissue was then mounted

on slides, coverslipped with anti-fade media and stored at 4°C until analysis was performed.

*Image analysis.* Following immunocytochemistry, the coding of tissue sections, the capturing of pictures (light and fluorescence) and the analyzing of images were performed as describes above in Experiment 1. The boundaries of the SCN and IGL were determined using archived NPY-stained (rabbit anti NPY; Bachem, Budendorf, Switzerland) sections overimposed on immunostained images (**Figure 2**).

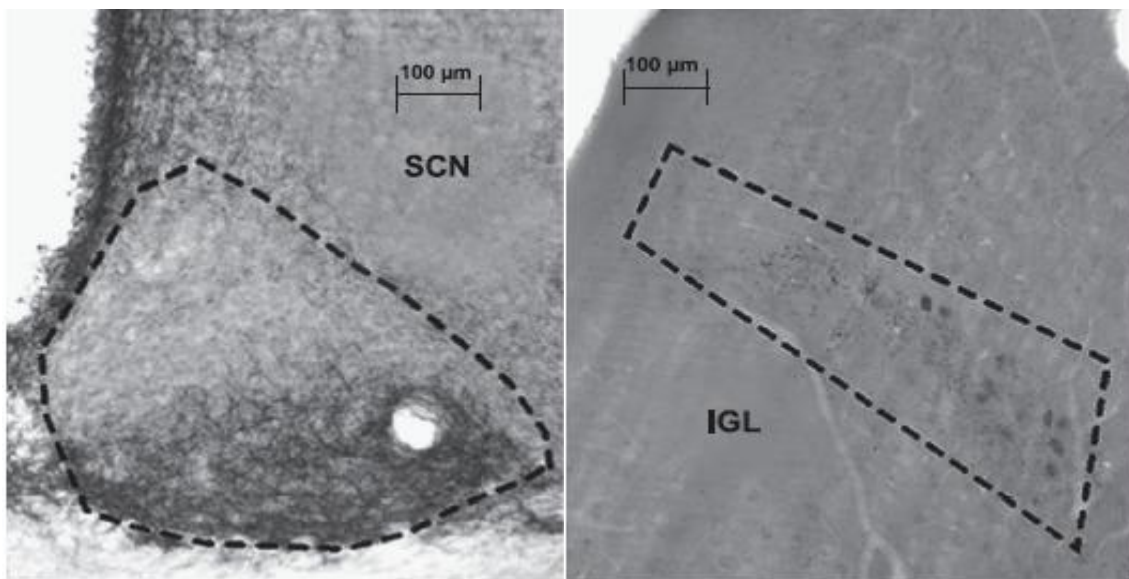


**Figure 2.** Representative pictures of the SCN (left panel) and IGL (right panel) immunostained for neuropeptide Y (NPY; rabbit anti-NPY 1:10,000, Bachem, Budendorf, Switzerland). As seen in this figure, NPY fibers densely enervate the ventral portion of the SCN and, to a lesser degree, the area dorsal to the dorsal SCN portion. The dorsal portion of the SCN, however, receives few NPY fibers. Similarly, NPY cell bodies are found in the IGL, but not in the adjacent lateral and dorsal geniculate bodies. These features allow for a specific delineation of the SCN boundaries. SCN=suprachiasmatic nucleus, IGL=intrageniculate leaflet.

A criterion was established so as to count only those cells with the densest staining. To do this, we quantified the degree of staining that was seen in the background of each individual section, and that seen in the cells showing the darkest labeling. It was then decided that cells would only be considered as densely stained if they attained a degree of staining that was 80% above that seen in the background. This particular procedure was

established to ensure that the raters were only counting cells in the surface of the section. Cell counts were performed by two independent raters, neither of whom was aware of the treatment group from which each animal came.

### **3.3. Experiment 3; estrogen's effect on the biological clock during adulthood**

#### **3.3.1. Animals**

Female Sprague Dawley rats (240-260g) were purchased from Charles River Farms (Kingston, NY, USA). Animals were kept under standard laboratory conditions, with tap water and regular rat chow available ad libitum, in a 12-h light/dark cycle (lights on from 06:30 to 18:30). Animals were group housed in plastic cages with no more than three animals per cage. Animals were acclimated to these housing conditions for 2 weeks before any experimental manipulation. All procedures in this study were also in accordance with USA National Institutes of Health animal care guidelines and were conducted with the approval of the Yale University Animal Care and Use Committee.

#### **3.3.2. Surgical and hormonal manipulations**

Female rats were OVX under general anesthesia (ketamine, 100 mg/kg; xylazine, 5 mg/kg; intraperitoneally). Two weeks after ovariectomy, rats were implanted with silastic capsules (Dow Corning, Midland, MI, USA) filled with crystalline E2 (Sigma-Aldrich, St Louis, MO, USA). Controls received implants with cholesterol (Sigma-Aldrich, St Louis, MO, USA). Capsules were 0.5 cm in length with an internal diameter of 1.98 mm and were placed subcutaneously in the intrascapular space under ether anesthesia.

#### **3.3.3. Light shifting procedures**

The light shifting procedures were initiated 48 hours following the capsule implantations. Animals (n = 24) were randomly assigned to four groups (n = 6 per group) according to the hormone treatment which they received and the manipulation of the light/dark cycle. The time at which the lights were turned on in the animal colony was termed Zeitgeber time (ZT) 0. A set of E2-treated and control animals was assigned to be killed at ZT1 to detect the expression of transcription factors that is induced by the regular onset of light within the colony. A second set of E2-treated and control animals was exposed to light at

ZT22, 2 h earlier than the regular onset of light, and was killed 1 h later at ZT23. The intensity of the light stimulus was measured at 300 lux in the colony rooms.

### **3.3.4. Fixation and tissue preparation**

Animals were deeply anesthetized with ether and perfused transcardially with 100mL of isotonic heparinized saline followed by 250 mL of fixative. The fixative consisted of 4% paraformaldehyde and 15% picric acid in 0.1 M sodium phosphate buffer (PB, pH 7.3). The brains were dissected out, postfixed for an additional 2 h in the same fixative at 4°C and immersed in a 30% sucrose solution for 48 h for cryoprotection. After rapid freezing, 30- $\mu$ m coronal sections were cut on a cryostat (CM3050S; Leica Microsystems, Nussloch, Germany) at -20°C to obtain sections across the rostrocaudal extent of SCN (from -0.94 to -1.4 mm from Bregma) and IGL (from -4.16 to -4.80 mm from Bregma) and the raphe nuclei (from -7.30 to -9.00 mm from Bregma) using a standard rat brain atlas (Paxinos and Watson, 1998). Six sets of serial sections were washed several times and placed in Watson anti-freeze solution (30% sucrose, 30% ethylene glycol in 0.1 M PB). Sections were stored at -20°C until immunohistochemistry was conducted.

### **3.3.5. Immunocytochemistry**

*Single labeling immunostaining in the SCN and IGL.* Sections containing the SCN and the IGL from each animal were processed for immunocytochemistry using antibodies that detect the Fos, pCREB, egr-1, CBP, and calbindin-D (28K) proteins (**Table 1**) using standard protocols - as described above in Experiment 1 - with a nickel-diaminobenzidine reaction resulting in a black reaction product.

*Single labeling immunostaining in the DRN and MRN for Fos and 5-HT.* Brain sections from a one in six series from each animal containing the DRN and MRN were processed for Fos immunoreactivity (rabbit anti Fos AB-5, Oncogene, Cambridge, MA, USA, 1:50,000) following a standard protocol as described previously resulting in a black reaction product using nickel–diaminobenzidine reaction. To demonstrate the distribution

of 5-HT neurons within the raphe nuclei a single immunostaining was performed using rabbit anti 5-HT antibody (Millipore, New York, NY, USA; 1:40,000).

**Table 1.** List of antibodies used in the SCN and IGL immunostainings.

Antibody	Dilution	Source
Rabbit anti Fos (AB-5)	1:50,000	Oncogene, Cambridge, MA, USA
Rabbit anti P-CREB	1:10,000	Millipore, New York, NY, USA
Mouse anti Calbindin-D	1:5,000	Sigma-Aldrich, St Louis, MO, USA
Rabbit anti egr-1	1:10,000	Santa Cruz Biotechnology, Santa Cruz, CA, USA
Mouse anti CBP	1:1,000	Santa Cruz Biotechnology, Santa Cruz, CA, USA

*Double labeling immunostaining in the raphe nuclei for Fos and 5-HT.* A second set of tissue sections from each animal was first processed for Fos immunocytochemistry and immediately after Fos staining sections were processed for 5-HT immunocytochemistry using the antisera and protocols described previously. Fos-positive cells resulting in a black, the 5-HT cells in a light brown reaction products. Sections were mounted on gelatin-coated slides, dehydrated, cleared in xylene and coverslipped using DePex. The colors of the two reaction products were readily distinguishable. In control double-immunostaining experiments, in which one of the primary antisera was replaced with normal serum, only single immunostaining could be detected. Tissues from every subject were processed simultaneously so that direct comparisons between groups were possible.

### **3.3.6. Image analysis**

After immunostaining, tissue sections containing SCN, IGL, DRN and MRN were coded and then pictures from each section were captured using a Axiophot microscope (Zeiss, Oberkochen, Germany) and imported into the Scion Image computer analysis system. *SCN and IGL.* The boundaries of the SCN and IGL were determined using archived Neuropeptide Y (NPY; rabbit anti NPY; Bachem, Budendorf, Switzerland) stained sections overlaid on immunostained images as shown before (**Figure 2**). A criterion

was established so as to only count cells with the densest staining. To do this, we quantified the degree of staining that was seen in the background of each individual section, and that seen in the cells showing the darkest labeling. It was then decided that cells would only be considered as densely stained if they attained a degree of staining that was 80% above that seen in the background. Cell counts were performed by two independent raters, neither of whom was aware of the treatment group that each animal belonged to and presented by mean number of stained cells per section.

*Raphe nuclei.* The DRN was divided into medial, lateral and caudal components as delineated previously (Jacobs and Azmitia, 1992; Paxinos and Watson, 1998) (**Figure 3**). The medial region of the DRN was further divided into dorsal and ventral components. Nevertheless, data from the dorsomedial and ventromedial regions of the DRN were grouped together into a single data set (medial DRN) given the low number and lack of differences in single or double labelling between these two regions. Similarly, data from the interfascicular DRN were pooled with those of the caudal DRN because of the small number of labelled nuclei and double-labelled cells found within this region. Sections were carefully matched to obtain counts that were anatomically comparable between animals in the different groups. For single label Fos staining, a criterion was established so as to only count cells with the densest staining within a grid of  $300 \times 300 \mu\text{m}$  using image software (NIH, Bethesda, MD, USA). Data from these cell counts are reported as the number of Fos-immunoreactive cells/ $\text{mm}^2 \times 10^2$ . For double-label immunocytochemistry, the total number of 5-HT cells and 5-HT/Fos cells (5-HT cells with a visible dark nucleus) was obtained by visual inspection of high resolution images captured within the same grid as described above. Cell counts of 5-HT cells are reported as the mean number of 5-HT cells/ $10^2 \text{ mm}^2$ . Double-labelled cells are reported as the percentage of 5-HT cells coexpressing Fos [(total double-labelled Fos/5-HT cells/total no. of 5-HT cells)  $\times 100$ ] and the percentage of Fos nuclei within 5-HT neurons [(total no. of double-labelled Fos/5-HT cells/total no. of Fos cells)  $\times 100$ ]. All cell counts were performed by two independent raters, neither of whom was aware of the treatment group that each animal belonged to at the time of quantification.

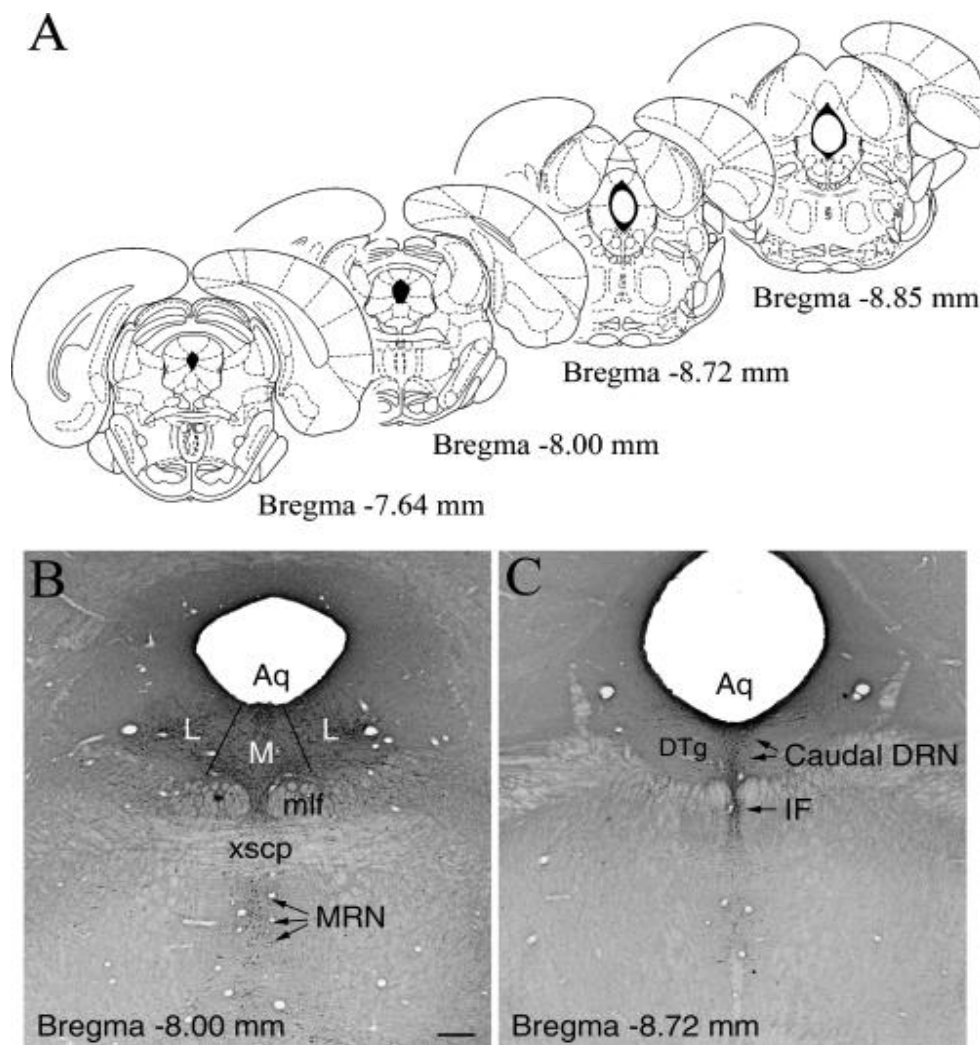


**Figure 3.** Anatomical delineation of the different raphe nuclei analysed in the present study. (A) Representative plates containing the raphe as described by Paxinos & Watson (1998). These sections were used as templates for the selection of sections in the immunocytochemical studies. (B) Representative digitized image of the anterior portion of the dorsal raphe nucleus (DRN) and the median raphe nucleus (MRN). This image depicts how the DRN was subdivided into medial (M) and lateral (L) portions. (C) Representative digitized image of the posterior portion of the raphe pointing to the caudal and interfascicular (IF) DRN. Serotonin immunocytochemistry was used as an aid in the delineation of these regions. Aq=aqueduct; DTg=dorsal tegmental nucleus; mlf=medial longitudinal fasciculus; xscp=decussation superior cerebellar peduncle. Scale bar, 200  $\mu$ m.

Values for each subject are expressed as the mean number of Fos nuclei, 5-HT or Fos/5-HT double-labelled cells within 0.25 mm<sup>2</sup> of each raphe nucleus for each assay. Raphe nuclei are located differently across the rostrocaudal extent of the raphe proper, with the

anterior portion of the raphe (Bregma -7.30 to -8.30 mm) containing both the MRN and the lateral and medial regions of the DRN and the posterior portion (Bregma -8.30 to -9.00 mm) containing the interfascicular and caudal DRN (**Figure 3**). In total, eight to 10 sections across the rostrocaudal extent of the raphe were used for each animal in each assay. Of these, at least six sections contained the medial portion of the DRN, four to five sections contained the lateral portion of the DRN and at least four sections contained the caudal portion of the DRN. At least eight sections per assay were used for quantification of the MRN. The number of sections used for quantification has been commonly used in studies using Fos as a marker for neuronal activation of the raphe in response to different stimuli (Grahn et al, 1999; Greenwood et al, 2003).

### **3.4. Statistical analyses**

All data are presented as mean  $\pm$  s.e.m. The statistical confidence was set at  $P \leq 0.05$  in all three experiments. The morphometric analysis was carried out in a blinded fashion.

*Experiment 1.* Statistical analysis was performed by unpaired t-test when applicable. F-test analysis was used with treatment (estradiol vs. vehicle) as one factor. The Kruskal-Wallis one-way nonparametric analysis of variance was selected for multiple statistical comparisons. The Mann-Whitney U-test was used to determine significance of differences between groups.

*Experiment 2.* Longitudinal data were compared using factorial 2 x 2 analysis of variance (ANOVA) with treatment (testosterone vs. vehicle) as one factor and sex (female vs. male) as the second factor; or 2 x 2 x 2 ANOVA with sex, treatment and SCN regions (core vs. shell). Fisher's LSD post-hoc analyses were performed as post-hoc tests when required.

*Experiment 3.* Factorial 2 x 2 ANOVA was used with treatment (estradiol vs. cholesterol) as one factor and time of light onset (ZT0 vs. ZT22) as the second factor. Fisher's LSD post-hoc analyses were performed as post-hoc tests when required.

## 4. RESULTS

### 4.1. Experiment 1; estrogen's effect on the energy homeostasis

#### 4.1.1. Estrogen increases the number of excitatory synapses on POMC perikarya in wild-type animals

To test the effect of estrogen on synaptology, we first studied axosomatic synapse type and number on POMC perikarya in ovariectomized wild-type female rats. Examination of POMC perikarya of ovariectomized rats revealed that symmetrical, putative inhibitory synapses outnumbered excitatory contacts ( $35.29 \pm 9.04$  versus  $10.75 \pm 4.6$  synapses per 100  $\mu\text{m}$  of perikaryal membrane;  $P < 0.05$ ; **Figure 4a**), whereas estrogen treatment resulted in a dominance of excitatory contacts over inhibitory synapses ( $28.5 \pm 7.25$  versus  $14.33 \pm 3.65$  synapses per 100  $\mu\text{m}$  perikaryal membrane,  $P < 0.05$ ; **Figure 4b**). The shift in synaptic balance on POMC perikarya (**Figure 4c**) with a corresponding decrease in appetite and adiposity is similar to what was previously observed in leptin-treated *ob/ob* mice (Pinto et al., 2004). Pre- and postembedding immunolabeling for GABA and glutamate confirmed that almost all of the asymmetric synapses on POMC perikarya were glutamatergic (**Figure 4d**). Immunocytochemistry further showed that all of the analyzed arcuate POMC neurons contained subunit 1 of the AMPA glutamate receptors (GluR1) (**Figure 4e**), whereas very few expressed GluR2 (**Figure 4f**). The GluR2 was more prominent in other hypothalamic regions, particularly in the dorsomedial hypothalamus (DMH). GluR1 incorporation into synapses is an important mechanism underlying long-term potentiation and experience-driven synaptic plasticity (Ehrlich and Malinow, 2004). GluR1 domination in arcuate POMC neurons predicts an increase in calcium influx upon glutamate binding of the receptor and a specific induction of the calcium binding protein, parvalbumin (Kondo et al., 1997). Thus, we tested whether the increase in the number of excitatory inputs on POMC neurons in the ARC induced by estrogen affects parvalbumin (PV) expression.

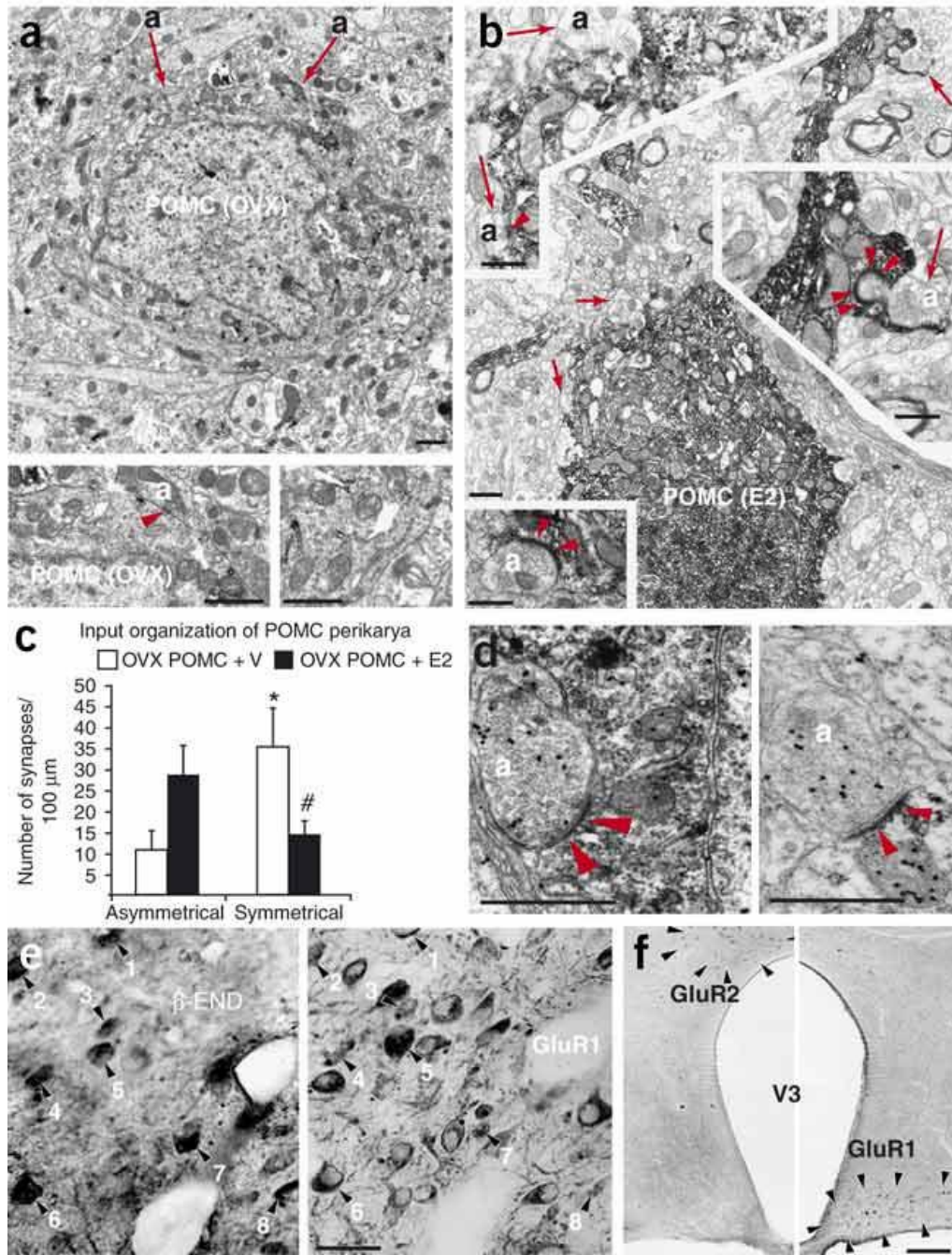


**Figure 4.** Estrogen regulates the type and number of axosomatic synapses on POMC perikarya in wild-type rodents of both sexes. (a,b) Electron microscopic examination of POMC perikarya of ovariectomized rats revealed that the number of putative inhibitory synapses (arrows in upper panel of a; 'a' in lower left panel) was much greater than that of putative excitatory contacts. In estrogen-replaced ovariectomized (OVX) females, excitatory contacts (arrows and arrowheads in b) were more numerous than inhibitory synapses. (c) Bar graph illustrating the total number of asymmetric (excitatory) and symmetric (inhibitory) synapses on POMC perikarya. In estrogen-

treated OVX rats, excitatory contacts onto the perikaryal membrane increased whereas inhibitory synapses decreased. \* $P < 0.05$ , # $P < 0.05$ . (d) Pre- and postembedding immunocytochemistry revealed that most boutons (marked 'a') establishing asymmetric (excitatory, arrowheads) synaptic contacts on POMC perikarya contained glutamate (5 nm immunogold particles). Scale bars, 1  $\mu\text{m}$ . (e) All of the analyzed arcuate POMC ( $\beta$ -endorphin,  $\beta$ -END) neurons colocalized (numbered cells) with AMPA glutamate receptor subunit 1 (GluR1). (f) In contrast, few, if any, of these cells expressed the GluR2 subunit. Scale bar, 20  $\mu\text{m}$  in e and 100  $\mu\text{m}$  in f. V3 represents third ventricle.

Indeed, we found in a pilot study that the estrogen regimen, which increased excitatory inputs on POMC neurons, robustly elevated the number of arcuate parvalbumin-expressing cells (**Figure 5a,b**), the vast majority of which were melanocortin cells (**Figure 5c,d**; preliminary results).

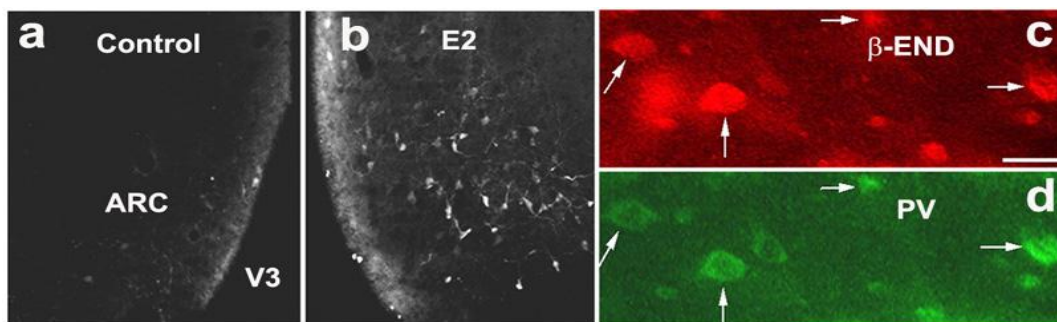


**Figure 5.** (a,b) Intracerebroventricular (i.c.v.) administration of water-soluble E2 (17- $\beta$  estradiol) induced the calcium binding protein, parvalbumin (PV) in the arcuate nucleus (ARC) compare to control. (c,d) The vast majority of PV (parvalbumin) cells were POMC cells ( $\beta$ -END). V3=third ventricle.

#### 4.1.2. Estrogen enhances POMC tone; the dynamics of feeding behavior and synaptic rewiring

In parallel with the morphological effect on synapses, E2 treatment increased the number of c-Fos-expressing POMC neurons in the ARC, indicating an increased activity of POMC neurons. The number of c-Fos-positive POMC neurons in the ARC of wild-type animals nearly doubled 4 h after a single subcutaneous injection of E2 treatment (**Figure 6a–c**). Thus, E2 may elevate POMC tone in wild-type animals, in part by increasing the number of excitatory synapses, an effect similar to that induced by leptin (Pinto et al., 2004).

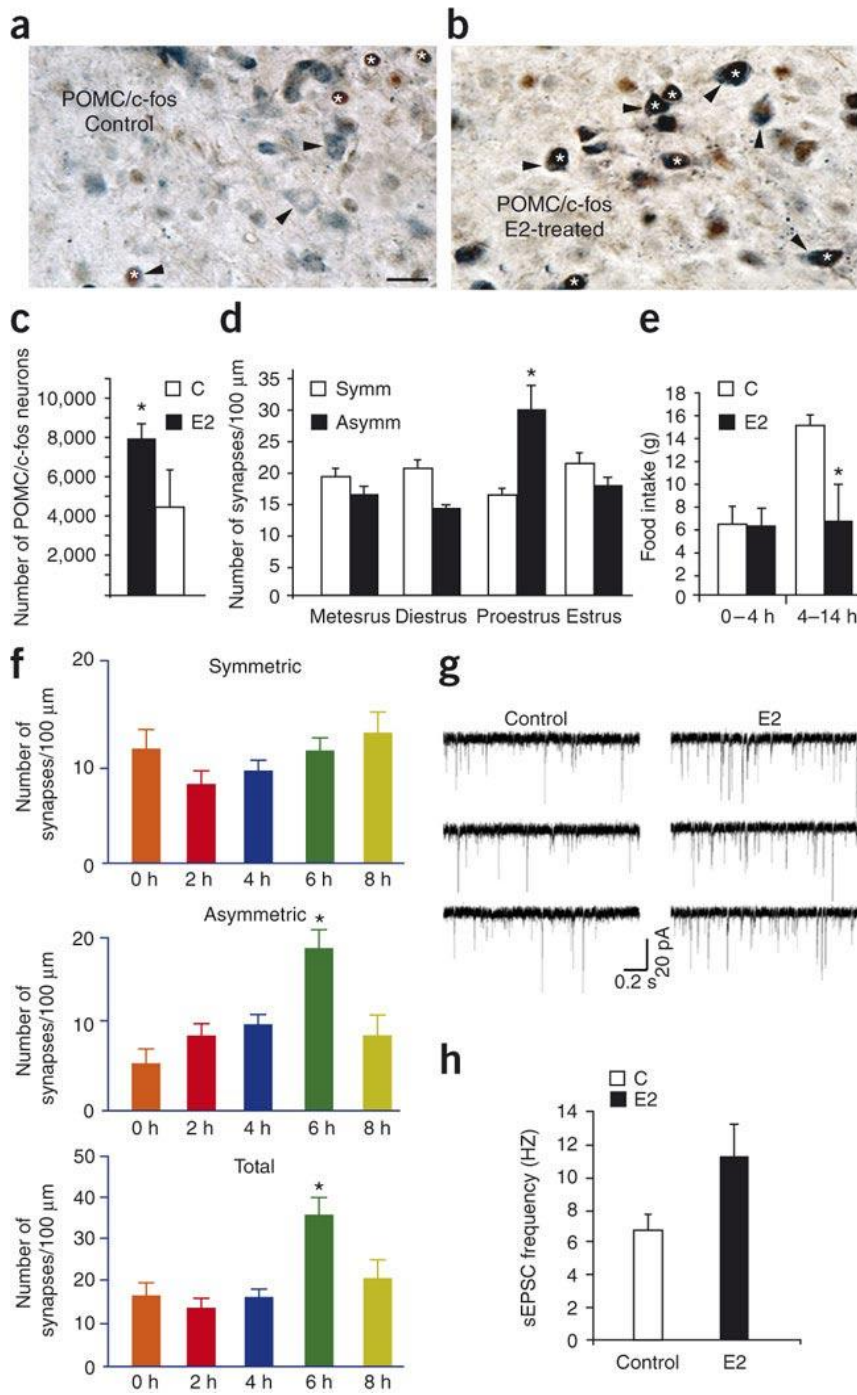


**Figure 6.** The increase in the number of glutamatergic, excitatory synapses on POMC perikarya increases arcuate POMC tone. (**a–c**) E2 significantly ( $P < 0.05$ ) increased the number of c-Fos-positive (white asterisk) POMC neurons (black arrowheads) in the arcuate nucleus, as compared to that in controls. Scale bar, 20  $\mu$ m. Total number of POMC and c-Fos double-positive neurons in the arcuate nucleus nearly doubled in animals treated with E2 (for 4 h). (**d**) Changes in the number of synapses on POMC perikarya during the estrus cycle, measured just before dark (6

p.m.). There were slightly fewer excitatory synapses than inhibitory synapses, except during proestrus (high E2 levels) when the number of excitatory synapses increased and the number of inhibitory synapses decreased. The ratio between inhibitory and excitatory synapses was reversed in proestrus. \* $P < 0.05$ . (e) Intracerebroventricular (i.c.v.) administration of water-soluble E2 had no effect on food intake for the first 4 h (0-4 h) after E2 treatment. However, 4-14 h after E2 treatment, food intake was significantly reduced in E2-treated animals. (f) Temporal kinetics of the increase in excitatory contacts on POMC perikarya induced by E2. The effect of E2 on excitatory synapses began at 4 h and peaked at 6 h after i.c.v. injection of E2. (g,h) Electrophysiologic recordings from POMC-GFP cells in acute arcuate slices showed an approximately 60% increase in the frequency of EPSCs in E2-treated versus control animals. \* $P < 0.05$ .

To address whether the effect of E2 on the synaptology of POMC neurons occurs under physiological conditions, we analyzed the synaptology of these neurons during estrus cycles. Rodents exhibit a 4-day estrus cycle in which E2 levels fluctuate, as does energy homeostasis, such that decreased food intake and body weight, and increased energy expenditure coincide with high levels of estrogen (Parker et al., 2001). In accordance with this, we observed an increase in the number of asymmetric synapses (confirmed to contain glutamate by postembedding labeling) on POMC perikarya, resulting in a dominance of excitatory synapses on the day of proestrus - when estrogen levels are high and feeding is low (**Figure 6d**).

To elucidate the relationship between synaptic changes and energy homeostasis, we studied the dynamics of feeding behavior and synaptic rewiring induced by E2. Intracerebroventricular (i.c.v.) administration of a water-soluble E2 initiated the reduction of food intake 4 h after E2 treatment (**Figure 6e**). In agreement with this, the induction of excitatory synapses on POMC perikarya was initiated 4 h ( $3.67 \pm 1.54$  to  $9.62 \pm 2.19$  per 100  $\mu\text{m}$  POMC perikaryal membrane) and peaked 6 h ( $20.65 \pm 3.35$  per 100  $\mu\text{m}$  POMC perikaryal membrane) after E2 administration (**Figure 6f**). The number of symmetric, inhibitory synapses on POMC perikarya, however, was only slightly reduced with quicker response dynamics when compared to the change in asymmetric synapses (from  $13.09 \pm 2.83$ , to  $8.05 \pm 2.69$  at 2 h and to  $8.35 \pm 2.13$  at 4 h, per 100  $\mu\text{m}$  POMC perikaryal membrane after E2 treatment) (**Figure 6f**). This is consistent with previous observations on the temporal kinetics of leptin-induced (Pinto et al., 2004) and estrogen-induced (Naftolin et al., 1996) arcuate synaptic plasticity.

To determine whether E2-induced synaptic changes on POMC neurons are reflected at the electrophysiological level, we studied miniature excitatory postsynaptic currents (mEPSCs) on the arcuate POMC neurons, by using patch-clamp recordings in acute arcuate slice preparations. POMC-GFP cells were held at -60 mV in the whole-cell voltage-clamp configuration (**Figure 6g**). The number of mEPSC was determined. POMC neurons from wild-type mice implanted with an E2 silastic capsule exhibited a 60% increase in mEPSCs when compared to those from control animals (**Figure 6h**).

#### **4.1.3. Estrogen exerts an antiobesity effect independent on leptin**

To address whether the estrogen-triggered plasticity of the anorexigenic melanocortin circuits is dependent on leptin signaling, we studied the effect of estrogen on the synaptology of melanocortin cells in leptin mutant, *ob/ob* and *db/db*, animals. Six week-old mutant mice of both sexes were used because at this stage, normal brain differentiation is established, while the body weight in the mutants is still rapidly increasing due to fat accumulation. Despite differential expression of ERs in various neuroendocrine nuclei in the brain in males and females, ERs are equally expressed in the ARC in both sexes (Brown et al., 1992) suggesting that estrogen's effect on the melanocortin system is not sexually dimorphic. The mutant males and females were subjected to 4 weeks of estrogen treatment through subcutaneous silastic capsule implants that result in physiological levels of circulating estrogen. The effect of estrogen on body weight was then measured daily. We observed a strong, about 50% reduction in body weight gain, which was similar in both sexes of *ob/ob* and *db/db* mice, in E2-treated mutants when compared to controls (**Figure 7a**). Similar to leptin, this effect of E2 on weight reduction is selective to fat mass, but not lean mass or linear body growth (**Figure 7b,c**). This effect was not limited to young, growing animals, as 4 weeks of E2 treatment caused a net loss of body weight (more than 10 g) in old, fully grown obese mutants in contrast to control mice, who had a slight increase in body weight (**Figure 7d**).

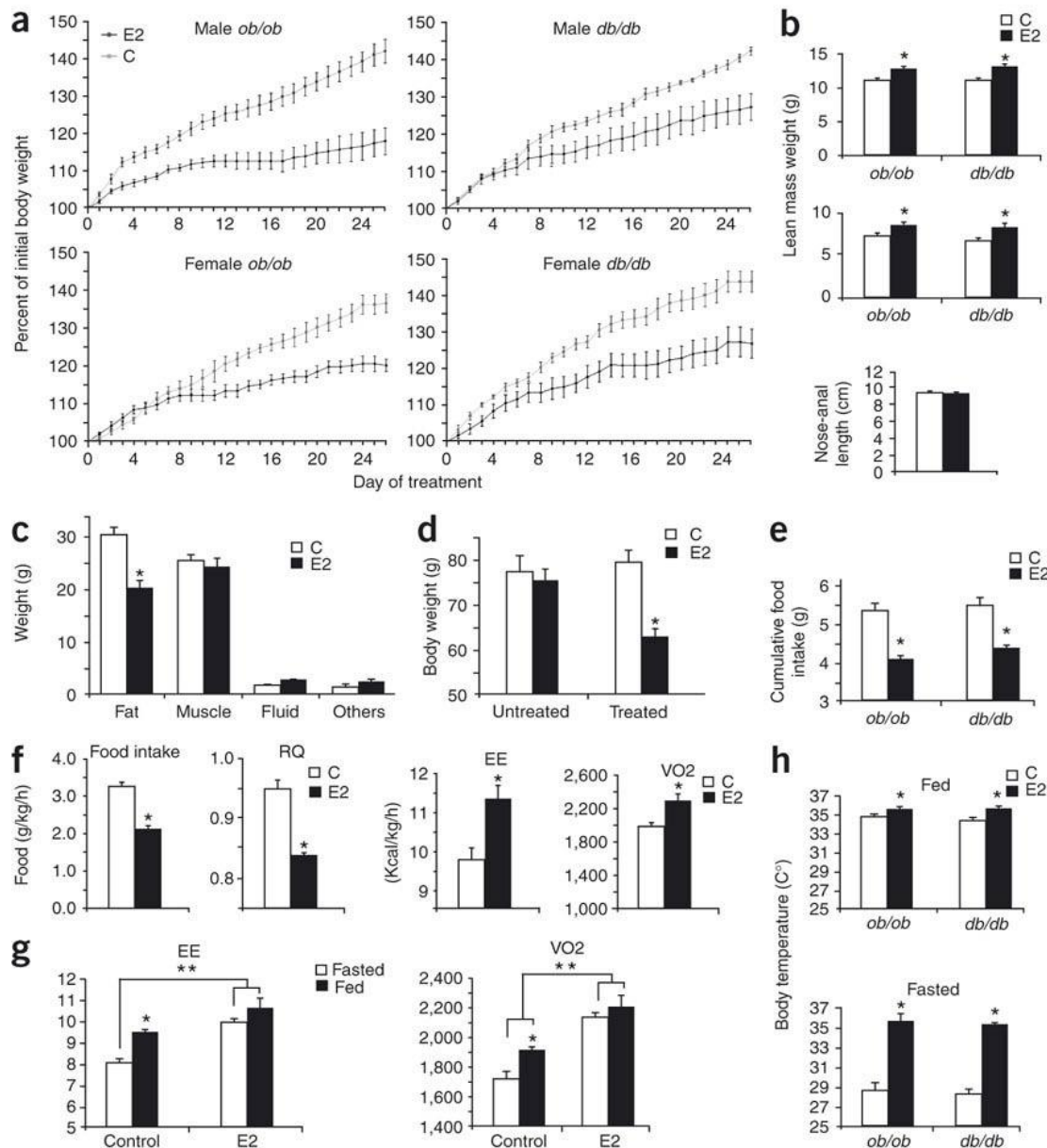


**Figure 7.** Estrogen exerts an antiobesity effect independent of functional genes encoding leptin and leptin receptor. **(a)** Both male and female *ob/ob* and *db/db* mice were sensitive to E2 treatment. Body weight gain was reduced by nearly 50% (40-58%) in all groups treated with E2 (for 4 weeks) when compared to controls. **(b)** In the same mice, the lean body mass was slightly increased in E2-treated mice (top, males; bottom, females), and the linear growth was unaffected. **(c)** Nuclear magnetic resonance imaging of *ob/ob* males with and without E2 treatment (4 weeks,  $n = 4$ ), showing total fat and lean mass as well as free fluid. There was a reduction in fat, but not muscle, fluid or other body components in E2-treated *ob/ob* mice. **(d)** E2 treatment caused a net loss of body weight in fully grown *ob/ob* mice. **(e)** E2-treated *ob/ob* and *db/db* mice consumed significantly less food in a 24-h period than did control mice. **(f)** The effect of E2 on food intake, respiratory quotient (RQ), energy expenditure (EE) and oxygen consumption (VO<sub>2</sub>) was detected

as early as the first day of treatment. **(g)** Fasting significantly reduced the energy expenditure and oxygen consumption of *ob/ob* mice, whereas E2 administration reversed this phenotype. **(h)** Basal body temperature was higher in E2-treated obese mice, and E2 treatment prevented fasting-induced drop in body temperature; this defect in diet-induced thermogenesis was reversed by E2 treatment  $P < 0.05$ .

Corresponding to the reduction in fat accumulation, E2 replacement decreased hyperphagia in both *ob/ob* and *db/db* mutants (**Figure 7e**). The anorectic effect of E2 was detected within the first 16 h of E2 treatment (**Figure 7f**), as was the reduction in the respiratory quotient (calculated as  $VCO_2/VO_2$ ), indicating that fat mobilization was increased. This quick effect of E2 on feeding in obese mutants is similar to that observed in wild-type animals treated with E2 in the brain (**Figure 4d**). E2 replacement also increased energy expenditure (**Figure 7f**), measured by a comprehensive mouse metabolic monitoring system. While fasting further reduced the energy expenditure of *ob/ob* mice, it had no significant effect on E2-treated mice (**Figure 7g**). Consistent with this, E2 treatment increased basal body temperature (measured rectally) and fully normalized the dysfunction of inducible thermogenesis in *ob/ob* and *db/db* mice: an overnight fast caused a  $>5^\circ\text{C}$  reduction in body temperature in *ob/ob* and *db/db* animals, but E2 treatment reversed this phenotype (**Figure 7h**). Thus, both reduced energy intake and increased energy expenditure contribute to the antiobesity effect of E2.

#### 4.1.4. Estrogen mimics leptin's effect on the rewiring POMC cells

Next, we analyzed the synaptology of POMC neurons in the *ob/ob* and *db/db* mice with and without E2 treatment. POMC perikarya of *ob/ob* and *db/db* animals were dominated by symmetric, inhibitory contacts ( $11.93 \pm 2.51$  versus  $3.42 \pm 0.92$  for *ob/ob*, and  $12.12 \pm 4.22$  versus  $3.3 \pm 0.8$  for *db/db*, per 100  $\mu\text{m}$  POMC perikaryal membrane) with an overall low density of perikaryal synapses ( $15.35 \pm 1.95$  for *ob/ob* and  $15.42 \pm 3.7$  for *db/db*, per 100  $\mu\text{m}$  POMC perikaryal membrane) (**Figure 8a,b**). The numbers of synapses were virtually identical between *ob/ob* and *db/db* mice, giving further credence to our proposition that it is the long form of the leptin receptor that mediates leptin's effect on POMC synaptology. The number of excitatory synapses on melanocortin perikarya,

however, was significantly ( $P < 0.01$ ) increased (from  $3.42 \pm 0.92$  to  $18.43 \pm 4.24$  for *ob/ob*, and from  $3.3 \pm 0.8$  to  $19.35 \pm 2.45$  for *db/db*, per 100  $\mu\text{m}$  POMC perikaryal membrane), with the total number of synapses doubled in E2-treated animals (**Figure 8a,b**). The increase in the number of synapses was due to changes in excitatory synapses only, presumably providing a high conductance 'hardware' that elevates the excitatory tone of POMC neurons. The number of inhibitory synapses, on the other hand, was not changed ( $11.93 \pm 2.51$  versus  $12.66 \pm 0.82$  for *ob/ob*, and  $12.12 \pm 4.22$  versus  $13.45 \pm 3.14$  for *db/db*, per 100  $\mu\text{m}$  POMC perikaryal membrane) by E2 treatment in obese mutants (**Figure 8a,b**), which is different from the results of E2 treatment in OVX wild-type animals (**Figure 4c**). The increase in the number of excitatory synapses on POMC perikarya predicted an overall enhancement of excitatory levels of arcuate melanocortin feeding circuits in E2-treated obese mice. This was evidenced by a significant ( $P < 0.05$ ) increase in the number of immunoreactive POMC neurons (**Figure 8c,d**), which mimics leptin action in the same neuronal circuits.

To test whether E2 is able to activate the downstream target of leptin signaling, STAT3, in the hypothalamus, we intraperitoneally injected a water-soluble E2 in both wild-type and *ob/ob* mice. We observed an acute increase in p-STAT3 levels in the hypothalamus upon E2 administration. The phosphorylation levels were induced within 30 min and peaked at about 60 min after E2 injection (**Figure 8e**). Chronic E2 administration with silastic capsule implants in a mouse model of brain STAT3 knockout had no effect on body weight reduction (presented as percentage of initial body weight), whereas it had a potent effect in control mice (**Figure 8f**). This later observation clearly suggests that the STAT3 activation is crucial for E2's effect in homeostasis.

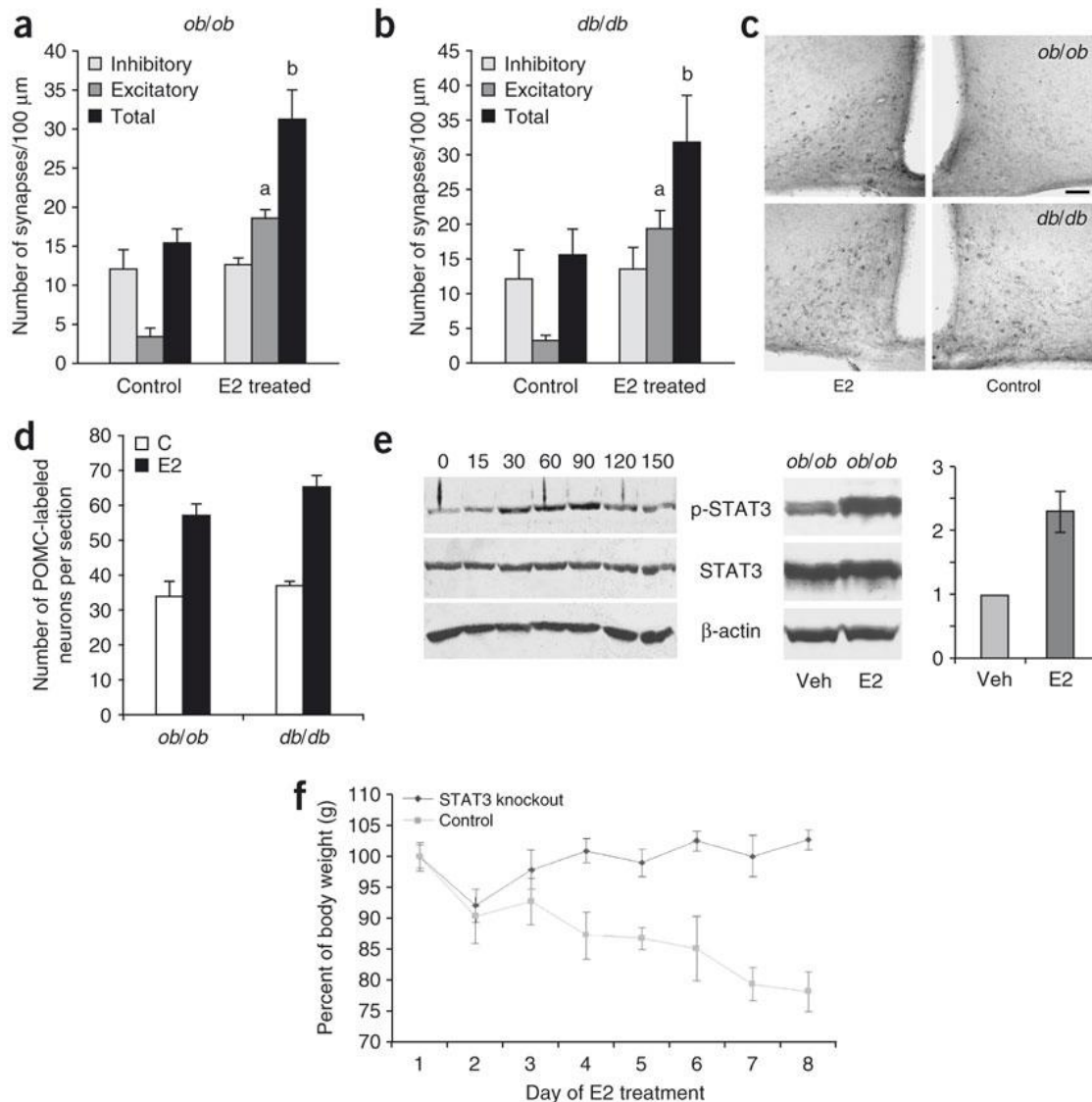


**Figure 8.** Estrogen mimics leptin's effect on the rewiring of melanocortin cells and increasing POMC tone, independent of leptin receptor-mediated signaling. **(a,b)** POMC perikarya of male *ob/ob* and *db/db* animals were dominated by inhibitory contacts; overall, there was a low density of perikaryal synapses. The number of excitatory synapses on POMC perikarya was significantly increased, and the total number of synapses doubled, in E2-treated animals  $P < 0.05$ . Data from leptin (*ob/ob*) and leptin receptor (*db/db*) mutants were virtually identical. **(c,d)** E2 treatment of male *ob/ob* and *db/db* mice resulted in a significant increase in the number of POMC neurons, from ~35 to 60 cells per section (both hemispheres of the arcuate nucleus), indicating an elevated POMC tone **(d)**. **(e)** E2 induced STAT3 phosphorylation in both wild-type and *ob/ob* mice. The phosphorylation levels were induced within 30 min and peaked at about 60 min after E2 injection. **(f)** Mice with brain-specific STAT3 knockout and their heterozygous littermates were implanted with silastic capsules filled with crystalline E2. E2 had no effect on body weight reduction (presented as percentage of initial body weight) in STAT3-knockout mice, whereas it had a potent effect in control mice.  $n = 4$ . Bar scale, 100  $\mu\text{m}$  in **c**.

We tested what effect, if any, elevated E2 levels had on POMC perikaryal synapses in ER $\alpha$ -null mice. The number of inhibitory synapses in obese ER $\alpha$ -null mice did not differ from that in wild-type littermates ( $10.28 \pm 0.98$  versus  $11.76 \pm 1.07$  synapses per 100  $\mu\text{m}$  POMC perikaryal membranes). Despite elevated levels of circulating E2 in ER $\alpha$ -null mice, the number of excitatory synapses on POMC perikarya in these mice ( $2.35 \pm 0.25$  per 100  $\mu\text{m}$  POMC perikaryal membrane) was significantly lower than that in E2-treated *ob/ob* or E2-treated *db/db* mice ( $18.43 \pm 4.24$  and  $19.35 \pm 2.45$ , respectively, per 100  $\mu\text{m}$  POMC perikaryal membrane;  $P < 0.01$ ). In addition, the number of observable POMC-immunopositive neurons in the arcuate nucleus was significantly reduced in ER $\alpha$ -null animals compared to controls (32.6 versus 50.7 per section). The number of POMC neurons in the arcuate nucleus in ER $\alpha$ -null mice was comparable to that in *ob/ob* and *db/db* mice (**Figure 8d**).

## 4.2. Experiment 2; estrogen's effects on the biological clock during early development

### 4.2.1. Distribution of BrdU-labeled cells in the SCN and IGL

In general, BrdU labeling was evident across various regions of the brain. Within the hypothalamus, BrdU-labeled cells were evident in the medial preoptic nucleus, medial preoptic area, lateral preoptic area, lateroanterior hypothalamic nucleus and bed nucleus of the stria terminalis. BrdU-labeled cells were also present in large numbers in the supraoptic nucleus, tuberomammillary nucleus and in the ARC. The SCN was subdivided into core and the shell of the rostral, medial and caudal SCN, as delineated previously (Moore et al., 2002) using sections immunostained for neuropeptide Y (NPY), which is selectively found in the SCN core (**Figure 9**).

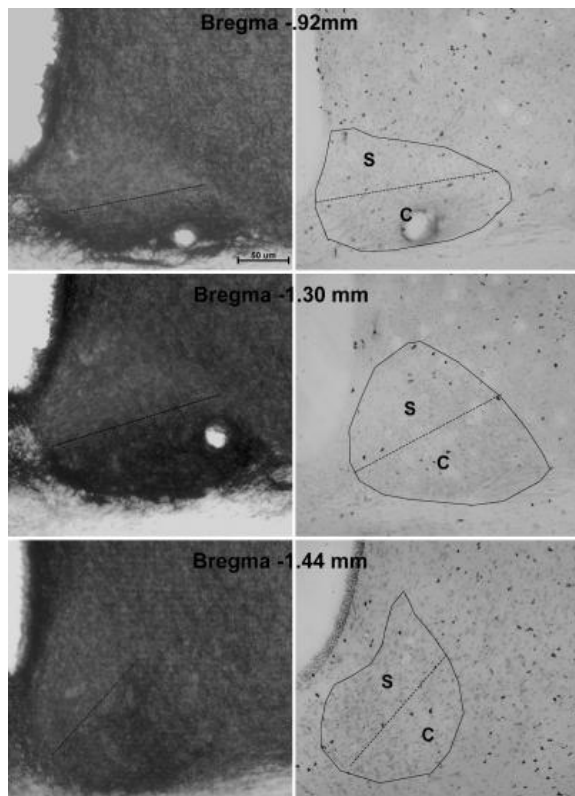


**Figure 9.** Photomicrographs depicting sample sections of the rostral (top panel), medial (middle panel) and caudal SCN (bottom panel). The left column show SCN sections stained for neuropeptide Y (NPY, rabbit anti-NPY 1:10,000, Bachem, Budendorf, Switzerland) counterstained with cresyl violet. NPY staining defines the ventral core (C) portion from the dorsal shell (S) portion of the SCN. Images in the right column show BrdU labeling in equivalent portions of the SCN at each level. Scale bar, 50µm.

BrdU-labeled cells were observed across the rostro-caudal extent of the nuclei. Overall cell count analyses showed that there were no differences in the number of BrdU-labeled cells per section across each segment of the SCN ( $P > 0.05$ ; rostral SCN =  $18.44 \pm 1.23$ , medial SCN =  $21.81 \pm 1.26$ , caudal SCN =  $19.12 \pm 1.62$ ), and the distribution of BrdU-labeled cells was observed in both core and shell portions of the SCN. Within the SCN core, BrdU-labeled cells were predominant in its dorsal portion, in an area bordering the shell. In the IGL, BrdU staining was sparse and appeared to label small nuclei, suggesting that BrdU labeled glia cells. In some cases, staining was completely absent in the IGL (data not shown).

#### 4.2.2. Sex differences in BrdU labeling in the SCN

To determine sex differences in the number of SCN cells that originate at the peak of the aromatase activity and that survive to adulthood, we counted the BrdU-labeled cells in the medial, anterior and rostral portion of the SCN.

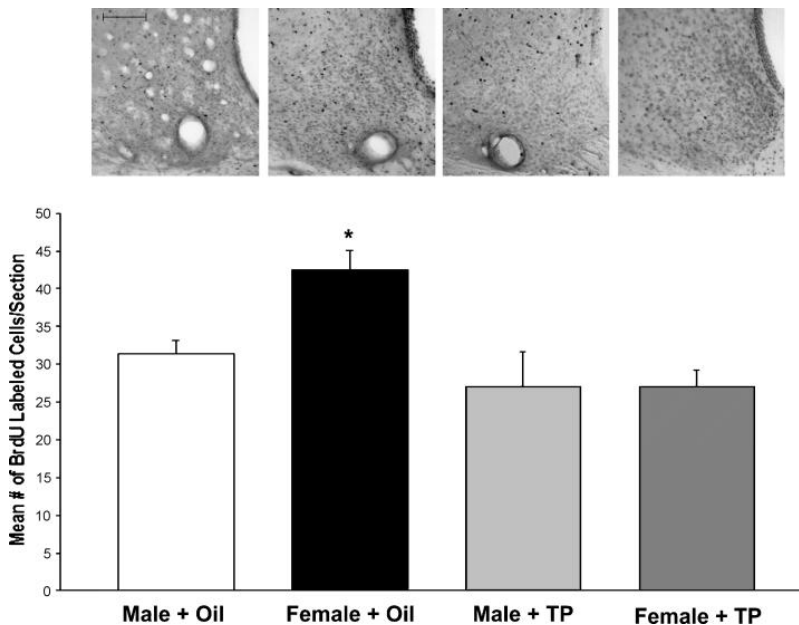


**Figure 10.** BrdU-labeled cells per section of the medial SCN of male and female rats treated prenatally with either oil or testosterone propionate (TP; 10 mg/0.1 mL). BrdU was predominantly expressed in the dorso-lateral portion of the SCN core and throughout the shell. Females treated prenatally with oil had more intense BrdU labeling and more nuclei present within the dorso-lateral portions of the core and in the shell of the SCN ( $*P < 0.05$ ). Scale bar, 50  $\mu$ m.

The number of BrdU-labeled cells appeared to be sexually differentiated in specific subregions across the rostro-caudal extent of the SCN. The counts from the medial

portion of the SCN revealed that females had an overall higher number of BrdU-labeled cells than males ( $F_{1,21} = 4.23$ ,  $P = 0.05$ ), and that TP decreased the overall number of BrdU-labeled cells ( $F_{1,21} = 13.3$ ,  $P < 0.05$ ) (**Figure 10**). A significant interaction effect ( $F_{1,21} = 4.176$ ,  $P = 0.05$ ) suggested that the sex difference in BrdU staining was dependent on the prenatal presence of testosterone. Statistical analyses of cells counts within the core or shell produced similar results, in which oil-treated females had a significantly higher number of BrdU-labeled cells in both core and shell, and prenatal TP treatment reduced this number.

Similarly, the caudal portion of the SCN of oil-treated female rats contained significantly more BrdU-labeled cells than the same portion of SCN in male or in TP-treated animals ( $P < 0.05$ ) (**Figure 11**). As for other portions of the SCN, testosterone decreased the number of BrdU-labeled cells dramatically. Although testosterone decreased BrdU-labeled cells in the caudal SCN of both males and females, it appeared to have a stronger effect in females than in males. These overall effects were not differentially expressed within the SCN core or shell.

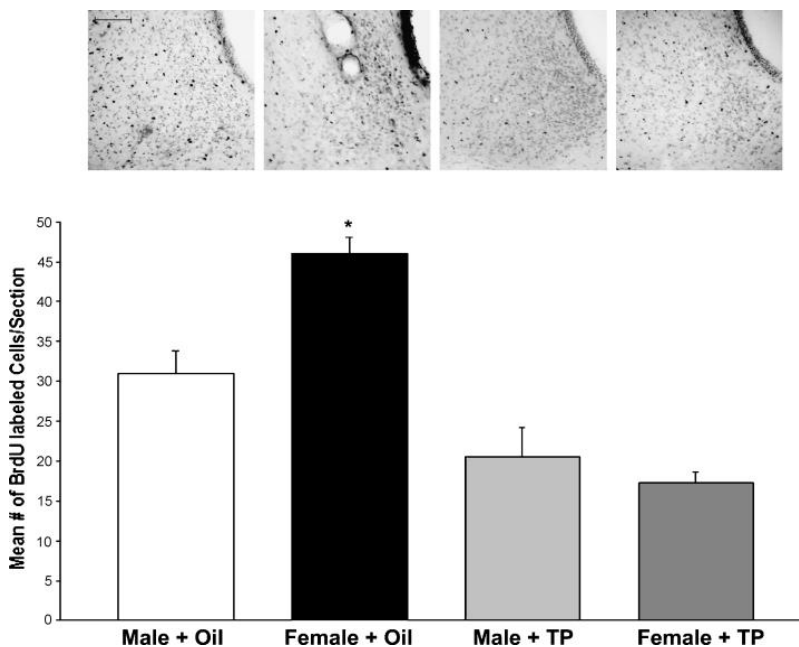


**Figure 11.** BrdU-labeled cells per section of the caudal SCN of male and female rats treated prenatally with either oil or testosterone propionate (TP; 10 mg/0.1 mL). BrdU was predominantly expressed in the dorso-lateral portion of the SCN core and throughout the shell. Females treated prenatally with oil had more intense BrdU labeling and more nuclei present within the dorso-lateral portions of the core and in the shell of the SCN ( $*P < 0.05$ ). Scale bar, 50  $\mu\text{m}$ .

In contrast with the medial and caudal SCN, there were no significant sex differences in the number of BrdU-labeled cells per section of the rostral SCN. TP treatment, however, did significantly reduce the overall number of BrdU-labeled cells in this subregion of the SCN, and these effects were more evident in females than in males. Using a 2 x 2 x 2 ANOVA, with sex, treatment and SCN regions (core vs. shell), it was observed that the SCN core of males had a higher number of BrdU cells per section than females ( $F_{1,17} = 8.79$ ,  $P < 0.05$ ), and that testosterone reduced this number overall ( $F_{1,17} = 10.034$ ,  $P < 0.05$ ). A post-hoc one-way ANOVA showed that females exposed to testosterone in utero had a significantly lower number of BrdU-stained nuclei than animals in the other groups. No significant differences were observed in the rostral SCN shell (**Figure 12**).

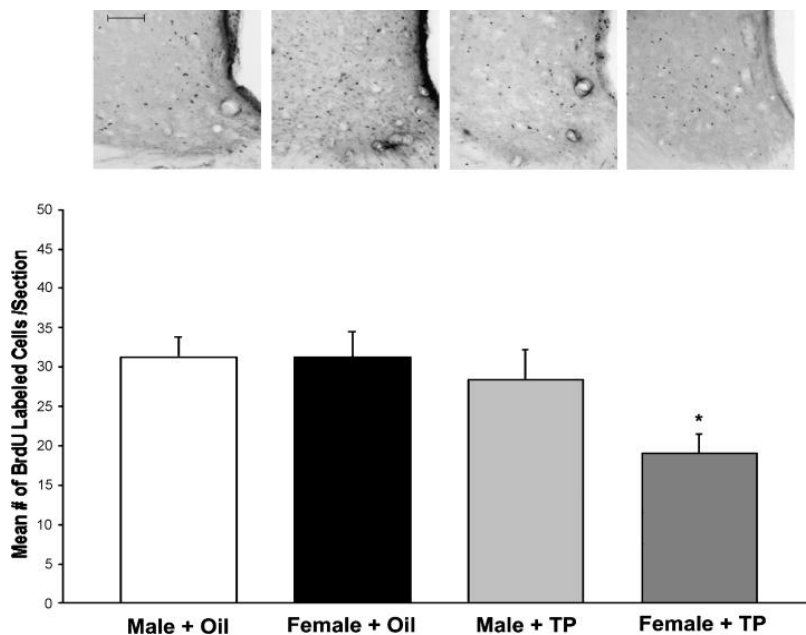


**Figure 12.** Mean ( $\pm$  SE) BrdU-labeled cells per section of the rostral SCN of male and female rats treated prenatally with either oil or testosterone propionate (TP; 10 mg/0.1 mL). BrdU was expressed in both SCN core and shell. Testosterone propionate treatment reduced the number of BrdU-labeled cells and this effect was significant only in the SCN of females ( $*P < 0.05$ ). Scale bar, 50  $\mu$ m.

#### 4.2.3. Phenotypical characterization of BrdU-labeled cells

In order to determine the nature of the cells tagged with BrdU on embryonic day 18, tissue sections were processed for double immunocytochemistry for BrdU and other neurochemicals that are known to be expressed in the SCN. Although the number of sections that were processed for each double immunocytochemistry assay was not

sufficient to conduct statistical analyses, these assays demonstrated that BrdU-labeled cells within the SCN were heterogeneous in nature, with no specific group of cells proliferating at the time of BrdU injection.

*BrdU and AVP immunoreactivity.* The location of BrdU-positive cells appeared to overlap that of previously reported AVP-immunoreactive cells in the SCN shell. Nevertheless, few AVP cells appeared to co-express BrdU (**Figure 13a**). BrdU-labeled cells, however, were observed in other hypothalamic regions that also contain AVP neurons, such as the supraoptic nuclei and medial preoptic area.

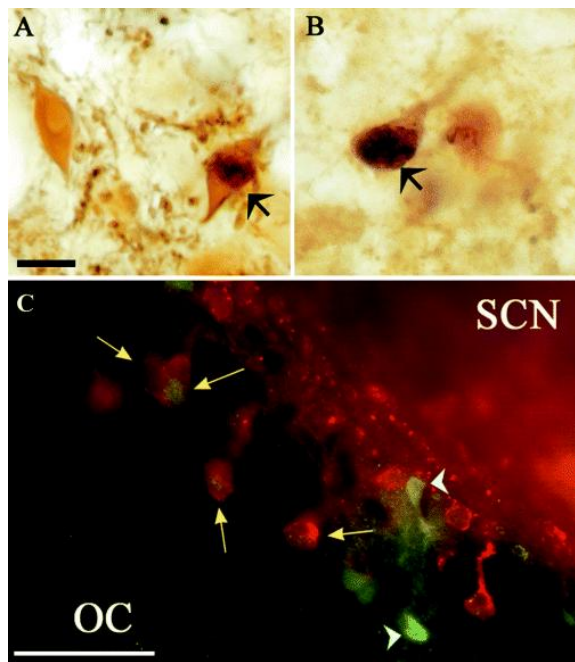


**Figure 13.** Double immunocytochemistry for BrdU and AVP (**A**), BrdU and calbindin-D (28K) (**B**), and BrdU and VIP (**C**) in the SCN. Very few SCN cells expressing BrdU colocalized with AVP-immunopositive cells in the SCN (large black arrow). BrdU was more abundantly co-expressed in cells that expressed the calcium binding protein, calbindin (large black arrow), within both the core and the shell regions of the SCN. Although BrdU was more prevalent in the shell and in the dorsolateral portion of the core, some VIP-immunopositive cells were also labeled with BrdU. Arrows point to cells double labeled with VIP- (Texas red) and BrdU- (green fluorescein) conjugated antibodies. Arrowheads point to single labeled BrdU cells. Scale bars, 10  $\mu$ m. OC=optic chiasma.

*BrdU and calbindin-D (28K) immunoreactivity.* Calbindin-D (28K) immunoreactivity was found in the core and shell portions of the SCN, particularly in its medial portion across the anterior–posterior plane. Double immunocytochemistry revealed the presence of several calbindin-D (28K)-immunoreactive cells that co-expressed BrdU in their nuclei. This was true for cells in other hypothalamic nuclei, such as the preoptic and supraoptic nuclei. Not all calbindin-D (28K)-immunopositive cells expressed BrdU (**Figure 13b**).

*BrdU and VIP immunoreactivity.* Cells labeled for VIP were found in the ventrolateral portion of the SCN. These were particularly evident in the ventral portion, embedded in the optic chiasm. As seen in **Figure 13c**, a number of VIP-immunoreactive cells also appeared to express BrdU-immunoreactive nuclei. The majority of double-labeled VIP cells were found in the ventrolateral portion of the SCN core, and in VIP cells embedded in the optic chiasm.

*BrdU and GFAP immunoreactivity.* BrdU immunoreactivity was not found within astrocytes that produce GFAP. In fact, GFAP-immunopositive astrocytes were more abundant in the ventromedial portion of the SCN, whereas BrdU-immunolabeled cells were located mostly on the dorsolateral portion of the SCN. Nevertheless, some GFAP-positive cells were seen surrounding cells labeled with BrdU (data not shown).

### 4.3. Experiment 3; estrogen's effect on the biological clock during adulthood

#### 4.3.1. Estrogen enhances light-induced Fos immunoreactivity in the SCN

First, we examined the ability of a phase shift to induce Fos immunoreactivity in the SCN. Animals presented with light at ZT22, 2 h prior to the regular onset of light within the colony room, showed a significant increase in Fos-immunoreactivity in the SCN than those sacrificed after the regular onset of light (ZT0) ( $F_{1,20} = 13.9, P < 0.05$ ) (**Figure 14**).

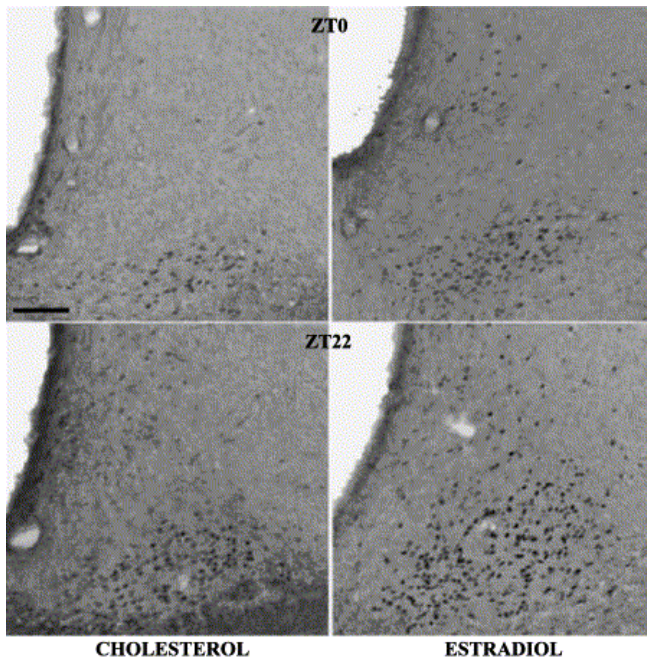
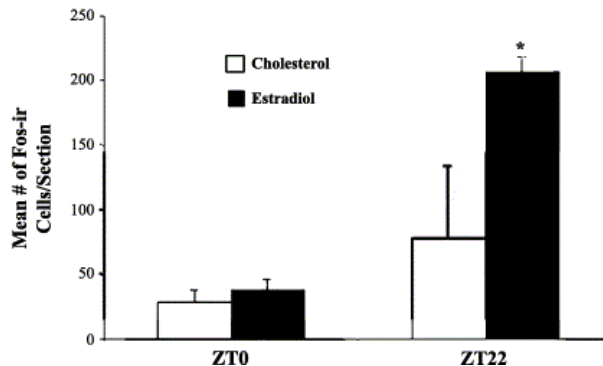


**Figure 14.** Patterns of Fos immunoreactivity (Fos-ir) in the SCN of OVX female rats treated with cholesterol or estradiol (E2) and sacrificed after the normal onset of light (ZT0), and cholesterol and E2-treated females sacrificed 1 h after a phase advance (ZT22). Analyses of cell counts demonstrated that the expression of the Fos protein in response to a phase advance was only enhanced in OVX females that received estradiol replacement. \*Significant from ZT0,  $P < 0.05$ ; scale bar, 50  $\mu\text{m}$ .



Then we examined the E2 effect during this phase shift. E2-treated animals had an overall higher number of Fos-immunoreactive nuclei than animals given cholesterol. A significant interaction effect suggested that E2-treated rats presented with light at ZT22 had more Fos-immunoreactive cells in the SCN than animals in the other groups ( $F_{1,20} = 4.15$ ,  $P = 0.05$ ). This was confirmed by one-way ANOVA followed by a Fisher's LSD test ( $F_{3,20} = 7.86$ ,  $P < 0.05$ ).

#### 4.3.2. Estrogen's effect on p-CREB immunoreactivity in the SCN

The phase advance of 2 h increased the overall number of p-CREB-ir cells ( $F_{1,20} = 41.88$ ,  $P < 0.05$ ) (Figure 15).

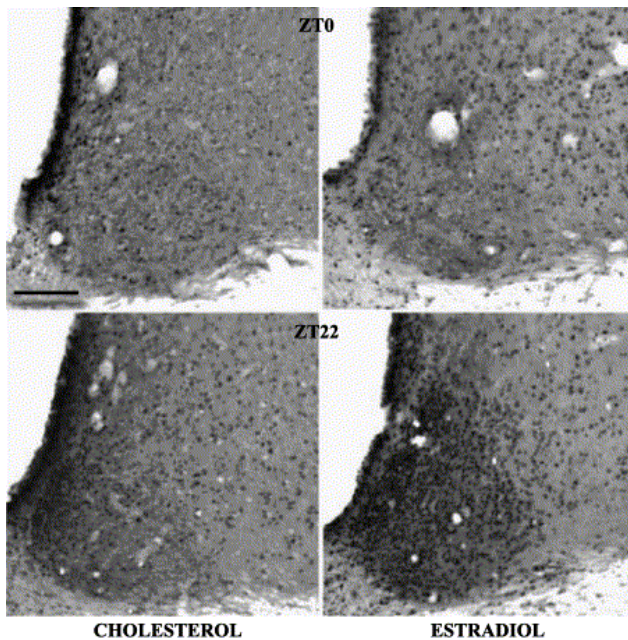
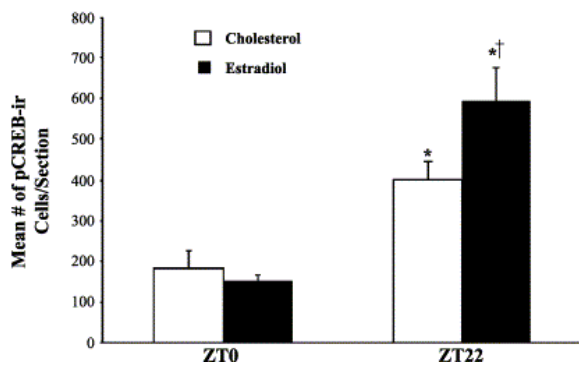


**Figure 15.** Immunoreactivity for p-CREB in the SCN of OVX animals in the different experimental groups. Data analysis revealed that the phase advance in the onset of light increased the expression of p-CREB in the SCN (\*Significantly different from ZT0,  $P < 0.05$ ), and this increase was significantly more pronounced in estradiol-treated OVX female rats ( $\dagger$ Significantly different from cholesterol at ZT22,  $P < 0.05$ ). Scale bar, 50  $\mu\text{m}$ .



Although there was no overall estradiol effect ( $F_{1,20} = 4.49, P > 0.05$ ), there was a significant interaction effect ( $F_{1,20} = 4.91, P < 0.05$ ). The post-hoc testing revealed a significant group effect ( $F_{3,20} = 16.43, P < 0.05$ ), where E2-treated animals exposed to light at ZT22, had more p-CREB positive cells than E2-treated animals exposed to light at ZT0, or cholesterol treated rats in either light condition.

#### 4.3.3. Estrogen has no effect on the calbindin-D (28K), egr-1 and CBP immunoreactivity in the SCN

The 2-h phase advance in the onset of light increased the number of calbindin-D (28K)- ( $F_{1,20} = 23.8, P < 0.05$ ), and egr-1- ( $F_{1,20} = 11.22, P < 0.05$ ) immunoreactive cells in the SCN (Figure 16, 17A,B).

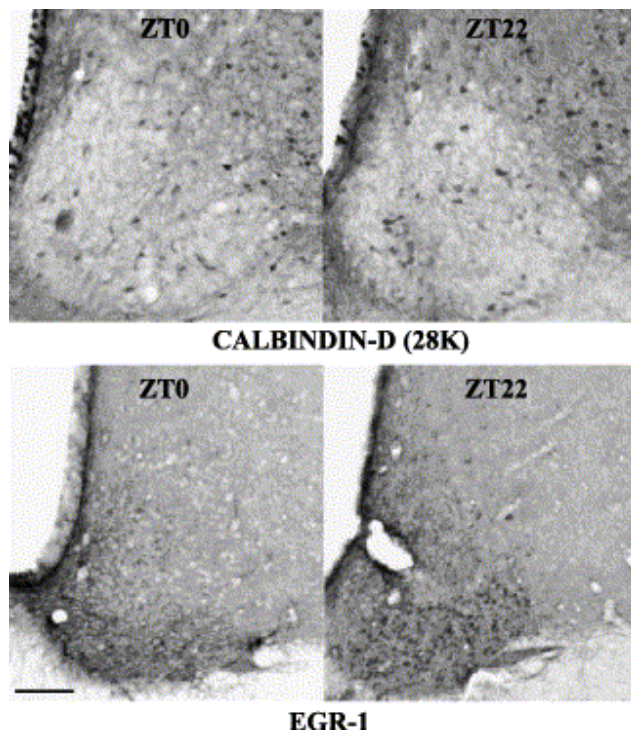


**Figure 16.** Expression of the calbindin-D (28K) (top panel) and egr-1 (bottom panel) proteins in control (ZT0) and phase-shifted (ZT22) OVX females. The phase advance increased the number of calbindin-D (28K)-, and egr-1-immunoreactive cells in the SCN. Scale bars, 50  $\mu$ m.

E2 treatment, however, had no effect in the expression of either of these proteins in the SCN. Neither the phase advance nor E2 affected the expression of CBP in the SCN of OVX rats (Figure 17C).

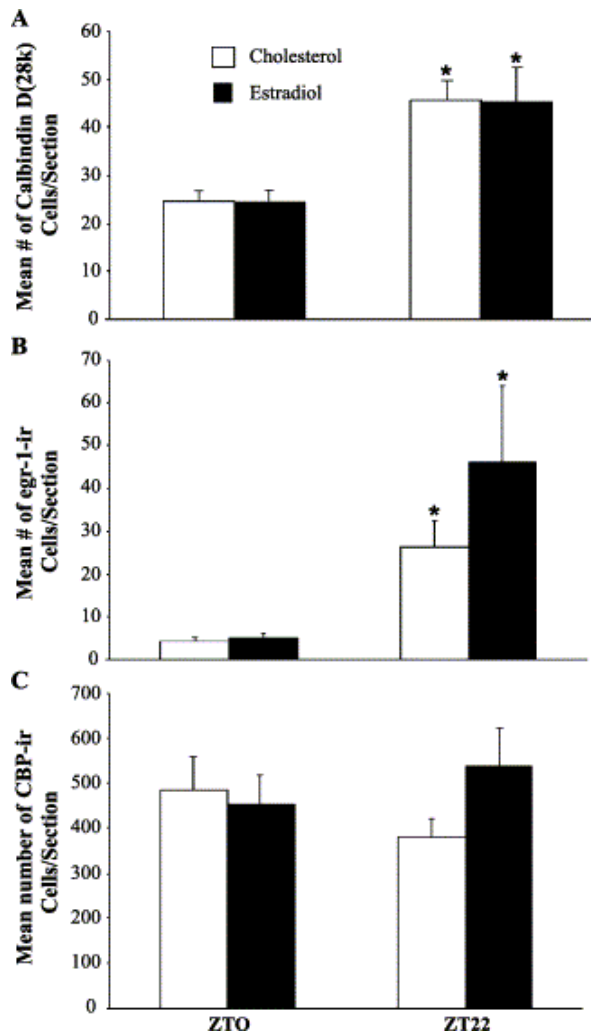


**Figure 17.** The number of calbindin-D (28K) (A), egr-1- (B), and CBP- (C) immunoreactive cells per section of the SCN of OVX females given cholesterol or estradiol and sacrificed following the regular onset of light (ZT0) or after a phase advance (ZT22). Although the phase shift increased both Calbindin-D (28K) and egr-1 protein expression (\*Significantly different from ZT0;  $P < 0.05$ ), E2 had no effect in the expression of any of these proteins.

#### 4.3.4. Estrogen has no effect on the light-induced p-CREB and calbindin-D (28K) immunoreactivity in the IGL

In contrast to the SCN, Fos-immunoreactivity was expressed at comparable levels in the IGL of OVX rats regardless of the hormone treatment, or the time at which they were presented with light on the day of sacrifice. The numbers of p-CREB- ( $F_{1,20} = 40.52$ ,  $P < 0.05$ ), and calbindin-D (28K)- ( $F_{1,20} = 10.36$ ,  $P < 0.05$ ) immunoreactive cells in the IGL were increased significantly by the 2-h phase advance in the onset of light. The expression of egr-1 and CBP in the IGL was not altered by the phase advance. Finally the E2 treatment did not affect the expression of any of these proteins in the IGL (Figure 18).

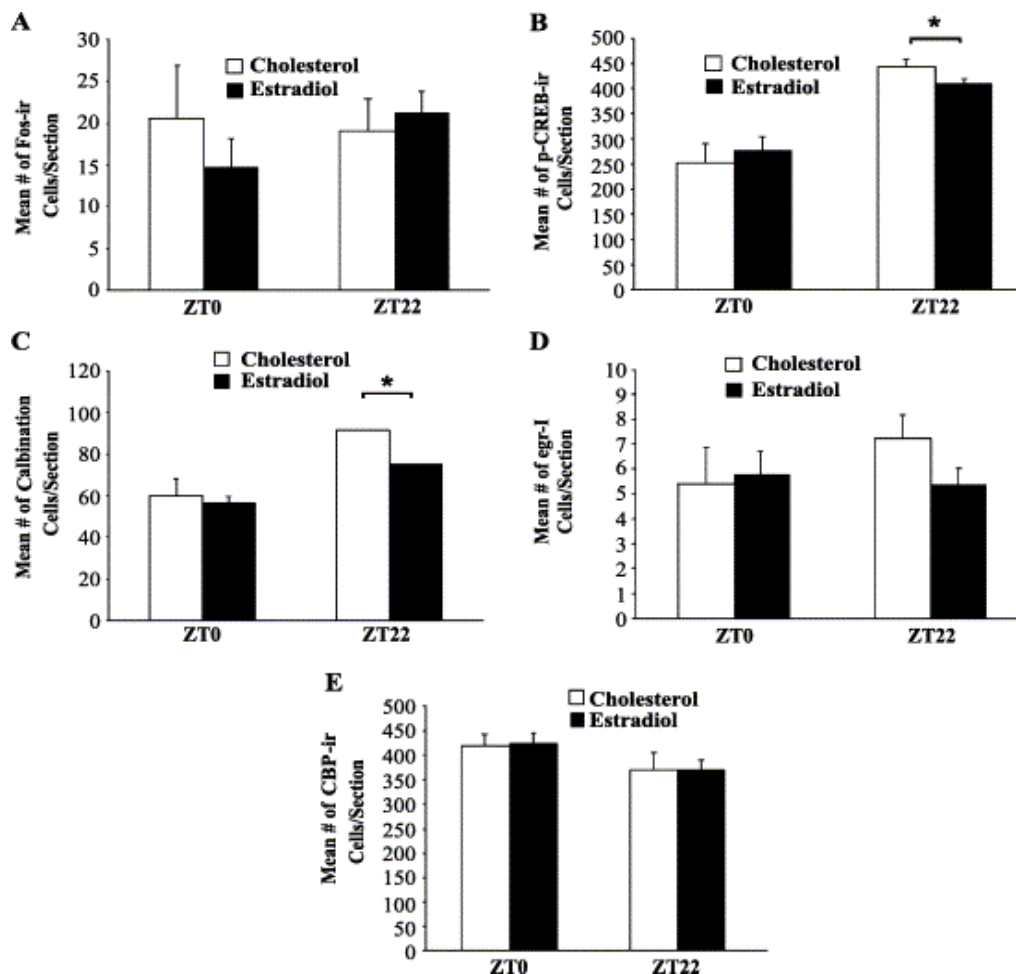


**Figure 18.** The number of Fos- (A), p-CREB- (B), calbindin-D (28K)- (C), egr-1- (D), and CBP- (E) immunoreactive cells per section of the IGL of OVX female rats treated with cholesterol or estradiol, and sacrificed at the different ZT times. As seen in these graphs, estradiol had no effect in the expression of these proteins within the IGL. \*Significant from ZT0,  $P < 0.05$ .

#### 4.3.5. Light induced Fos expression in the DRN, but not in the MRN

Fos-immunoreactive nuclei were observed in all regions of the dorsal raphe nucleus (Figure 19) for the four experimental groups. Photomicrographs of the medial, lateral and caudal regions of the DRN examined from representative cholesterol-treated control rats presented with light at ZT0 or ZT22 are shown in Figure 19.

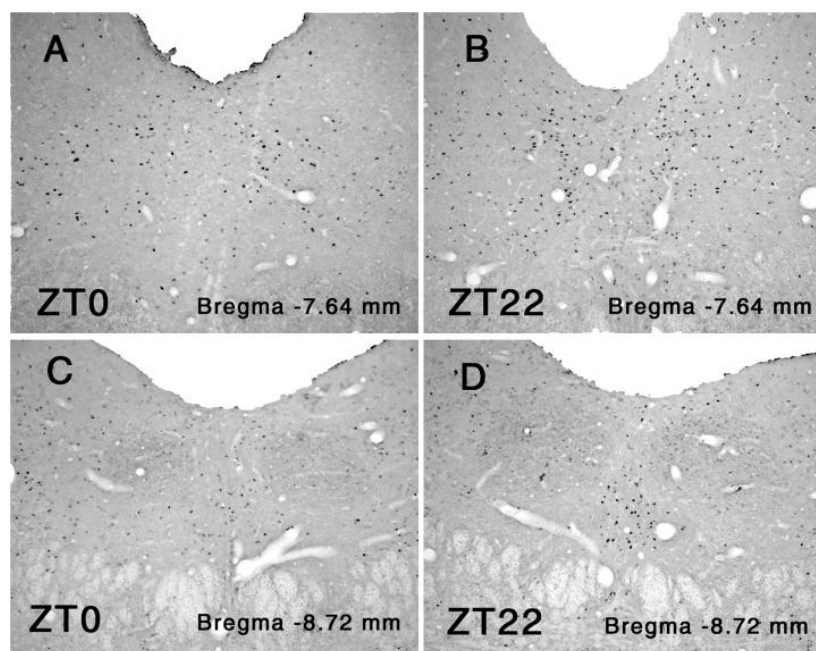


**Figure 19.** Samples of Fos-immunoreactive nuclei in the medial, lateral (A,B) and caudal (C,D) dorsal raphe nucleus of ovariectomized control female rats killed 60 min after regular onset of light [Zeitgeber time (ZT)0] (A,C) or 60 min after a phase advance (ZT22) (B,D). Scale bar, 200 $\mu$ m.

We examined the ability of a phase shift to induce Fos immunoreactivity in the DRN and in the MRN. Statistical analyses revealed that animals presented with light at ZT22, 2 h before the regular onset of light within the colony room, showed a significant increase in Fos expression in the medial ( $F_{1,20} = 4.52$ ,  $P < 0.05$ ) (**Figure 20A**), lateral ( $F_{1,20} = 5.89$ ,  $P < 0.05$ ) (**Figure 20B**) and caudal ( $F_{1,20} = 6.96$ ,  $P < 0.05$ ) (**Figure 20C**) regions of the DRN compared with those killed after the regular onset of light (ZT0). E2 treatment, however, had no effect on the expression of Fos protein in any regions of the DRN. In contrast to the DRN, neither the 2-h phase advance nor the E2 treatment affected the number of Fos-immunoreactive nuclei in the MRN (**Figure 20D**).

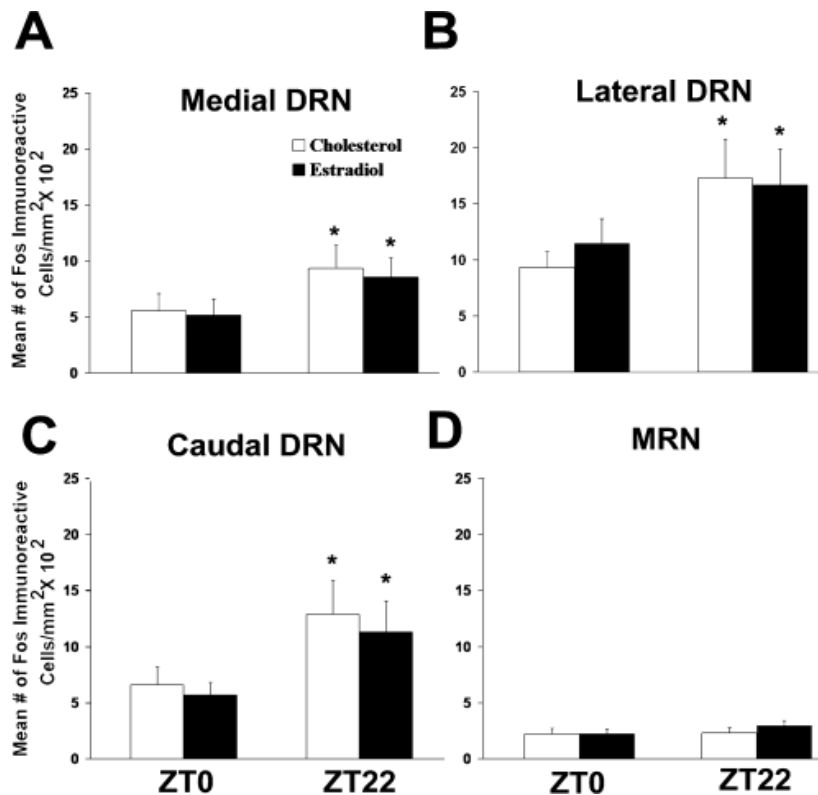


**Figure 20.** Phase advances increase the density of Fos-immunoreactive nuclei in all portions of the dorsal raphe nucleus (DRN) but not in the median raphe nucleus (MRN). (A-C) Fos-immunoreactive cells in different portions of the DRN. (D) Means and SEM of Fos-immunoreactive cells in the MRN (\* $P < 0.05$ ). Estradiol treatment had no effect on the overall expression of the Fos protein in any of the DRN regions.

#### 4.3.6. Estrogen increases the proportion of serotonin (5-HT) cells expressing Fos after a phase shift in the DRN

To test our hypothesis, that estradiol enhances light-induced transcription in the SCN indirectly by modulating 5-HT release from the raphe into the SCN, we examined the ability of E2 to increase the proportion of 5-HT cells expressing Fos after a phase shift. First we stained the serotonin- (5-HT) immunoreactive neurons in the DRN in all four experimental groups. **Table 2** shows the mean number of 5-HT-immunoreactive cells in the medial, lateral and caudal regions of DRN for the four experimental groups. As shown, neither the phase shift nor the E2 treatment altered the number of 5-HT-immunolabelled cells in the DRN.

**Table 2.** 5-HT-immunoreactive cells in the DRN. The number (mean  $\pm$  SEM) of serotonin (5-HT)-immunoreactive cells/mm<sup>2</sup>  $\times$  10<sup>2</sup> was determined in the medial, lateral or caudal region of the dorsal raphe nucleus (DRN). Adult ovariectomized female rats were treated with estradiol or cholesterol and killed 1 h after the normal onset of light [Zeitgeber time (ZT0)] or 1 h after a phase advance (ZT22). n = number of rats.

#### 5-HT-immunoreactive cells

ZT and treatment	(n)	Medial DRN	Lateral DRN	Caudal DRN
ZT0				
Cholesterol	6	23.39 $\pm$ 2.98	21.25 $\pm$ 1.86	28.45 $\pm$ 3.35
Estradiol (E2)	6	24.88 $\pm$ 2.80	24.85 $\pm$ 3.28	30.75 $\pm$ 4.66
ZT22				
Cholesterol	6	26.11 $\pm$ 1.83	21.88 $\pm$ 0.99	30.91 $\pm$ 2.40
Estradiol (E2)	6	26.82 $\pm$ 1.86	24.54 $\pm$ 3.26	32.24 $\pm$ 2.27

Next, using double-labeling staining for 5-HT and Fos (**Figure 21**), we revealed that exposure to an advance in the onset of light (ZT22) significantly increased the percentage of 5-HT cells co-expressing Fos in the medial ( $F_{1,20} = 12.54$ ,  $P < 0.05$ ), lateral ( $F_{1,20} = 11.50$ ,  $P < 0.05$ ) and as well as in the caudal ( $F_{1,20} = 4.74$ ,  $P < 0.05$ ) regions of the DRN compared with those killed after the regular onset of light (ZT0).

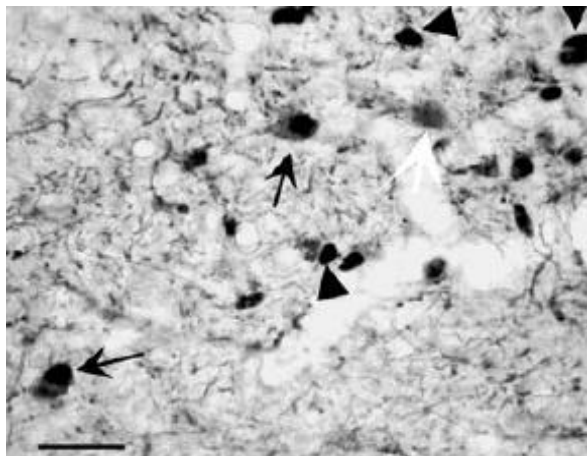


**Figure 21.** Fos and 5-HT immunolabelling in the lateral region of the DRN of an estradiol-(E2) treated OVX female rat killed 60 min after a phase advance. Black arrowheads, Fos-immunoreactive nuclei; white arrows, 5-HT-immunoreactive cells; black arrows, double-labelled cells. Scale bar, 25 $\mu$ m.

E2-treated animals had an overall higher percentage of double-labelled 5-HT cells in the lateral DRN ( $F_{1,20} = 6.03$ ,  $P < 0.05$ ) and a near significant higher percentage in the medial DRN ( $F_{1,20} = 3.52$ ,  $P = 0.07$ ) but not in the caudal DRN ( $F_{1,20} = 0.07$ ,  $P > 0.05$ ) compared

with animals given cholesterol implants (**Figure 22**). Our findings are suggesting that there is an effect of light on Fos expression in the lateral subregion of the DRN and this effect is enhanced by estrogen.

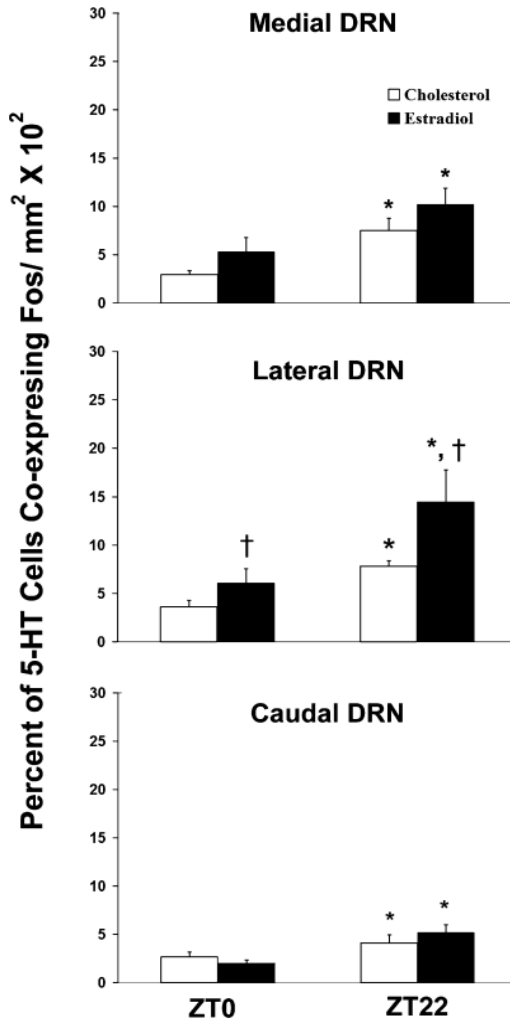


**Figure 22.** Mean and SEM of the proportion of serotonin (5-HT) cells that were also immunopositive for Fos in the dorsal raphe nucleus (DRN) of OVX female rats treated with estradiol or cholesterol and killed at either Zeitgeber time (ZT)0 or ZT22. Estradiol treatment significantly increased the activation of 5-HT cells in the lateral and tended to increase it in the medial but not in the caudal DRN at both ZT0 and ZT22. \*Significantly different from ZT0,  $P < 0.05$ ; †Significantly different from cholesterol-treated subjects.

## 5. DISCUSSION

The present dissertation is the essence of a number of studies targeting the mechanism of estrogen effect on the hypothalamic regulation of energy homeostasis and circadian rhythm. Here we demonstrated clear evidences about the important role of gonadal steroid estrogen in these hypothalamic regulatory processes. Our results perhaps will guide further research aiming to better understand these mechanisms and hopefully will help researchers to draw conclusions relevant for clinical settings.

### 5.1. Estrogen and the hypothalamic regulation of energy homeostasis

Obesity is a major health problem in modern society, affecting more than one-quarter of all adults. Leptin, the most potent antiobesity hormone regulates energy homeostasis by acting as a feedback signal indexing body energy stores to the hypothalamus. Estrogen is also a potent energy regulator; both reduced energy intake and increased energy expenditure contribute to the antiobesity effect of estrogen. Here we have shown that estrogen increases excitatory synapses on the hypothalamic POMC neurons and enhances POMC tone, while decreasing food intake and body weight similar to leptin. The fact, that this effect was also observed in leptin-mutant obese animals clearly suggests that estrogen exerts its antiobesity effect independent on leptin. This effect seems to be mediated by ER $\alpha$  and by the STAT3, but further studies is needed to determine more of the intracellular processes that bring about these synaptic alterations. Elaborating further these processes will eventually allow for the testing of a direct causal relationship between presynaptic reorganization of POMC inputs and feeding and metabolism.

Estrogen increases the number of excitatory synapses on POMC perikarya in wild-type animals. The shift in synaptic balance on POMC perikarya with a corresponding decrease in appetite and adiposity is similar to what was previously observed in leptin-treated *ob/ob* mice (Pinto et al., 2004). The fact that the hypothalamus is not hard-wired, i.e., it goes through continuous synaptic reorganization, is not novel. Rapid

rearrangement of synapses have been shown to occur in the magnocellular system during changes in water homeostasis (Theodosis et al., 1991; Miyata et al., 1994), the ARC interneuronal system during changes in the gonadal steroid milieu (Garcia-Segura et al., 1994; Parducz et al., 2003), the ARC melanocortin neurons during changes in ghrelin levels (Pinto et al., 2004) and on the perikarya of GnRH neurons during changes in the gonadal steroid milieu (Zsarnovszky et al., 2001; Naftolin et al., 2007) or during changes in photoperiod lengths (Xiong et al., 1997). Our observations further support the notion that synaptic plasticity is a key component in the hypothalamic regulation of energy homeostasis and that, under pathological conditions, the synaptic constellation and its plasticity is impaired.

An important question is whether these synaptic alterations influence neuronal activity and, consequently, metabolic phenotype. Even if it does not directly affect action potentials, the changing input organization of NPY/AgRP and POMC perikarya should influence the setpoint of these cells under various circumstances. For example, a trans-synaptic excitatory signal is more likely to trigger an action potential if this input is located proximally with few surrounding inhibitory connections than if it is bordered by numerous inhibitory synapses. If the synaptic wiring indeed participates in determining the setpoint of the central feeding circuit rather than acutely determining postsynaptic activity, then it is possible that subjects who are sensitive to diet-induced obesity have a wiring and plasticity of the melanocortin system different from those who are resistant to obesity, even before obesity develops. If this is the case, then one could argue that developmental programming of hypothalamic circuits (Bouret et al., 2004) contributes not to obesity per se but to predisposing individuals to the development of obesity. For example, there is a critical developmental period during which the development of efferents from the melanocortin system is affected by leptin (Bouret et al., 2004). This event may affect the hardwiring of at least some parts of the feeding circuits, thereby determining the set point of this system.

Almost all of the asymmetric synapses on POMC perikarya were glutamatergic. It is known already, that estrogen increases the levels of AMPA glutamate receptors (GluR)

in the hypothalamus (Diano et al., 1997). Here we showed that all of the analyzed arcuate POMC neurons contained mostly subunit 1 of the AMPA glutamate receptors (GluR1). GluR1 incorporation into synapses is an important mechanism underlying long-term potentiation and experience-driven synaptic plasticity (Ehrlich and Malinow, 2004). GluR1 domination in arcuate POMC neurons predicts an increase in calcium influx upon glutamate binding of the receptor and a specific induction of the calcium binding protein, parvalbumin (Kondo et al., 1997). Indeed, we have found in our preliminary study that this might be the case.

Interestingly and informatively, estrogen's effect on energy regulation was effective in leptin mutant (*ob/ob*) and leptin-receptor mutant (*db/db*) mice consistent with previous observations (Dubuc, 1986; Grasa et al., 2000). The estrogen's effect in these obese animals is clearly suggesting that estrogen exerts its anti-obesity effect independent on leptin. Estrogen reduced body weight (selective to fat mass, not lean mass or linear body growth), decreased hyperphagia and parallel increased energy expenditure in *ob/ob* and *db/db* mice. Estrogen also increased basal body temperature (measured rectally) and fully normalized the dysfunction of inducible thermogenesis in these mice. Animals with a deficiency in brain-specific leptin signaling, such as the brain-specific STAT3-knockout mice, exhibit a similar defect, suggesting a central mode of control of these processes (Gao et al., 2004). Inducible thermogenesis is regulated mostly through the sympathetic nervous system and involves both brown and white adipose tissues (Bachmann et al., 2002). Together, our results argue that estrogen induces neuronal responses to lower the homeostatic set-point, rather than simply causing a taste aversion in wild-type and leptin-mutant mice (Flanagan-Cato et al., 2001).

We were able to demonstrate that, estrogen triggers robust increases in the number of excitatory synapses on the ARC POMC perikarya in *ob/ob* and *db/db* mice, mimicking leptin's effect on the rewiring POMC cells. This leads to a corresponding change in the electronic tone in these cells, measured as an increase in the events of random presynaptic release. These findings are suggesting that estrogen and leptin signals in regulating energy homeostasis are, in part, translated to similar synaptic adaptations in

the POMC neurons to induce an antiobese neuronal response. The STAT3 is thought to have a dominant role in the intracellular signal transduction of leptin's antiobesity effect. Our observations strongly support the notion that STAT3 proteins are positioned downstream of estrogen signaling in neurons and required for estrogen's antiobesity effect and estrogen and leptin signaling interact via these proteins.

In a recent study estrogen increases leptin-induced STAT3 activities in ARC neurons (Clegg, 2006). The brain-specific STAT3 knockout mice are obese and diabetic, highly resembling leptin mutant phenotypes (Gao et al.; 2004) and therefore provides a unique experimental system for dissecting the interactive mechanism between leptin-STAT3 and estrogen signaling. Surprisingly, unlike the leptin and leptin receptor deficiencies that are sensitive to estrogen's treatment, the brain STAT3 knockout mice were insensitive to estrogen treatment, indicates that the estrogen's effect in homeostasis is mediated centrally through the STAT3 pathway just like the leptin's one. Consistent with our findings, numerous other molecular endocrinology studies also indicated that STAT3 is a downstream target of estrogen signaling in various cellular systems (Bjornstrom and Sjoberg, 2002). Distinct molecular mechanisms by which estrogen activates STAT3 were observed. STAT3 is activated in response to estrogen treatment in cells (Bjornstrom and Sjoberg, 2002; Sekine et al., 2004). The cross-talk requires ERs and involves the mitogen-activated protein kinase (MAPK), Src-kinase and Phosphoinositide-3 kinase (PI3K) pathways. Other interactive mechanisms include direct association of ERs and STAT3 (Ciana et al., 2003). In a human neuroblastoma cell line, called SK-N-BE, ER $\alpha$  blocks the mitogenic effect of tumor growth factor- $\alpha$  (TGF- $\alpha$ ) signaling and induces differentiation independent of ER $\alpha$ 's DNA binding activity, but requires a transcriptionally active STAT3. In this process, ER $\alpha$  is directly associated with STAT3 (Ciana et al., 2003). Finally, ER $\alpha$  and STAT3 are known to associate with common co-regulators, such as CREB binding protein p300 (CBP/P300), and nuclear co-activator SRC1a (NcoA/SRC1a) (Robyr et al., 2000; Edwards, 2000). The interaction between ERs and STAT3 may, therefore, involve co-regulators. In any case, the ER-

STAT3 interaction provides “shortcut” mechanisms in which membrane associated receptors are bypassed.

Consistent with the aforementioned *in vitro* data, ER $\alpha$  has been suggested as the main ER that mediates estrogen’s antiobesity effect in both sexes (Geary et al., 2001). In the ARC, ER $\alpha$  is the dominant ER, and levels of ER $\beta$  are negligible (Osterlund et al., 1998). Notably, levels of circulating estrogen in obese ER $\alpha$ -null animals are 10 times higher than those in their wild-type littermates, revealing estrogen resistance in these mice. Our observations with ER $\alpha$ -null mice, when estrogen failed to increase the number of excitatory synapses on POMC perikarya in compared to the estrogen-treated *ob/ob* or *db/db* mice, further supported this notion.

In term of the intracellular mechanism of estrogen’s effect and the cross-talk between estrogen and leptin several interesting questions remain to be assessed in the future:

First, where do estrogen and leptin signaling meet? Whether STAT3 activation by estrogen occurs in LRB-expressing neurons, and if so, which subpopulation(s) of those neurons in the hypothalamus may be involved has not yet been assessed. Since ER $\alpha$  is found only in a subset of LRB-expressing neurons in the hypothalamic nuclei associated with feeding and metabolism, and estrogen’s effect on homeostasis is less potent than leptin, it is possible that estrogen only activates STAT3 in a subset of leptin-sensitive neurons in the hypothalamus. Similarly, estrogen may activate STAT3 in non-LRB neurons as well. This question is also related to the issue of whether estrogen signaling-STAT3 interaction is indeed occurring in the same cells, which is supported by cell culture studies, or whether it is a secondary effect.

Second, how do ERs trigger STAT3 phosphorylation in cells? Even if estrogen signaling and STAT3 directly interact (as acute phosphorylation of STAT3 by estrogen was observed both in cells and in the hypothalamus), it is not known how this process is accomplished in cells. Because ERs themselves are transcription factors possessing no tyrosine kinase activity, a tyrosine kinase must be activated upon estrogen administration. It was suggested that MAPK, Src kinase, and PI3K pathways were required for estrogen activation of STAT3 in cultured cells, but it is not clear how

estrogen via ERs triggers these pathways. We found that, in the hypothalamus, estrogen acutely activates Src kinase but does not affect the Janus kinases (JAKs) and other tyrosine kinases that are known to phosphorylate STAT3 (unpublished data). Src kinase is a potent tyrosine kinase known to directly bind to and phosphorylate STAT3. This raised the possibility that Src kinase may be the downstream effector of estrogen signaling in STAT3 phosphorylation. However, how does estrogen activate Src kinase through ERs, remains still unanswered.

Finally, how might estrogen and leptin regulate synaptology? One possibility is that both leptin and estrogen regulate genes involving synaptogenesis. Candidate genes such as postsynaptic density-95 (PSD-95), which regulates the balance between excitatory and inhibitory synapses in the primary neuronal cultures prepared from hippocampi of embryonic day 18/19 (Prange et al., 2004), and brain-derived neurotrophic factor (BDNF), a neurotrophin that regulates synaptic formation and function and has an anti-obesity effect (Rios et al., 2001). Both genes are regulated by estrogen *in vivo* (Akama and McEwen, 2003; Solum and Handa, 2002). PSD-95 is a protein that recruits the cAMP-dependent protein kinase (PKA) to the glutamate receptor complex through interaction with A-kinase-anchoring protein (AKAP79/150) (Colledge et al., 2000). The formation of the PSD-95/AKAP79/150 complexes is required for the regulation of activity and quantity on the cell surface of AMPA glutamate receptor, especially its subunit 1 (GluR1) (Colledge et al., 2000). We found that GluR1, but not GluR2, is associated with the excitatory synapses on POMC neurons of the ARC. PSD-95-controlled AMPA receptor incorporation to synapses is an important mechanism underlying long-term potentiation and experience-driven synaptic plasticity (Edwards, 2000); its role in energy homeostasis is not known. The role of BDNF in energy regulation, on the other hand, is well established (Rios et al., 2001; Friedel et al., 2005). It affects various aspects of homeostasis, including eating behavior (Kernie et al., 2000) and energy expenditure (Nonomura et al., 2001); however, the mechanism underlying this effect is not known. It would not be surprising that BDNF is involved in synaptic

plasticity in the melanocortin neurons associated with feeding. This also raises question of whether BDNF is involved in hypothalamic reproduction.

Whereas potential roles for recently uncovered membrane estrogen receptors (Qiu et al., 2006) in these synaptic alterations cannot be ruled out, our observations raise the possibility that decreased stimulation of ER $\alpha$  in menopausal conditions may confer susceptibility to weight gain. These mechanisms are targets of current studies.

While our studies focused on the ARC melanocortin system, it is important to emphasize that energy metabolism regulation from the brain is organized from various sites, which is not limited to the hypothalamus, but also includes other regions, most notably the brain stem (Schwartz, 2000; Grill and Kaplan, 2002). Thus, it is important to determine whether synaptic plasticity is characteristic of other systems in the adult brain that are associated with metabolic regulation.

Despite the amount of intellectual talent and monetary resources being directed to deeper understand the development of metabolic disorders and obesity, the medical breakthrough has not yet occurred. Whether or not it is reasonable to anticipate breakthrough discoveries in metabolism regulation (the dream of patients and the pharmaceutical industry!) will largely depend upon our ability to understand the fine points of the brain's role in the regulatory process and how these brain processes couple with the activity of peripheral tissues. Further research needed to address these issues.

## **5.2. Estrogen and the hypothalamic regulation of circadian rhythm**

The SCN is the master clock that generates and maintains circadian and seasonal rhythms by integrating changes in photic conditions to the brain. Estrogen has significant effects on the biological clock during both development and adulthood maintaining the synchrony of endocrine and autonomic mechanisms. We have shown that the locally formed estrogen's developmental effect on the biological clock is, at least in part, responsible for the sexually dimorphism of the adult SCN, and taking place mostly late prenatally at the peak of aromatase activity in the brain. During adulthood, estrogen modulates the light-induced activity of SCN neurons directly and/or indirectly through

the raphe serotonin system. Our data further support the notion, that estrogen is important for optimal responses of the biological clock to changes in environmental light.

Our experiments show that female control animals have more BrdU-labeled cells in the medial and caudal SCN than males, and that the testosterone regimen given in the present study dramatically decreases the number of BrdU-labeled cells across the female SCN. The developmental mechanisms that underlie the sex difference in BrdU-labeled cells within the SCN remain to be determined, although it is likely that steroid-induced apoptotic mechanisms play an important role in mediating this effect. Previous studies on sexual differentiation of other hypothalamic structures, such as AVPV or SDN-POA, point to a steroid hormone modulation of apoptosis as the main mechanism producing sexual dimorphism (Jacobson et al., 1985; Gorski et al., 1978; Arai et al., 1994). Most sexually dimorphic nuclei within the hypothalamus are larger in males than in females. In these nuclei, the estrogen that results from the aromatization of testosterone is thought to protect neurons from programmed cell death by increasing the production of anti-apoptotic proteins such as Bcl-2 (Zup et al., 2003), as well as by increasing the production of neuroprotective agents such as the calcium binding proteins (Stuart and Lephart, 1999; Brager et al., 2000). Interestingly, the development of the AVPV, which is larger in females than in males, is also affected by prenatal testosterone treatment (Sumida et al., 1993). In contrast to other sexually dimorphic hypothalamic regions, testosterone enhances cell death in the AVPV and perhaps in the SCN through mechanisms that include the modulation of the antiapoptotic protein Bcl-2, given that male mice overexpressing this protein have a larger AVPV than their control wild-type counterparts (Zup et al., 2003). Similarly, it has been proposed that the neuroprotective effects of aromatized androgens during development are mediated by their actions on cells containing ER $\alpha$ , whereas apoptosis of developing neurons may be mediated by the actions of these estrogens on ER $\beta$  (Nilsen et al., 2000). Given that cells in the SCN of neonatal rats contain predominantly ER $\beta$ , it is possible that estrogen-sensitive SCN cells in the neonatal rat undergo increased programmed cell death when aromatase and

testosterone levels peak. Alternatively, androgens and/or their metabolites may decrease neuronal proliferation in the SCN of gestating rats, advance the timing of SCN proliferation and/or differentiation, arrest proliferation at an earlier embryonic date, or disturb post-mitotic migration of cells to the SCN (Beyer et al., 1994; Beyer & Hutchison, 1997; Brannvall et al., 2002). Finally, proliferation or survival of SCN cells may be modulated indirectly by the action of testosterone or its metabolites at sites that are more sensitive to androgens or estrogen, and that project to the SCN, such as the AVPV, bed nucleus of the stria terminalis or the raphe nucleus (De La Iglesia et al., 1999; Bethea et al., 2002).

The neurochemical identity of SCN cells that develop on embryonic day 18 that are more numerous in female rats remains to be fully determined. Double immunocytochemistry studies were only effective in showing that BrdU-containing cells were heterogeneous in nature, with no specific phenotype being generated at the time of BrdU injection. The localization of BrdU cells in both core and shell suggested that these cells would express VIP in the core, AVP in the shell and calbindin D (28K) in both core and shell (Moore et al., 2002). Although BrdU-labeled cells were primarily concentrated in the dorsal core region and shell of the SCN, cells that were expressed in the ventral SCN co-localized with VIP neurons. Studies addressing cell proliferation in rats and hamsters have shown that the ventral portion of the SCN develops earlier than the dorsal portion, although some cells proliferate in this region late in gestation (Altman and Bayer, 1986). Although VIP cells can be detected early in SCN development (Botchkina and Morin, 1995a), our results show that a small portion of VIP neurons are generated late in rat SCN development.

It remains unclear whether the cells labeled with BrdU on embryonic day 18 produce vasopressin. Although there were some cells that showed both AVP and BrdU, these were few in number. Given that proliferation of neurons in the shell portion of the SCN appears to peak at an earlier gestational age (Altman and Bayer, 1986) this finding is not particularly surprising. Nevertheless, AVP-immunoreactive fibers in the SCN often obscured cell body labeling and made the detection of the double staining difficult.

Of particular interest was the finding revealed by double immunocytochemical studies that some BrdU-labeled cells also expressed calbindin-D (28K) immunoreactivity. Calbindin-D (28K) belongs to a family of calcium-binding proteins implicated in developmental mechanisms underlying neuronal cell fate such as apoptosis, proliferation and protection from neurochemical insults (Mattson, 1992). Immunoreactivity for calbindin-D (28K) is highly expressed in the SCN of neonatal mice, but not in adults (Ikeda and Allen, 2003). Interestingly, the hypothalamic expression of this protein is sexually dimorphic in late gestation and early in postnatal life, with males having more calbindin-D28K expression from E17 to PN2 (Lephart, 1996; Stuart and Lephart, 1999). Considering these data, it is possible that calbindin-D (28K), or other calcium-buffering proteins, participates in the mechanisms that determine the sexually dimorphic proliferation/survival of cells within the SCN.

Because the IGL of adult females has been found to synthesize steroid hormone receptors, and to be connected with neuroendocrine cell groups that are involved in sexually differentiated physiological functions (Horvath et al., 1999), it was expected that BrdU labeling would reveal sex differences in this region. Unlike the SCN, however, the IGL did not show a sex difference in the number of BrdU-labeled cells on embryonic day 18. Moreover, there were few cells labeled with BrdU in the animals used in the present study, suggesting that proliferation of cells within this region occurs at a different time than in the SCN (Botchkina and Morin, 1995b). Nevertheless, the lack of an effect in the IGL does not preclude the possibility that retinal inputs into the IGL as well as the distribution of axons that originate from the IGL are sexually differentiated.

Also of interest were the findings that BrdU was expressed in both VIP- and AVP-secreting cells. Although it remains to be determined if BrdU is differentially expressed in VIP and AVP cells in the SCN of male and female rats, both of these peptidergic systems are known to be sexually differentiated, and these differences underlie sex-specific physiological and behavioural aspects of reproduction (Van der Beek et al., 1997; Horvath et al., 1998; Kalsbeek and Buijs, 2002). Our results leave the door open

for the speculation that there are sex differences in the neurogenesis and/or survival of cells producing these peptides.

In term of the adulthood effect of estrogen, we demonstrated that estrogen replacement enhances neuronal responses to a phase advance in the onset of light. Thus, the mean number of Fos- and p-CREB-immunoreactive cells seen in the SCN of estrogen-treated female rats exposed to light 2 h prior to their regular lights on schedule were higher than the means seen in cholesterol treated controls. While the phase advance increased the levels of *egr-1* and calbindin-D (28K) in the SCN of the same animals, estrogen had no effect in the expression of these proteins.

The expression of Fos and p-CREB has been linked to the molecular mechanisms that regulate the circadian expression of clock genes and their entrainment to changes in light from the environment (Aronin et al., 1990; Gau et al., 2002; Kako and Ishida, 1998). The activation of retinal ganglion cells by light results in the release of glutamate from their terminals in the ventral portion of the SCN. This, in turn, stimulates glutamate receptor subtypes and causes the rapid influx of calcium into the cell that, through the activation of calcium signaling intracellular pathways, results in the phosphorylation of CREB, and the transcription of the message for Fos (Gillette and Mitchell, 2002; Kako and Ishida, 1998). The data presented here suggest that estrogen enhances the responses of ventral SCN cells to glutamatergic inputs. This study, however, cannot discern if the estrogen-induced enhanced expression of Fos and p-CREB is due to increased glutamate release from retinal fibers, increased sensitivity of SCN cells to glutamate, or to changes in the degree of signaling that occurs following the glutamate-dependant calcium influx into SCN cells.

The expression of *egr-1* and calbindin-D (28K) was increased by the 2-h phase advance in both the estrogen-treated and control animals. These results confirm that previous data demonstrating that the SCN expression of both *egr-1* and calbindin-D (28K) are enhanced by changes in photic conditions and play a role in the synchronization of the circadian master clock to changes in light schedules (Arvanitogiannis et al., 2000; Guido et al., 1999). Nevertheless, the overall expression of *egr-1* in the SCN was considerably

low. Given that the expression of the message for *egr-1* in the SCN peaks 2 h after photic stimulation (Guido et al., 1999), it remains possible that the time at which the animals were sacrificed in the present study was not appropriate for the detection of differences in the immunoexpression of *egr-1* after estrogen treatment.

The expression of the coactivator protein CBP in the SCN was not altered by either the phase shift in photic information, or by the hormone treatment. While this is a protein that has been previously reported to potentiate p-CREB-mediated transcription in estrogen sensitive tissues (Fiore and Gannon, 2003), it seems that it does not play a similar role in response to estrogen treatment, and a to a phase advance. Although there are changes in the daily expression of CBP in the SCN, CBP expression appears to peak during the dark phase and to decrease by the middle of the light phase, perhaps playing a role in the downstream regulation of clock genes, but not in the entrainment to light. Whether other coactivator proteins serve to enhance p-CREB-mediated transcription remains to be determined. It is interesting that CBP immunoreactivity in the IGL was decreased while p-CREB immunoreactivity was increased by the advance in the onset of photic stimulation, suggesting that this coactivator is recruited in p-CREB-mediated transcription in this region. Nevertheless, the increases in p-CREB immunoreactivity in the IGL were not followed by increases in either Fos or *egr-1* expression, perhaps because photic induced neuronal activation of IGL cells is attained via p-CREB-mediated transcription signaling pathways that do not increase the transcription of the *c-fos* or *egr-1* genes.

These findings suggest that estrogen is important for optimal responses of the master clock to changes in environmental light. They also provide for a mechanism underlying previously reported effects of estrogen on circadian rhythms of activity. For example, the present data may explain the clear changes seen in activity rhythms of female rodents across the estrous cycle, and the shortening of the circadian period by estrogen treatment to OVX female rats (Albers, 1981). Interestingly, estrogen treatment to OVX female rodents prevents the split in circadian rhythms of locomotion that is seen under prolonged constant light conditions, suggesting that estrogen acts as a coupling agent

within the SCN (Morin and Cummings, 1982). Indeed, estrogen treatment increases the expression of connexin-46 in the SCN, leading to the speculation that estrogen can synchronize the activity of SCN cells by increasing gap junction-mediated cell to cell communication (Shinohara et al., 2000; Shinohara et al., 2001). This, in addition to experiments where gap junction blockers disrupt light-induced phase shifts (Michel and Colwell, 2001), suggests that a decrease in circulating estrogen may therefore lead to asynchrony in SCN responses to changes in environmental light and ultimately result in altered circadian rhythms such as those seen in aging animals, including humans (Wise et al., 2002). Given that disruptions of circadian and seasonal rhythms are associated with a myriad of pathological conditions including sleep disorders, depression, addiction, and various neurological and endocrine conditions, further examination of the effects of hormones on the circadian system are fully warranted (Bunney and Bunney, 2000; Turek et al., 2001).

In our studies, estrogen was given systemically, and, therefore, it remains unclear whether estrogen was acting directly upon the SCN, or indirectly on afferents to the SCN, to enhance Fos and p-CREB immunoreactivity. The SCN expresses the message for the ER $\beta$  receptor subtype, albeit at low levels (Shughrue et al., 1997; Mitra et al., 2003). Nevertheless, the activity of the SCN could be modulated by estrogen sensitive regions that project to the SCN. One region that could possibly modulate neuronal responses in the SCN is the raphe nucleus, which contains estrogen receptors (Leranth et al., 1999; Bethea et al., 2002; Mitra et al., 2003), sends a strong serotonergic projection to the SCN to regulate circadian rhythms (Pickard et al., 1996; Pickard and Rea, 1997; Meyer-Bernstein and Morin, 1999; Morin, 1999; Lu et al., 2001; Hay-Schmidt et al., 2003) and receives direct projections from the retina (Shen and Semba, 1994). In addition, estrogen-sensitive cells within the preoptic area and the AVPV also project to the SCN, and, hence, could indirectly have an effect in modulating the responses of the SCN to photic stimulation (De La Iglesia et al., 1999). Interestingly, it has been suggested that behavioral activity may interact with photic information to regulate circadian rhythms and immediate early gene expression in the SCN of rodents

(Mrosovsky, 1989; Mikkelsen et al., 1998). Given that both endogenous and exogenous estrogen increase spontaneous locomotor activity as well as various measures of arousal in female rats (Ogawa et al., 2003), it is also possible that the estrogen-induced enhancement of the expression of transcription factors in the SCN is mediated through estrogen sensitive regions that underlie arousal-mediated phase shifts (Ruiz de Elvira et al., 1992). This proposition is particularly intriguing given that both the raphe and the preoptic area: (1) are estrogen sensitive (2) project to the SCN and (3) play a role in the mechanisms that regulate locomotor activity (Mistlberger et al., 2000; Fahrbach et al., 1985).

Here we investigated the putative role of the midbrain raphe; whether hormonal information is integrated in the raphe nucleus to modulate responses to changes in photic stimulation. We demonstrated that, an advance in the onset of light increased the expression of the activity marker Fos in the DRN. Although overall Fos expression in the DRN was not altered by estrogen treatment, the proportion of 5-HT neurons that expressed Fos in the lateral and medial portions of the DRN after phase shift was increased in estrogen-treated animals. However, the MRN is not sensitive to either the phase shift or estrogen treatment.

Indeed, previous studies have shown that the DRN of several rodent species receives direct retinal inputs, particularly the lateral DRN (Shen and Semba, 1994; Fite et al., 1999). Moreover, 5-HT neurons show a short-lived increase in excitatory activity after light flashes and there are clear circadian patterns of activity in DRN neurons (Rasmussen et al., 1986; Cagampang et al., 1993). Therefore, the present findings support the idea that 5-HT neurons in the DRN are sensitive to photic stimulation and that light modulates daily fluctuations in a variety of functions either through connections between the raphe and the circadian pacemaker, the SCN (Prosser et al., 1994; Kennaway and Moyer, 1998; Kohler et al., 1999; Morin, 1999), or via the projections of the raphe throughout the central nervous system (Vertes, 1991; Vertes et al., 1999). The effect of light on Fos expression in the DRN may therefore be mediated by the direct retinal projections to this region, in addition to indirect retinal multisynaptic

pathways that ultimately target the DRN (Jacobs and Azmitia, 1992; Hermann et al., 1997).

Taking together with the aforementioned evidences our data further support the notion, that neurons within the DRN, particularly the lateral DRN, play a role integrating photic information with hormonal cues to modulate 5-HT release and ultimately circadian rhythms of activity in female rodents (Morin et al., 1977; Albers, 1981; Morin and Cummings, 1982; Meyer-Bernstein and Morin, 1999). However, it is not known whether estrogen acts directly on 5-HT cells or indirectly on other neighboring cell groups within the DRN. It is noteworthy that, although the phase shift increased the proportion of 5-HT cells that expressed the Fos protein, many Fos-immunoreactive cells observed in this study appeared to be non-serotonergic, indicating that the phase shift may also alter Fos expression in other cell types within the DRN. In addition, while estrogen increased the number of 5-HT cells that expressed Fos in the DRN, it did not enhance overall Fos expression in this or any other raphe nucleus. This would suggest that estrogen increases gene transcription in 5-HT neurons while decreasing the activation of neighboring non-serotonergic cells. This may indeed be the case in lateral DRN, where the proportion of Fos-immunoreactive cells seen in 5-HT neurons increased in response to estrogen treatment even though the total number of Fos-immunoreactive cells was not affected by estrogen. One possibility is that the phase advance and/or estrogen also modulate the expression of Fos in GABAergic cells, given that many neurons in the DRN contain GABA and that these modulate the activity of DRN 5-HT cells (Tortero et al., 2000). In addition, neurons within the DRN also express a variety of neurotransmitters and peptides that may be differentially expressed and/or activated after a phase shift and under varying hormonal conditions (Jacobs and Azmitia, 1992).

Differences in the expression of Fos due to the phase shift and in the presence of estrogen were evident in the DRN but not in the MRN of OVX rats. Nonetheless, the MRN appears to provide the primary serotonergic innervations to the SCN (Meyer-Bernstein and Morin, 1996, 1998; Dudley et al., 1999; Hay-Schmidt et al., 2003) and 5-HT cells in the MRN contain estrogen receptors (Leranth et al., 1999). Lesions of the

DRN, however, alter circadian rhythms of activity in rodents by decreasing 5-HT levels in the SCN (Kam and Moberg, 1977; Szafarczyk et al., 1980). In addition, electrical stimulation of the DRN produces 5-HT release and inhibits light-induced Fos expression in the SCN (Meyer-Bernstein and Morin, 1998; Dudley et al., 1999) indicating that both DRN and MRN neuronal changes influence SCN activity. The existence of intensive reciprocal serotonergic connections between the MRN and DRN is also known (Vertes, 1991; Vertes et al., 1999; Glass et al., 2003). While the direct DRN→SCN projection is weak by comparison, the DRN may influence the activity of the SCN via a multisynaptic DRN→MRN→SCN pathway as described previously (Dudley et al., 1999; Glass et al., 2003). Interestingly, most 5-HT projections from the DRN target the intrageniculate leaflet and are thought to play a role in the non-photoc entrainment of circadian rhythms via this pathway (Meyer-Bernstein and Morin, 1996, 1998). Therefore, 5-HT cells in the DRN could also influence the circadian system by another multisynaptic pathway to the SCN through the intrageniculate leaflet (DRN→intrageniculate leaflet→SCN).

While our data suggests that the activity of 5-HT neurons in the raphe is directly affected by photic and hormonal stimuli, it is also possible that the effects of photic stimulation and estrogen on Fos expression in the raphe could result indirectly from changes in locomotor activity that, in turn, modulate the activity of serotonergic cells (Ruiz de Elvira et al., 1992; Mikkelsen et al., 1998; Mistlberger et al., 2000). Nevertheless, the expression of Fos in the raphe appears to be increased after forced locomotor activity (Brudzynski and Wang, 1996). These results would predict that a decrease in locomotor activity after a phase advance in the onset of light would result in a decrease in Fos expression within the DRN, a result that would be in sharp contrast to those obtained in our studies. While our findings cannot determine the mechanisms by which the photic and hormonal stimuli affect gene expression in the DRN, it could be argued that photic stimulation upon the retina induces Fos expression in the raphe via a direct monosynaptic connection given that Fos expression is concurrently enhanced at other brain sites targeted by the retina in a paradigm similar to that followed in our study. Estrogen, however, increases locomotor activity in females and may enhance the effect

of light on Fos expression in the DRN through non-photic mechanisms (Gerall et al., 1973; Ruiz de Elvira et al., 1992). The complex interaction between photic and hormonal cues in the regulation of neuronal activity in the DRN and the ultimate consequences of this interaction on behavioral outputs warrant further investigation.

In both animals and humans, alterations in circadian rhythms, sleep/arousal patterns, mood and learning and memory are often reported after a drop in circulating estrogen levels (Wise et al., 2002). Chronically, however, these alterations are the hallmark of affective disorders such as depression, a psychiatric disorder that has been linked to abnormal function in the 5-HT neuronal system (Halbreich and Kahn, 2001; Parry and Newton, 2001; Gibbs and Gabor, 2003). Moreover, the marked sex differences in the prevalence of affective disorders suggest that a better understanding of how the serotonergic system responds to sensory stimulation, and the role of estrogen in modulating these responses, is crucial in devising better treatment strategies.

The appropriate entrainment of brain functions to the environment is normally achieved by the circadian clock. Altered activity of the biological clock in the absence of gonadal hormones may be a key trigger in initiating and maintaining the discomforting side effects of gonadal failure including post partum depression, premenstrual and perimenopausal mood swings and hot flushes. In light of the fact that interactions between the biological clock and the neuroendocrine hypothalamus seem to share similarities in rats and higher primates, the results gained in our studies could guide further research and help to establish a fundamental hormone-dependent mechanism by which the biological clock functions. This, in turn, may offer new avenues to enhance the clinical management of the aforementioned sexually dimorphic symptoms.

## 6. CONCLUSIONS

Our findings provided key evidences to better understand the mechanism of estrogen's effect on the central control of homeostasis and circadian rhythm, which might be highly relevant in the clinical setting. The followings are our most important conclusions.

### *Estrogen's effect on energy homeostasis*

1. We were first able to demonstrate that estrogen increases excitatory synapses on the hypothalamic POMC perikarya. This effect is similar what was seen after leptin administration to leptin deficient animals.
2. Almost all of these excitatory synapses are glutamatergic, the vast majority of them mediated by GluR1. These receptors are thought to be responsible for the specific induction of the calcium binding protein, parvalbumin.
3. In parallel with the morphological effect on synapses, estrogen enhances the activity of POMC neurons in the ARC.
4. Estrogen is able to change the synaptology of POMC neurons under physiological conditions as well during the rodent estrus cycle further supporting the notion, that synaptic plasticity has an element role in the hypothalamic regulatory systems.
5. We also clearly demonstrated, that the temporal kinetics of the synaptic rewiring induced by estrogen correlate well with the dynamics of the feeding behavior.
6. The estrogen-induced synaptic changes on POMC neurons are reflected also at the electrophysiological level. This finding is further supporting our hypothesis.
7. Furthermore, we demonstrated that estrogen-triggered anorexigenic behavior is completely independent of leptin.
8. One of our major discoveries is that estrogen mimics leptin's effect on the rewiring of POMC neurons and enhancing their tones. This finding further support the notion that the synaptic plasticity has a major role in the hypothalamic control of energy homeostasis.

9. In term of intracellular mechanism we have presented evidence, that estrogen activates the downstream target of leptin signaling, STAT3, independent of leptin.
10. And finally, our data strongly suggest, that estrogen's antiobesity effect on synapses of melanocortin system is mediated mostly by the ER $\alpha$ .

These observations unveiled, that the estrogen's antiobesity effect is mediated through a rapid synaptic changes of the hypothalamic feeding circuits independent of leptin, supporting the notion that the synaptic plasticity of ARC feeding circuits is an inherent element in the hypothalamic regulation of energy homeostasis. Our findings may offer alternative approaches to reducing adiposity under conditions of failed leptin receptor signaling.

#### *Estrogen's effect on the biological clock during early development*

1. The number and the distribution of SCN neurons, which are newly originated during the late prenatal period, are gender specific. Female animals have more BrdU-labeled cells in the medial and caudal SCN than males. However, no sex differences are seen in the IGL.
2. Testosterone treatment during the late prenatal period reverses this sex difference in the SCN suggesting that the sex difference was dependent on the prenatal presence of testosterone and the degree of aromatisation. No such an effect was observed in the IGL.
3. By investigating the phenotypical characterization of these newly originated cells in the SCN, we showed that these cells expressing calbindin-D (28K), VIP and, to a lesser degree AVP, suggesting that these cells are primarily involved in the sex dimorphic functions of the circadian clock.

We have shown that the locally formed estrogen's developmental effect on the biological clock is, at least in part, responsible for the sexually dimorphism of the adult SCN, and taking place mostly late prenatally at the peak of aromatase activity in the brain. Our results unveiled a previously unknown effect of gonadal steroids on the

developing SCN, which may contribute to the emergence of gender-specific circadian rhythms.

*Estrogen's effects on the biological clock during adulthood*

1. Estrogen modulates the light-induced expression of various transcription factors in the SCN but not in the IGL.
2. Changes in the onset of light enhances the activity of the neurons in the raphe nuclei and this effect is modulates by estrogen.

Our observations demonstrated that estrogen modulates the light-induced activity of SCN neurons directly or indirectly through the raphe serotonin system. These data further support the notion, that estrogen is important for optimal responses of the biological clock to changes in environmental light.

## 7. SUMMARY

In addition to its well-described key role in the regulation of reproductive function, estrogen significantly modulates a variety of centrally regulated physiological functions. Cessation of ovarian function (natural or iatrogenic menopause) leads to imbalanced energy homeostasis favoring obesity and altered circadian rhythms. Estrogen is a potent antiobesity hormone that reduces food intake and increases energy expenditure. Its effect is comparable to leptin, which is believed to be the most potent anorectic. Estrogen also maintains the synchrony of endocrine and autonomic mechanisms by modulating the function of the biological clock in the suprachiasmatic nucleus (SCN) of the hypothalamus. The mechanisms, however, underlying these effects are not well understood. The aim of my thesis was to identify these mechanisms. Here we report that estrogen triggers a prompt and robust increase in the number of excitatory synapses on the proopiomelanocortin neurons in the hypothalamic arcuate nucleus, causing a decrease in food intake and body weight similar to leptin. This synaptic rearrangement is leptin independent since it was also observed in leptin-mutant obese animals. This effect seems to be mediated by the estrogen receptor  $\alpha$  (ER $\alpha$ ) and by the signal transducer and activator of transcription 3 molecule (STAT3). These above findings support the notion that the synaptic plasticity of feeding circuits is an inherent element in energy homeostasis regulation. Here we have also shown that locally formed estrogen has a developmental effect on the biological clock, and it may contribute to the emergence of gender-specific circadian rhythms. This effect takes place mostly late prenatally at the peak of aromatase activity in the brain. In the adult SCN estrogen enhances the light-induced activity of neurons. Estrogen might act directly on the SCN, and/or indirectly through the raphe serotonin system. The impressive developments of knowledge about these pathways suggest that targeting the estrogen cascade could be a real addition to the treatment of metabolic disorders and biological rhythm abnormalities.

## ÖSSZEFOGLALÁS

A reprodukció szabályozásában betöltött szerepén kívül az ösztrogén számos központilag szabályozott élettani funkcióra van hatással. A petefészkek működésének megszűnése (természetes vagy orvosi eredetű menopauza) az energiahomeosztázis megbomlásához, elhízáshoz és a circadián ritmus zavaraihoz vezet. Az ösztrogén egy erős elhízás elleni hormon, hatását a táplálékfelvétel csökkentése és az energialeadás növelése révén valósítja meg. Hatásának erőssége összemérhető a leptinével, amit a legjelentősebb anorexigén hormonnak tartunk számon. Az ösztrogén továbbá számottevő hatással van a hipotalamusz suprachiasmaticus nukleuszában (SCN) található biológiai óra működésére is, ahol az endocrin és az autonóm mechanizmusok összehangolásáért felelős. Az ösztrogén fenti hatásainak mechanizmusa azonban nem ismert pontosan. A disszertációm célja ezen mechanizmusok vizsgálata volt. Eredményeinkből kitűnik, hogy az ösztrogén egy gyors és robusztus növekedést vált ki a hipotalamikus arcuate nukleuszban található proopiomelanocortin neuronok serkentő szinapszisainak számában, és ezáltal valósul meg a táplálékfelvétel és a testsúly csökkenése csakúgy, mint a leptin esetében. Ez a szinaptikus átrendeződés azonban a leptintől függetlenül valósul meg, mivel a leptin-mutáns elhízott állatokban is megfigyelhető. A hatásmechanizmusában az  $\alpha$  típusú ösztrogén receptor ( $ER\alpha$ ) és a STAT3 molekula játszhatnak meghatározó szerepet. Ezek a megfigyelések alátámasztják azt a hipotézist, miszerint a szinaptikus plaszticitás az energiahomeosztázis szabályozásának egy jellemző eleme. Másfelől kimutattuk, hogy a lokálisan képződött ösztrogénnek fontos hatása van a biológiai óra fejlődésére, így járulva hozzá a nemre specifikus circadian ritmus kialakulásához. Ez a hatás a késői praenatalis korban következik be amikor az aromatáz enzim aktivitása a csúcson van az agyban. A felnőtt SCN esetében az ösztrogén képes serkenteni a fény által kiváltott neurális aktivitást. Ez létrejöhet direkt hatás következtében és/vagy indirekt mechanizmuson keresztül a raphe szerotonin rendszer közreműködésével. Eredményeink felvetik annak a lehetőségét, hogy az ösztrogén kaszkád terápiás célbavétele hasznos lehet a metabolikus betegségek és a biológiai ritmuszavarok kezelésében.

## 8. REFERENCES

1. Abizaid A, Liu ZW, Andrews ZB, Shanabrough M, Borok E, Elsworth JD, Roth RH, Sleeman MW, Picciotto MR, Tschöp MH, Gao XB, Horvath TL. (2006) Ghrelin modulates the activity and synaptic input organization of midbrain dopamine neurons while promoting appetite. *J Clin Invest*, 116: 3229-3278.
2. Ainslie DA, Morris MJ, Wittert G, Turnbull H, Proietto J, Thorburn AW. (2001) Estrogen deficiency causes central leptin insensitivity and increased hypothalamic neuropeptide Y. *Int J Obes Relat Metab Disord*, 25: 1680-1688.
3. Akama KT, McEwen BS. (2003) Estrogen stimulates postsynaptic density-95 rapid protein synthesis via the Akt/protein kinase B pathway. *J Neurosci*, 23: 2333-2339.
4. Albers HE. (1981) Gonadal hormones organize and modulate the circadian system of the rat. *Am J Physiol*, 214: 62-66.
5. Albers HE, Moline ML, Moore-Ede MC. (1984) Sex differences in circadian control of LH secretion. *J Endocrinology*, 100: 101-105.
6. al-Shamma HA, De Vries GJ. (1996) Neurogenesis of the sexually dimorphic vasopressin cells of the bed nucleus of the stria terminalis and amygdala of rats. *J Neurobiol*, 29: 91-98.
7. Altman J, Bayer SA. (1986) The development of the rat hypothalamus. *Adv Anat Embryol Cell Biol*, 100: 1-178.
8. Anand BK, Brobeck JR. (1951) Localization of a feeding center in the hypothalamus of the rat. *Proc Soc Exp Biol Med*, 77: 323-324.
9. Arai Y, Murakami S, Nishizuka M. (1994) Androgen enhances neuronal degeneration in the developing preoptic area: apoptosis in the anteroventral periventricular nucleus (AVPvN-POA). *Hormones Behav*, 28: 313-319.
10. Aronin N, Sagar SM, Sharp FR, Schwartz WJ. (1990) Light regulates expression of a Fos-related protein in rat suprachiasmatic nuclei. *Proc Natl Acad Sci USA*, 87: 5959-5962.

11. Arvanitogiannis A, Robinson B, Beaulieu C, Amir S. (2000) Calbindin-D28k immunoreactivity in the suprachiasmatic nucleus and the circadian response to constant light in the rat. *Neuroscience*, 99: 397-401.
12. Asarian L, Geary N. (2002) Cyclic estradiol treatment normalizes body weight and restores physiological patterns of spontaneous feeding and sexual receptivity in ovariectomized rats. *Horm Behav*, 42: 461-471.
13. Asarian L, Geary N. (2006) Modulation of appetite by gonadal steroid hormones. *Phil Trans R Soc B*, 361: 1251-1263.
14. Augoulea A, Mastorakos G, Lambrinoudaki I, Christodoulakos G, Creatsas G. (2005) Role of postmenopausal hormone replacement therapy on body fat gain and leptin levels. *Gynecol Endocrinol*, 20: 227-235.
15. Bachman ES, Dhillon H, Zhang CY, Cinti S, Bianco AC, Kobilka BK, Lowell BB. (2002)  $\beta$ AR signaling required for diet-induced thermogenesis and obesity resistance. *Science*, 297: 843-845.
16. Benoit S, Schwartz M, Baskin D, Woods SC, Seeley RJ. (2000) CNS melanocortin system involvement in the regulation of food intake. *Horm Behav*, 37: 299-278.
17. Bethea CL, Lu NZ, Gundlach C, Streicher JM. (2002) Diverse actions of ovarian steroids in the serotonin neural system. *Front Neuroendocrinol*, 23: 41-100.
18. Beyer C, Green S, Hutchison J. (1994) Androgens influence sexual differentiation of embryonic mouse hypothalamic aromatase neurons in vitro. *Endocrinology*, 135: 1220-1226.
19. Beyer C, Hutchison JB. (1997) Androgens stimulate the morphological maturation of embryonic hypothalamic aromatase-immunoreactive neurons in the mouse. *Dev Brain Res*, 98: 74-81.
20. Bjornstrom L, Sjoberg M. (2002) Signal transducers and activators of transcription as downstream targets of nongenomic estrogen receptor actions. *Mol Endocrinol*, 16: 2202-2214.

21. Botchkina GI, Morin LP. (1995a) Ontogeny of radial glia, astrocytes and vasoactive intestinal peptide immunoreactive neurons in hamster suprachiasmatic nucleus. *Dev Brain Res*, 86: 48-56.
22. Botchkina GI, Morin LP. (1995b) Specialized neuronal and glial contributions to development of the hamster lateral geniculate complex and circadian visual system. *J Neurosci*, 15: 190-201.
23. Bouret SG, Draper SJ, Simerly RB. (2004) Trophic action of leptin on hypothalamic neurons that regulate feeding. *Science*, 304: 108-110.
24. Brager DH, Sickel MJ, McCarthy MM. (2000) Developmental sex differences in calbindin-D (28K) and calretinin immunoreactivity in the neonatal rat hypothalamus. *J Neurobiol*, 42: 315-322.
25. Brown TJ, Naftolin F, Maclusky NJ. (1992) Sex differences in estrogen receptor binding in the rat hypothalamus: effects of subsaturating pulses of estradiol. *Brain Res*, 578: 129-134.
26. Brown-Grant K, Raisman G. (1977) Abnormalities in reproductive function associated with destruction of the suprachiasmatic nuclei in female rats. *Proc R Soc London*, 198: 279-296.
27. Brudzynski SM, Wang D. (1996) C-Fos immunohistochemical localization of neurons in the mesencephalic locomotor region in the rat brain. *Neuroscience*, 75: 793-803.
28. Bunney WE, Bunney BG. (2000) Molecular clock genes in man and lower animals: possible implications for circadian abnormalities in depression. *Neuropsychopharmacology*, 22: 335-345.
29. Bunt SM, Lund RD, Land PW. (1983) Prenatal development of the optic projection in albino and hooded rats. *Dev Brain Res*, 6: 149-168.
30. Butera PC, Czaja JA. (1984) Intracranial estradiol in ovariectomized guinea pigs: effects on ingestive behaviors and body weight. *Brain Res*, 322: 41-48.
31. Cagampang FR, Yamazaki S, Otori Y, Inouye SI. (1993) Serotonin in the raphe nuclei: regulation by light and an endogenous pacemaker. *Neuroreport*, 5: 49-52.

32. Carr MC. (2003) The emergence of the metabolic syndrome with menopause. *J Clin Endocrinol Metab*, 88: 2404-2411.
33. Ciana P, Di Luccio G, Belcredito S, Pollio G, Vegeto E, Tatangelo L, Tiveron C, Maggi A. (2001) Engineering of a mouse for the in vivo profiling of estrogen receptor activity. *Mol Endocrinol*, 15: 1104-1113.
34. Clegg DJ, Brown LM, Woods SC, Benoit SC. (2006) Gonadal hormones determine sensitivity to central leptin and insulin. *Diabetes*, 55: 978-987.
35. Coleman DL. (1978) Obese and diabetes: two mutant genes causing diabetes-obesity syndromes in mice. *Diabetologia*, 14: 141-178.
36. Coleman DL, Hummel KP. (1969) Effects of parabiosis of normal with genetically diabetic mice. *Am J Physiol*, 217: 1298-1304.
37. Colledge M, Dean RA, Scott GK, Langeberg LK, Haganir RL, Scott JD. (2000) Targeting of PKA to glutamate receptors through a MAGUK-AKAP complex. *Neuron*, 27: 107-119.
38. Colvin GB, Sawyer CH. (1969) Induction of running activity by intracerebral implants of estrogen in ovariectomized rats. *Neuroendocrinology*, 4: 309-320.
39. Couse JF, Curtis SW, Washburn TF, Lindzey J, Golding TS, Lubahn DB, Smithies O, Korach KS. (1995) Analysis of transcription and estrogen insensitivity in the female mouse after targeted disruption of the estrogen receptor gene. *Mol Endocrinol*, 9: 1441-1454.
40. De La Iglesia HO, Blaustein JD, Bittman EL. (1999) Oestrogen receptor-alpha-immunoreactive neurones project to the suprachiasmatic nucleus of the female Syrian hamster. *J Neuroendocrinol*, 11: 481-490.
41. Diano S, Naftolin F, Horvath TL. (1997) Gonadal steroids target AMPA glutamate receptor-containing neurons in the rat hypothalamus, septum and amygdala: a morphological and biochemical study. *Endocrinology*, 138: 778-789.
42. Diano S, Kalra SP, Sakamoto H, Horvath TL. (1998) Leptin receptors in estrogen receptor-containing neurons of the female rat hypothalamus. *Brain Res*, 812: 256-259.

43. Diano S, Farr SA, Benoit SC, McNay EC, da Silva I, Horvath B, Gaskin FS, Nonaka N, Jaeger LB, Banks WA, Morley JE, Pinto S, Sherwin RS, Xu L, Yamada KA, Sleeman MW, Tschöp MH, Horvath TL. (2006) Ghrelin controls hippocampal spine synapse density and memory performance. *Nat Neurosci*, 9: 381-388.
44. Dudley TE, Dinardo LA, Glass JD. (1999) In vivo assessment of the midbrain raphe nuclear regulation of serotonin release in the hamster suprachiasmatic nucleus. *J Neurophysiol*, 81: 1469-1477.
45. Dubuc PU. (1985) Effects of estrogen on food intake, body weight, and temperature of male and female obese mice. *Proc Soc Exp Biol Med*, 180: 468-473.
46. Edwards DP. (2000) The role of coactivators and corepressors in the biology and mechanism of action of steroid hormone receptors. *J Mammary Gland Biol Neoplasia*, 5: 307-324.
47. Ehrlich I, Malinow R. (2004) Postsynaptic density 95 controls AMPA receptor incorporation during long-term potentiation and experience-driven synaptic plasticity. *J Neurosci*, 24: 916-927.
48. Fahrbach S, Meisel RL, Pfaff DW. (1985) Preoptic implants of estradiol increase wheel running but not the open field activity of female rats. *Physiol Behav*, 35: 985-992.
49. Fiore P, Gannon RL. (2003) Expression of the transcriptional coactivators CBP and p300 in the hamster suprachiasmatic nucleus: possible molecular components of the mammalian circadian clock. *Brain Res Mol Brain Res*, 111: 1-7.
50. Fite KV, Janusonis S, Foote W, Bengston L. (1999) Retinal afferents to the dorsal raphe nucleus in rats and Mongolian gerbils. *J Comp Neurol*, 414: 469-484.
51. Flanagan-Cato LM, Grigson PS, King, JL. (2001) Estrogen-induced suppression of intake is not mediated by taste aversion in female rats. *Physiol Behav*, 72: 549-558.
52. Friedel S, Fontenla Horro F, Wermter AK, Geller F, Dempfle A, Reichwald K, Smidt J, Bronner G, Konrad K, Herpertz-Dahlmann B, Warnke A, Hemminger U, Linder M, Kiefl H, Goldschmidt HP, Siegfried W, Remschmidt H, Hinney A,

- Hebebrand J. (2005) Mutation screen of the brain derived neurotrophic factor gene BDNF: identification of several genetic variants and association studies in patients with obesity, eating disorders, and attention-deficit/hyperactivity disorder. *Am J Med Genet B Neuropsychiatr Genet*, 132: 96-99.
53. Garcia-Segura LM, Chowen JA, Parducz A, Naftolin F. (1994) Gonadal hormones as promoters of structural synaptic plasticity: cellular mechanisms. *Prog Neurobiol*, 44: 279-307.
  54. Gao Q, Wolfgang MJ, Neschen S, Morino K, Horvath TL, Shulman GI, Fu XY. (2004) Disruption of neural signal transducer and activator of transcription 3 causes obesity, diabetes, infertility, and thermal dysregulation. *Proc Natl Acad Sci USA*, 101: 4661-4666.
  55. Gao Q, Horvath TL. (2008) Cross-talk between estrogen and leptin signaling in the hypothalamus. *Am J Physiol Endocrinol Metab*, 294: 817-826.
  56. Gau D, Lemberger T, von Gall C, Kretz O, Le Minh N, Gass P, Schmid W, Schibler U, Korf HW, Schutz G. (2002) Phosphorylation of CREB Ser142 regulates light-induced phase shifts of the circadian clock. *Neuron*, 34: 245-253.
  57. Geary N, Asarian L, Korach KS, Pfaff DW, Ogawa S. (2001) Deficits in E2-dependent control of feeding, weight gain, and cholecystokinin satiation in ER-alpha null mice. *Endocrinology*, 142: 4751-4757.
  58. Gerall AA, Napoli AM, Cooper UC. (1973) Daily and hourly estrous running in intact, spayed and estrone implanted rats. *Physiol Behav*, 10: 225-229.
  59. Gibbs RB, Gabor R. (2003) Estrogen and cognition: applying preclinical findings to clinical perspectives. *J Neurosci Res*, 74: 637-643.
  60. Gillette MU, Mitchell JW. (2002) Signaling in the suprachiasmatic nucleus: selectively responsive and integrative. *Cell Tissue Res*, 309: 99-107.
  61. Gorski RA, Gondon JH, Shryne JE, Southam AM. (1978) Evidence for a morphological sex difference within the medial preoptic area of the rat brain. *Brain Res*, 148: 333-346.

62. Grahn RE, Will MJ, Hammack SE, Maswood S, McQueen MB, Watkins LR, Maier SF. (1999) Activation of serotonin-immunoreactive cells in the dorsal raphe nucleus in rats exposed to an uncontrollable stressor. *Brain Res*, 826: 35-43.
63. Grasa MM, Vila R, Esteve M, Cabot C, Fernandez-Lopez J, Remesar X, Alemany M. (2000) Oleoyl-estrone lowers the body weight of both *ob/ob* and *db/db* mice. *Horm Metab Res*, 32: 246-250.
64. Glass JD, Grossman GH, Farnbauch L, DiNardo L. (2003) Midbrain raphe modulation of nonphotic circadian clock resetting and 5-HT release in the mammalian suprachiasmatic nucleus. *J Neurosci*, 23: 7451-7460.
65. Gray JM, Wade GN. (1981) Food intake, body weight, and adiposity in female rats: actions and interactions of progestins and antiestrogens. *Am J Physiol*, 240: 474-481.
66. Greenwood BN, Foley TE, Day HE, Campisi J, Hammack SH, Campeau S, Maier SF, Fleshner M. (2003) Freewheel running prevents learned helplessness/behavioral depression: role of dorsal raphe serotonergic neurons. *J Neurosci*, 23: 2889-2898.
67. Grill HJ, Kaplan JM. (2002) The neuroanatomical axis for control of energy balance. *Front Neuroendocrinol*, 23: 2-40.
68. Guido ME, Goguen D, De Guido L, Robertson HA, Rusak B. (1999) Circadian and photic regulation of immediate-early gene expression in the hamster suprachiasmatic nucleus. *Neuroscience*, 90: 555-571.
69. Halbreich U, Kahn LS. (2001) Role of estrogen in the aetiology and treatment of mood disorders. *CNS Drugs*, 15: 797-817.
70. Hay-Schmidt A, Vrang N, Larsen PJ. & Mikkelsen JD. (2003) Projections from the raphe nuclei to the suprachiasmatic nucleus of the rat. *J Chem Neuroanat*, 25: 293-310.
71. Heine PA, Taylor JA, Iwamoto GA, Lubahn DB, Cooke PS. (2000) Increased adipose tissue in male and female estrogen receptor-alpha knockout mice. *Proc Natl Acad Sci USA*, 97: 12729-12734.

72. Hermann DM, Luppi PH, Peyron C, Hinckel P, Jouvet M. (1997) Afferent projections to the rat nuclei raphe magnus, raphe pallidus and reticularis gigantocellularis pars alpha demonstrated by iontophoretic application of cholera toxin (subunit b). *J Chem Neuroanat*, 13: 1-21.
73. Hervey GR. (1959) The effects of lesions in the hypothalamus in parabiotic rats. *J Physiol*, 145: 336-378.
74. Hetherington AW, Ranson SW. (1940) Hypothalamic lesions and adiposity in the rat. *Anat Rec*, 78: 149.
75. Horvath TL. (2005) The hardship of obesity: a soft-wired hypothalamus. *Nat Neurosci*, 8: 561-565.
76. Horvath TL, Bechmann I, Kalra SP, Naftolin F, Leranath C. (1997). Heterogeneity in the neuropeptide Y-containing neurons of the rat arcuate nucleus: GABAergic and non-GABAergic subpopulations. *Brain Res*, 756: 283-278.
77. Horvath TL, Diano S, Sakamoto H, Shughrue PJ, Merchenthaler I. (1999) Estrogen receptor beta and progesterone receptor mRNA in the intergeniculate leaflet of the female rat. *Brain Res*, 844: 196-200.
78. Horvath TL, Cela V, van der Beek EM. (1998) Gender specific apposition of vasoactive intestinal peptide-containing axons on gonadotrophin-releasing hormone neurons in the rat. *Brain Res*, 795: 277-281.
79. Horvath TL, Gao XB. (2005) In vivo organization and plasticity of hypocretin neurons: possible clues for obesity's association with insomnia. *Cell Metab*, 1: 279-278.
80. Horvath TL, Wikler KC. (1999) Aromatase in developing sensory systems of the rat brain. *J. Neuroendocrinol*, 11: 77-84.
81. Huang XF, Xin X, McLennan P, Storlien L. (2004) Role of fat amount and type in ameliorating diet-induced obesity: insights at the level of hypothalamic arcuate nucleus leptin receptor, neuropeptide Y and pro-opiomelanocortin mRNA expression. *Diabetes Obes Metab*, 6: 35-44.

82. Huszar D, Lynch CA, Fairchild-Huntress V, Dunmore JH, Fang Q, Berkemeier LR, Gu W, Kesterson RA, Boston BA, Cone RD, Smith FJ, Campfield LA, Burn P, Lee F. (1997) Targeted disruption of the melanocortin-4 receptor results in obesity in mice. *Cell*, 88: 131-141.
83. Ikeda M, Allen CN. (2003) Developmental changes in calbindin-D28k and calretinin expression in the mouse suprachiasmatic nucleus. *Eur J Neurosci*, 17: 1111-1118.
84. Jacobs BL, Azmitia EC. (1992) Structure and function of the brain serotonin system. *Physiol Rev*, 72: 165-229.
85. Jacobson CD, Davis FC, Gorski RA. (1985) Formation of the sexually dimorphic nucleus of the preoptic area: neuronal growth, migration, and changes in cell number. *Dev Brain Res*, 21: 7-18.
86. Jones ME, Thorburn AW, Britt KL, Hewitt KN, Wreford NG, Proietto J, Oz OK, Leury BJ, Robertson KM, Yao S, Simpson ER. (2000) Aromatase-deficient (ArKO) mice have a phenotype of increased adiposity. *Proc Natl Acad Sci USA*, 97: 12735-12740.
87. Kako N, Ishida N. (1998) The role of transcription factors in circadian gene expression. *Neurosci Res*, 31: 257-264.
88. Kalsbeek A, Buijs RM. (2002) Output pathways of the mammalian suprachiasmatic nucleus: coding circadian time by transmitter selection and specific targeting. *Cell Tissue Res*, 309: 109-118.
89. Kam LM, Moberg GP. (1977) Effect of raphe lesions on the circadian pattern of wheel running in the rat. *Physiol Behav*, 18: 213-217.
90. Kernie SG, Liebl DJ, Parada LF. (2000) BDNF regulates eating behavior and locomotor activity in mice. *EMBO J*, 19: 1290-1300.
91. Kohler M, Kalkowski A, Wollnik F. (1999) Serotonin agonist quipazine induces photic-like phase shifts of the circadian activity rhythm and c-Fos expression in the rat suprachiasmatic nucleus. *J Biol Rhythms*, 14: 131-140.

92. Kondo M, Sumino R, Okado H. (1997) Combinations of AMPA receptor subunit expression in individual cortical neurons correlate with expression of specific calcium-binding proteins. *J Neurosci*, 17: 1570-1581.
93. Le Blond CB, Morris S, Karakiulakis G, Powell R, Thomas PJ. (1982) Development of sexual dimorphism in the suprachiasmatic nucleus of the rat. *J Endocrinol*, 95: 137-145.
94. Legan SJ, Karsch FJ. (1975) A daily signal for the LH surge in the rat. *Endocrinology*, 96: 57-62.
95. Lenn NJ, Beebe B, Moore RY. (1977) Postnatal development of the suprachiasmatic hypothalamic nucleus of the rat. *Cell Tiss Res*, 178: 463-475.
96. Lephart ED. (1996) A review of brain aromatase cytochrome P450. *Brain Res Brain Res Rev*, 22: 1-26.
97. Leranth C, Shanabrough M, Horvath TL. (1999) Estrogen receptor- $\alpha$  in the raphe serotonergic (5-HT) and supramammillary (SUM) are calretinin (CR)-containing neurons of the female rat. *Exp Brain Res*, 128: 417-420.
98. Ley CJ, Lees B, Stevenson JC. (1992) Sex- and menopause-associated changes in bodyfat distribution. *Am J Clin Nutr*, 55: 950-954.
99. Lu H, Ozawa H, Nishi M, Ito T, Kawata M. (2001) Serotonergic neurones in the dorsal raphe nucleus that project into the medial proptic area contain oestrogen receptor  $\beta$ . *J Neuroendocrinol*, 13: 839-845.
100. Maffei M, Halaas J, Ravussin E, Pratley RE, Lee GH, Zhang Y, Fei H, Kim S, Lallone R, Ranganathan S. (1995) Leptin levels in human and rodent: measurement of plasma leptin and ob RNA in obese and weight-reduced subjects. *Nat Med*, 1: 1155-1161.
101. Mattson MP. (1992) Calcium as sculptor and destroyer of neural circuitry. *Exp Gerontol*, 27: 29-49.
102. McEwen BS. (2001) Invited review: Estrogens effects on the brain: multiple sites and molecular mechanisms. *J Appl Physiol*, 91: 2785-2801.

103. McEwen BS, Alves SE. (1999) Estrogen actions in the central nervous system. *Endocr Rev*, 20: 279-307.
104. Meli R, Pacilio M, Raso GM, Esposito E, Coppola A, Nasti A, Di Carlo C, Nappi C, Di Carlo R. (2004) Estrogen and raloxifene modulate leptin and its receptor in hypothalamus and adipose tissue from ovariectomized rats. *Endocrinology*, 145: 3115-3121.
105. Mercer JG, Hoggard N, Williams LM, Lawrence CB, Hannah LT, Trayhurn P. (1996) Localization of leptin receptor mRNA and the long splice variant (O-Rb) in mouse hypothalamus and adjacent brain regions by in situ hybridization. *FEBS Lett*, 387: 113-116.
106. Meyer-Bernstein EL, Morin LP. (1996) Differential serotonergic innervation of the suprachiasmatic nucleus and the intergeniculate leaflet and its role in circadian rhythm modulation. *J Neurosci*, 16: 2097-2111.
107. Meyer-Bernstein EL, Morin LP. (1998) Destruction of serotonergic neurons in the median raphe nucleus blocks circadian rhythm phase shifts to triazolam but not to novel wheel access. *J Biol Rhythms*, 13: 494-505.
108. Meyer-Bernstein EL, Morin LP. (1999) Electrical stimulation of the median or dorsal raphe nuclei reduces light-induced FOS protein in the suprachiasmatic nucleus and causes circadian activity rhythm phase shifts. *Neuroscience*, 92: 267-279.
109. Michel S, Colwell CS. (2001) Cellular communication and coupling within the suprachiasmatic nucleus. *Chronobiol Int*, 18: 579-600.
110. Mikkelsen JD, Vran N, Mrosovsky N. (1998) Expression of Fos in the circadian system following nonphotic stimulation. *Brain Res Bull*, 47: 367-376.
111. Milewicz A, Bidzinska B, Mikulski E, Demissie M, Tworowska U. (2000) Influence of obesity and menopausal status on serum leptin, cholecystokinin, galanin and neuropeptide Y levels. *Gynecol Endocrinol*, 14: 196-203.
112. Mistlberger RE, Antle MC, Glass JD, Miller JD. (2000) Behavioral and serotonergic regulation of circadian rhythms. *Biol. Rhythm Res*, 31: 240-283.

113. Mitra SW, Hoskin E, Yudkovitz J, Pear L, Wilkinson HA, Hayashi S, Pfaff DW, Ogawa S, Rohrer SP, Schaeffer JM, McEwen BS, Alves, SE. (2003) Immunolocalization of estrogen receptor beta in the mouse brain: comparison with estrogen receptor alpha. *Endocrinology*, 144: 2055-2067.
114. Miyata S, Nakashima T, Kiyohara T. (1994) Structural dynamics of neural plasticity in the supraoptic nucleus of the rat hypothalamus during dehydration and rehydration. *Brain Res Bull*, 34: 169-78.
115. Moore RY. (1983) Organization and function of a central nervous system circadian oscillator: the suprachiasmatic hypothalamic nucleus. *Fed Proc*, 42: 2783-2789.
116. Moore RY, Speh JC, Leak RK. (2002) Suprachiasmatic nucleus organization. *Cell Tissue Res*, 309: 89-98.
117. Morin LP. (1999) Serotonin and the regulation of mammalian circadian rhythmicity. *Ann Med*, 31: 12-33.
118. Morin LP, Cummings LA. (1982) Splitting of wheelrunning rhythms by castrated or steroid treated male and female hamsters. *Physiol Behav*, 29: 665-675.
119. Morin LP, Fitzgerald KM, Zucker I. (1977) Estradiol shortens the period of hamster circadian rhythms. *Science*, 196: 305-307.
120. Mrosovsky N. (1989) Nonphotic enhancement of adjustment to new light-dark cycles: masking interpretation discounted. *J Biol Rhythms*, 4: 365-370.
121. Naftolin F, Garcia-Segura LM, Horvath TL, Zsarnovszky A, Demir N, Fadiel A, Leranath C, Vondracek-Klepper S, Lewis C, Chang A, Parducz A. (2007) Estrogen-induced hypothalamic synaptic plasticity and pituitary sensitization in the control of the estrogen-induced gonadotrophin surge. *Reprod Sci*, 14: 101-116.
122. Naftolin F, Horvath TL, Balthazart J. (2001) Estrogen synthetase (aromatase) immunohistochemistry reveals concordance between avian and rodent limbic systems and hypothalami. *Exp Biol Med (Maywood)*, 226: 717-725.
123. Nilsen J, Mor G, Naftolin F. (2000) Estrogen-regulated developmental neuronal apoptosis is determined by estrogen receptor subtype and the Fas/Fas ligand system. *J Neurobiol*, 43: 64-78.

124. Nonomura T, Tsuchida A, Ono-Kishino M, Nakagawa T, Taiji M, Noguchi H. (2001) Brain-derived neurotrophic factor regulates energy expenditure through the central nervous system in obese diabetic mice. *Int J Exp Diabetes Res*, 2: 201-209.
125. Ogawa S, Chan J, Gustafsson JA, Korach KS, Pfaff DW. (2003) Estrogen increases locomotor activity in mice through estrogen receptor  $\alpha$ : specificity for the type of activity. *Endocrinology*, 144: 230-239.
126. Ollmann MM, Wilson BD, Yang YK, Kerns JA, Chen Y, Gantz I, Barsh GS. (1997) Antagonism of central melanocortin receptors in vitro and in vivo by agouti-related protein. *Science*, 278: 135-138.
127. Osterlund M, Kuiper GG, Gustafsson JA, Hurd YL. (1998) Differential distribution and regulation of estrogen receptor- $\alpha$  and - $\beta$  mRNA within the female rat brain. *Brain Res Mol Brain Res*, 54: 175-180.
128. Palmer K, Gray JM. (1986) Central vs. peripheral effects of estrogen on food intake and lipoprotein lipase activity in ovariectomized rats. *Physiol Behav*, 37: 187-189.
129. Parducz A, Zsarnovszky A, Naftolin F, Horvath TL. (2003) Estradiol affects axosomatic contacts of neuroendocrine cells in the arcuate nucleus of adult rats. *Neuroscience*, 117: 791-794.
130. Parker GC, McKee ME, Bishop C, Coscina DV. (2001) Whole-body metabolism varies across the estrous cycle in Sprague-Dawley rats. *Physiol Behav*, 74: 399-403.
131. Parry BL, Newton RP. (2001) Chronobiological basis of female-specific mood disorders. *Neuropsychopharmacology*, 25: 102-108.
132. Pickard GE, Weber ET, Scott PA, Riberdy AF, Rea MA. (1996) 5HT<sub>1B</sub> receptor agonists inhibit light-induced phase shifts of behavioral circadian rhythms and expression of the immediate-early gene c-fos in the suprachiasmatic nucleus. *J Neurosci*, 16: 8208-8220.

133. Pickard GE, Rea MA. (1997) Serotonergic innervation of the hypothalamic suprachiasmatic nucleus and photic regulation of circadian rhythms. *Biol Cell*, 89: 513-523.
134. Pinto S, Roseberry AG, Liu H, Diano S, Shanabrough M, Cai X, Friedman JM, Horvath TL. (2004) Rapid rewiring of arcuate nucleus feeding circuits by leptin. *Science*, 304: 110-115.
135. Poehlman ET. (2002) Menopause, energy expenditure, and body composition. *Acta Obstet Gynecol Scand*, 81: 603-611.
136. Prange O, Wong TP, Gerrow K, Wang YT, El-Husseini A. (2004) A balance between excitatory and inhibitory synapses is controlled by PSD-95 and neuroligin. *Proc Natl Acad Sci USA*, 101: 13915-13920.
137. Prosser RA, Macdonald ES, Heller HC. (1994) C-fos mRNA in the suprachiasmatic nuclei in vitro shows a circadian rhythm and responds to a serotonergic agonist. *Brain Res Mol Brain Res*, 25: 151-156.
138. Qiu J, Bosch MA, Tobias SC, Krust A, Chambon P, Scanlan TS, Rønnekleiv OK, Kelly MJ. (2006) A G-protein-coupled estrogen receptor is involved in hypothalamic control of energy homeostasis. *J Neurosci*, 26: 5649-5655.
139. Rasmussen K, Strecker RE, Jacobs BL. (1986) Single unit response of noradrenergic, serotonergic and dopaminergic neurons in freely moving cats to simple sensory stimuli. *Brain Res*, 369: 336-340.
140. Rios M, Fan G, Fekete C, Kelly J, Bates B, Kuehn R, Lechan RM, Jaenisch R. (2001) Conditional deletion of brain-derived neurotrophic factor in the postnatal brain leads to obesity and hyperactivity. *Mol Endocrinol*, 15: 1748-1757.
141. Robyr D, Wolffe AP, Wahli W. (2000) Nuclear hormone receptor coregulators in action: diversity for shared tasks. *Mol Endocrinol*, 14: 329-347.
142. Roesch DM. (2006) Effects of selective estrogen receptor agonists on food intake and body weight gain in rats. *Physiol Behav*, 87: 39-44.
143. Roselli CE, Resko JA. (1993) Aromatase activity in the brain: hormonal regulation and sex differences. *J Steroid Biochem Mol Biol*, 44: 499-508.

144. Ruiz de Elvira MC, Persaud R, Coen CW. (1992) Use of running wheels regulates the effects of the ovaries on circadian rhythms. *Physiol Behav*, 52: 277-284.
145. Rusak B, Zucker I. (1975) Biological rhythms and animal behavior. *Annual Review of Psychology*, 26: 137-171.
146. Schwartz GJ. (2000) The role of gastrointestinal vagal afferents in the control of food intake: current prospects. *Nutrition*, 16: 866-873.
147. Schwartz MW, Seeley RJ, Campfield LA, Burn P, Baskin DG. (1996) Identification of leptin action in rat hypothalamus. *J Clin Invest*, 98: 1101-1106.
148. Seeley RJ, Yagaloff KA, Fisher SL, Burn P, Thiele TE, van Dijk G, Baskin DG, Schwartz MW. (1997) Melanocortin receptors in leptin effects. *Nature*, 390: 349.
149. Sekine Y, Yamamoto T, Yumioka T, Imoto S, Kojima H, Matsuda T (2004) Cross-talk between endocrine-disrupting chemicals and cytokine signaling through estrogen receptors. *Biochem Biophys Res Commun*, 315: 692-698.
150. Shen H, Semba K. (1994) A direct retinal projection to the dorsal raphe nucleus in the rat. *Brain Res*, 635: 159-168.
151. Shinohara K, Funabashi T, Mitushima D, Kimura F. (2000) Effects of estrogen on the expression of connexin32 and connexin43 mRNAs in the suprachiasmatic nucleus of female rats. *Neurosci Lett*, 286: 107-110.
152. Shinohara K, Funabashi T, Nakamura TJ, Kimura F. (2001) Effects of estrogen and progesterone on the expression of connexin-36 mRNA in the suprachiasmatic nucleus of female rats. *Neurosci Lett*, 309: 37-40.
153. Shughrue PJ, Lane MV, Merchenthaler I. (1997) Comparative distribution of estrogen receptor-alpha and -beta mRNA in the rat central nervous system. *J Comp Neurol*, 388: 507-525.
154. Silver R, LeSauter J, Tresco PA, Lehman MN. (1996) A diffusible coupling signal from the transplanted suprachiasmatic nucleus controlling circadian locomotor rhythms. *Nature*, 382: 810-813.

155. Solum DT, Handa RJ. (2002) Estrogen regulates the development of brain-derived neurotrophic factor mRNA and protein in the rat hippocampus. *J Neurosci*, 22: 2650-2659.
156. Stellar E. (1954) The physiology of motivation. *Psychol Rev*, 61: 5-22.
157. Stuart E, Lephart ED. (1999) Dimorphic expression of medial basal hypothalamic-preoptic area calbindin-D (28K) mRNA during perinatal development and adult distribution of calbindin-D (28K) mRNA in Sprague-Dawley rats. *Brain Res Mol Brain Res*, 73: 60-67.
158. Su JD, Qiu J, Zhong YP, Chen YZ. (2001) Expression of estrogen receptor -alpha and -beta immunoreactivity in the cultured neonatal suprachiasmatic nucleus: with special attention to GABAergic neurons. *Neuroreport*, 12: 1955-1959.
159. Sumida H, Nishizuka M, Kano Y, Arai Y. (1993) Sex differences in the anteroventral periventricular nucleus of the preoptic area and in the related effects of androgen in prenatal rats. *Neurosci Lett*, 151: 41-44.
160. Swanson LW, Cowan WM, Jones EG. (1974) An autoradiographic study of the efferent projections of the ventral lateral geniculate nucleus in the albino rat and cat. *J Comp Neurol*, 156: 143-164.
161. Szafarczyk A, Alonso G, Ixart G, Malaval F, Nouguiet-Soule J, Assenmacher I. (1980) Serotonergic system and circadian rhythms of ACTH and corticosterone in rats. *Am J Physiol*, 239: 482-489.
162. Tartaglia LA, Dembski M, Weng X, Deng N, Culpepper J, Devos R, Richards GJ, Campfield LA, Clark FT, Deeds J, Muir C, Sanker S, Moriarty A, Moore KJ, Smutko JS, Mays GG, Wool EA, Monroe CA, Tepper RI. (1995) Identification and expression cloning of a leptin receptor, OB-R. *Cell*, 83: 1263-1278.
163. Theodosis DT, Rougon G, Poulain DA. (1991) Retention of embryonic features by an adult neuronal system capable of plasticity: polysialylated neural cell adhesion molecule in the hypothalamo-neurohypophysial system. *Proc Natl Acad Sci USA*, 88: 5494-5498.

164. Torterolo P, Yamuy J, Sampogna S, Morales FR, Chase MH. (2000) GABAergic neurons of the cat dorsal raphe nucleus express c-fos during carbachol-induced active sleep. *Brain Res*, 884: 68-76.
165. Turek FW, Dugovic C, Zee PC. (2001) Current understanding of the circadian clock and the clinical implications for neurological disorders. *Arch Neurol*, 58: 1781-1787.
166. Van der Beek EM, Horvath TL, Wiegant VM, Van den Hurk R, Buijs RM. (1997) Evidence for a direct neuronal pathway from the suprachiasmatic nucleus to the gonadotropin-releasing hormone system: combined tracing and light and electron microscopic immunocytochemical studies. *J Comp Neurol*, 384: 569-579.
167. Vertes RP. (1991) A PHA-L analysis of ascending projections of the dorsal raphe nucleus in the rat. *J Comp Neurol*, 313: 643-668.
168. Vertes RP, Fortin WJ, Crane AM. (1999) Projections of the median raphe nucleus in the rat. *J Comp Neurol*, 407: 555-582.
169. Wade GN, Gray JM, Bartness TJ. (1985) Gonadal influences on adiposity. *Int J Obes*, 9 (Suppl 1): 83-92.
170. Watts AG, Swanson LW. (1987) Efferent projections of the suprachiasmatic nucleus: II. Studies using retrograde transport of fluorescent dyes and simultaneous peptide immunohistochemistry in the rat. *J Comp Neurol*, 258: 230-252.
171. Wise PM, Smith MJ, Dubal DB, Wilson ME, Rau SW, Cashion AB, Bottner M, Rosewell KL. (2002) Neuroendocrine modulation and repercussions of female reproductive aging. *Recent Prog Horm Res*, 57: 235-256.
172. Xiong JJ, Karsch FJ, Lehman MN. (1997) Evidence for seasonal plasticity in the gonadotropin-releasing hormone (GnRH) system of the ewe: changes in synaptic inputs onto GnRH neurons. *Endocrinology*, 138: 1240-1278.
173. Zhang Y, Proenca R, Maffei M, Barone M, Leopold L, Friedman JM. (1994) Positional cloning of the mouse obese gene and its human homologue. *Nature*, 372: 425-478.

174. Zsarnovszky A, Horvath TL, Garcia-Segura LM, Horvath B, Naftolin F. (2001) Oestrogen-induced changes in the synaptology of the monkey (*Cercopithecus aethiops*) arcuate nucleus during gonadotropin feedback. *J Neuroendocrinol*, 13: 22-78.
175. Zup SL, Carrier H, Waters EM, Tabor A, Bengston L, Rosen GJ, Simerly RB, Forger NG. (2003) Overexpression of bcl-2 reduces sex differences in neuron number in the brain and spinal cord. *J Neurosci*, 23: 2357-2362.

## 9. THE AUTHOR'S PUBLICATIONS ASSOCIATED WITH THE THESIS

1. Abizaid A, **Mezei G**, Horvath TL. (2004) Estradiol enhances light-induced expression of transcription factors in the SCN. **Brain Res**, 1010: 35-44. **IF: 2.389**
2. Abizaid A, **Mezei G**, Sotonyi P, Horvath TL. (2004) Sex differences in adult suprachiasmatic nucleus neurons emerging late prenatally in rats. **Eur J Neurosci**, 19: 2488-2496. **IF: 3.820**
3. Abizaid A\*, **Mezei G\***, Thanarajasingam G, Horvath TL. (2005) \***Co-first authors**. Estrogen enhances light-induced activation of dorsal raphe serotonergic neurons. **Eur J Neurosci**, 21: 1536-1546. **IF: 3.949**
4. Gao Q, **Mezei G**, Nie Y, Rao Y, Choi C.S, Bechmann I, Leranth C, Toran-Allerand D, Priest CA, Roberts JL, Gao XB, Mobbs C, Shulman GI, Diano S, Horvath TL. (2007) Anorectic estrogen mimics leptin's effect on the rewiring of melanocortin cells and Stat3 signaling in obese animals. **Nat Med**, 13: 89-94. **IF: 26,382**
5. **Mezei G**, Rigo J Jr, Horvath TL. (2009) Estrogen as metabolic hormone. The role of estrogen in the hypothalamic regulation of energy homeostasis. **Metabolismus**, 7: 111-114. Hungarian.

### Abstracts

1. Abizaid A, **Mezei G**, Horvath TL. (2003) Estradiol enhances light induced fos immunoreactivity (Fos-IR) within the suprachiasmatic nucleus (SCN) of ovariectomized (OVX) female rats. Program No. 511.3 Neuroscience Abstract, New Orleans, LA, USA: Society of Neuroscience, 2003. Online **IF: 8.306**
2. Abizaid A, **Mezei G**, Horvath TL. (2003) Estradiol enhances neuronal activation in the SCN of female rats after an advance in the onset of light. **Horm Behav**, 44: 36. **IF: 3.222**

3. Abizaid A, Sotonyi P, Borok E, **Mezei G**, Horvath TL. (2003) Sexually dimorphic proliferation of cells in the suprachiasmatic nucleus (SCN). ENDO 2003. The Endocrine Society's 85<sup>th</sup> Annual Meeting, Philadelphia, PA, USA.
4. Qian G, **Mezei G**, Diano S, Horvath TL. (2004) Estradiol mimics leptin's effect on synaptic plasticity of POMC cells. ENDO 2004, The Endocrine Society's 86<sup>th</sup> Annual Meeting, New Orleans, LA, USA.

## 10. THE AUTHOR'S PUBLICATIONS NOT ASSOCIATED WITH THE THESIS

1. Marton T, Tanko A, **Mezei G**, Papp Z. (2001) Diagnosis of an unusual form of iniencephaly in the first trimester of pregnancy. **Ultrasound Obstet Gynecol**, 18: 549-551.
2. Papp C, Beke A, **Mezei G**, Toth-Pal E, Papp Z. (2002) Chorionic villus sampling: a 15-year experience. **Fetal Diagn Ther**, 17: 218-227. **IF: 1.053**
3. Papp C, Beke A, Ban Z, **Mezei G**, Toth-Pal E, Papp Z. (2003) Chorionic villus sampling: a 15-year experience. **Magy Noorv L**, 66: 271-282. Hungarian.
4. Szigeti Z, Toth-Pal E, Papp C, Beke A, Joo JG, Ban Z, **Mezei G**, Papp Z. (2004) Cytogenetic investigation of fetuses conceived by intracytoplasmic sperm injection. **Prenat Diagn**, 24: 579-580.
5. **Mezei G**, Papp C, Toth-Pal E, Beke A, Papp Z. (2004) Factors influencing parental decision making in prenatal diagnosis of sex chromosome aneuploidy. **Obstet Gynecol**, 104: 94-101. **IF: 3.512**
6. Beke A, Papp C, Toth-Pal E, **Mezei G**, Oroszne NJ, Joo JG, Csaba A, Papp Z. (2004) Cytogenetic exploration of fetal ultrasound anomalies. **Orv Hetil**, 145: 2123-2133. Hungarian.
7. Joo JG, Beke A, Csaba A, **Mezei G**, Papp Z. (2004) Obstetric, prenatal diagnostic and phenotype characteristics of holoprosencephaly. **Magy Noorv L**, 67: 3-10. Hungarian.
8. Szigeti Z, Toth-Pal E, Papp C, Beke A, Joo JG, Ban Z, **Mezei G**, Papp Z. (2004) Cytogenetic investigation of fetuses conceived by intracytoplasmic sperm injection. **Magy Noorv L**, 67: 137-142. Hungarian.
9. Beke A, Papp C, Toth-Pal E, **Mezei G**, Oroszne NJ, Joo JG, Csaba A, Papp Z. (2005) Trisomies and other chromosome abnormalities detected following positive sonographic findings. **J Reprod Med**, 50: 675-691. **IF: 0.778**

10. Papp Z, **Mezei G**, Hidvegi J, Hupuczi P. (2005) Abdominal partial resection of the vagina and colpexy: experiences with the procedure for posthysterectomy vault prolapse in 74 cases. **Orv Hetil**, 146: 2641-2645. Hungarian.
11. Papp C, Hajdu J, Beke A, **Mezei G**, Szigeti Z, Ban Z, Papp Z. (2006) Prenatal diagnosis of Turner syndrome. A report on 69 cases. **J Ultrasound Med**, 25: 711-717. **IF: 1.189**
12. Papp Z, **Mezei G**, Gavai M, Hupuczi P, Urbancsek J. (2006) Reproductive performance after transabdominal metroplasty: A review of 157 consecutive cases. **J Reprod Med**, 51: 544-552. **IF: 0.835**
13. Papp C, Ban Z, Szigeti Z, Hajdu J, Beke A, Toth-Pal E, Csaba A, Joo JG, **Mezei G**, Papp Z. (2006) The role of ultrasound examination in second trimester screening for fetal aneuploidies. **Orv Hetil**, 147: 2131-2137. Hungarian.
14. Papp C, Hajdu J, Beke A, Ban Z, Szigeti Z, Toth-Pal E, Csaba A, Joo JG, **Mezei G**, Papp Z. (2007) Prenatal diagnosis of Turner syndrome. A report on 69 cases. **Magy Noorv L**, 70: 37-43. Hungarian.
15. Papp C, Hajdu J, Beke A, Ban Z, Szigeti Z, Toth-Pal E, Csaba A, Joo JG, **Mezei G**, Papp Z. (2006) Prenatal diagnosis of trisomy 13: a report on 28 cases. **Magy Noorv L**, 69: 555-561. Hungarian.
16. Beke A, Barakonyi E, Belics Z, Joo JG, Csaba A, Papp C, Toth-Pal E, **Mezei G**, Ban Z, Papp Z. (2007) The risk of aneuploidies in cases of unilateral and bilateral choroids plexus cysts.. **Magy Noorv L**, 70: 29-36. Hungarian.
17. Szigeti Z, Hajdu J, Csapo Z, Toth-Pal E, Joo JG, Csaba A, **Mezei G**, Papp Z, Papp C. (2007) Correlation of prenatal ultrasound diagnosis and pathological findings following induced abortions, in fetuses with trisomy 21. **Magy Noorv L**, 70: 219-227. Hungarian.
18. Szigeti Z, Hajdu J, Csapo Z, Toth-Pal E, Joo JG, Csaba A, **Mezei G**, Pete B, Papp Z. (2007) Quality control of prenatal sonography in detecting trisomy 18. The value of perinatal autopsy. **Magy Noorv L**, 70: 281-288. Hungarian.

19. Papp C, Hajdu J, Beke A, Ban Z, Szigeti Z, Joo JG, Csaba A, Toth-Pal E, **Mezei G**, Papp Z. (2007) Prenatal sonographic findings in 207 fetuses with trisomy 21. **Magy Noorv L**, 70: 83-90. Hungarian.
20. Papp C, Szigeti Z, Hajdu J, Csapo Z, Lazar L, Toth-Pal E, Joo JG, Csaba A, **Mezei G**, Papp Z. (2007) Correlation of prenatal ultrasound diagnosis and pathological findings following induced abortions, in fetuses with trisomies. **Gyermekgyogy**, 58: 422-428. Hungarian.
21. Joo JG, Beke A, Szigeti Z, Csaba A, **Mezei G**, Toth-Pal E, Rab A, Papp Z, Papp C. (2007) Role of fetopathological investigations in the clinical assessment of urinary tract malformations. **Magy Noorv L**, 70: 355-362. Hungarian.
22. Joo JG, Beke A, Toth-Pal E, Papp C, Szigeti Z, Csaba A, **Mezei G**, Lazar L, Papp Z. (2007) Major diagnostic and pathological features of iniencephaly based on twenty-four cases. **Magy Noorv L**, 70: 211-218. Hungarian.
23. Joo JG, Beke A, Szigeti Z, Csaba A, **Mezei G**, Toth-Pal E, Papp C. (2008) Craniospinal malformations in a twelve-year fetopathological study; the efficiency of ultrasonography in view of fetopathological investigations. **Early Hum Dev**, 84: 115-119. **IF: 1.850**
24. Joo JG, Beke A, Szigeti Z, Csaba A, **Mezei G**, Toth-Pal E, Papp Z, Papp C. (2008) Craniospinal malformations in a twelve-year fetopathological study; the efficiency of ultrasonography in view of fetopathological investigations. **Orv Hetil**, 149: 23-27. Hungarian.

### **Book chapters**

1. Szigeti Z, Toth-Pal E, Papp C, Beke A, Joo JG, Ban Z, **Mezei G**, Papp Z. Cytogenetic investigation of fetuses conceived through intracytoplasmic sperm injection. In: Eds. Papp Z, Rodeck C. **Recent Advances in Prenatal Genetic Diagnosis**. Medimond, Bologna, 2004: 153-156.
2. Beke A, Barakonyi E, Belics Z, Joo JG, Csaba A, Papp C, Toth-Pal E, **Mezei G**, Ban Z, Papp Z. The risk of aneuploidies in cases of choroids plexus cysts. In: Eds.

Kurjak A, Chervenak FA, **Perinatal Medicine**. Medimond, Bologna, 2005: 237-240.

### Abstracts

1. Beke A, Papp C, Toth-Pal E, **Mezei G**, Oroszne NJ, Joo JG, Csaba A, Papp Z. (2002) Chromosomal abnormalities detected following positive ultrasound finding. *Fetal Diagn Ther*, 17 (Supp. 1): 47. IF: 1.053
2. Jenei K, Beke A, Csabay L, Sipos Z, Barakonyi E, Ban Z, Sziller I, **Mezei G**, Papp C, Toth-Pal E. (2002) Incidence of Toxoplasma and CMV infection in cases with positive ultrasound findings. *Fetal Diagn Ther*, 17 (Supp. 1): 47. IF: 1.053
3. Joo JG, Papp C, Toth-Pal E, Beke A., Csaba A, **Mezei G**, Papp Z. (2002) Successful enucleation of a necrotizing fibroid causing oligohydramnios and fetal postural deformity in the 25<sup>th</sup> week of gestation. *Fetal Diagn Ther*, 17 (Supp. 1): 52. IF: 1.053
4. **Mezei G**, Beke A, Toth-Pal E, Papp Cs, Papp Z. (2002) Factors influencing parental decision-making in prenatal diagnosis of sex chromosome aneuploidy: 12-year-experience. *Fetal Diagn Ther*, 17 (Supp. 1): 98. IF: 1.053
5. Beke A, Papp C, Toth-Pal E, **Mezei G**, Oroszne NJ, Joo JG, Csaba A, Papp Z. (2002) Cytogenetic exploration of fetal ultrasound anomalies. *Nogygyaszati és Szuleszeti Tovabbkepzo Szemle*, 4 (Supp.): 25. Hungarian.
6. Jenei K, Beke A, Csabay L, Sipos Zs, Barakonyi E, Ban Z, Sziller I, **Mezei G**, Papp C, Toth-Pal E. (2002) Incidence of Toxoplasma and CMV infection in cases with positive ultrasound findings. *Fetal Diagn Ther, Nogygyaszati és Szuleszeti Tovabbkepzo Szemle*, 4 (Supp.): 28.
7. **Mezei G**, Papp C, Toth-Pal E, Beke A, Papp Z. (2002) Factors influencing parental decision-making in prenatal diagnosis of sex chromosome aneuploidy: 12-year-experience. *Nogygyaszati és Szuleszeti Tovabbkepzo Szemle*, 4 (Supp.): 29. Hungarian.

8. Joo JG, Papp C, Toth-Pal E, Beke A, Csaba A, **Mezei G**, Papp Z. (2002) Successful enucleation of a necrotizing fibroid causing oligohydramnios and fetal postural deformity in the 25<sup>th</sup> week of gestation. *Nogyogyaszati és Szuleszeti Tovabbkepzo Szemle*, 4 (Supp.): 110. Hungarian.
9. Papp C, Toth-Pal E, Beke A, **Mezei G**, Ban Z, Papp Z. (2003) Chorionic villus sampling: our experience. *Ultrasound Obstet Gynecol*, 22 (Supp. 1): 137.  
IF: 1.973
10. Beke A, Barakonyi E, Belics Z, Joo JG, Csaba A, Papp C, Toth-Pal E, **Mezei G**, Ban Z, Papp Z. (2005) The risk of aneuploidies in cases of choroids plexus cysts. *J Perinat Med*, 33 (Supp): 162. IF: 0.713

Number of peer-reviewed publications in international journals:	12 ( <b>IF: 45.814</b> )
From these as a first author:	2 ( <b>IF: 7.461</b> )
Number of peer-reviewed publications in Hungarian journals:	17
Number of book chapters:	2
Number of abstract presentations:	14 (IF: 18.426)
Cumulative impact factor:	<b>ΣIF: 64.440</b>

## 11. ACKNOWLEDGEMENTS

I would like to express my gratefulness to my supervisor **Prof. János Rigó Jr., M.D. Ph.D.**, the chairman of the 1<sup>st</sup> Department of Obstetrics and Gynecology at Semmelweis University Faculty of Medicine who encouraged and supported me full hearted throughout the research and the preparation of my thesis even from a great distance. I am also very grateful to **Prof. Tamás Horváth D.V.M., Ph.D.**, the chairman of Department of Comparative Medicine and Professor at the Department of Obstetrics, Gynecology and Reproductive Sciences Yale University School of Medicine, New Haven, Connecticut, USA who gave me the opportunity and honor to work with him in his laboratory at Yale University, to be part of many breakthrough discoveries and who introduced the deeper aspects of neuroendocrinology to me. I also thank to **Prof. Péter Sótónyi D.V.M., Ph.D.**, the chairman of the Department of Anatomy and Histology, Szent István University, Faculty of Veterinary Science for endearing biology and anatomy to me, for the support throughout my entire carrier and for the deep friendship lasting almost 20 years.

I would thank to **Prof. Rácz Károly M.D., Ph.D.**, 2<sup>nd</sup> Department of Internal Medicine, Semmelweis University Faculty of Medicine for the program leader in this work.

I would like to thank to **Prof. Zoltán Papp M.D., Ph.D.**, the former chairman of the 1<sup>st</sup> Department of Obstetrics and Gynecology, who guided me through my residency and through my clinical and research work in the field of prenatal genetics.

I am thankful to **Tóth-Pál Ernő M.D., Ph.D.**, **Papp Csaba M.D., Ph.D.**, **Beke Arthúr M.D., Ph.D.** and to all the colleagues and co-workers in the division of clinical genetics and in the genetic laboratory at the 1<sup>st</sup> Department of Obstetrics and Gynecology at Semmelweis University Faculty of Medicine, all are very close to my heart.

I was lucky to have excellent colleagues and friends like **Alfonso Abizaid Ph.D.** and **Prof. Qian Gao M.D., Ph.D.** at Yale University to work with, who were helping and teaching me on a daily basis. I also received a lots of professional technical support from **Erzsébet Borok** and **Marya Shanabrough**, I am thankful for them as well.